STUDY OF ELASTIC AND INELASTIC ELECTRON AND POSITRON SCATTERING FROM METASTABLE HYDROGEN IN THE GLAUBER AND WALLACE APPROXIMATIONS

ZONGCHAO YAN, M.Sc

Study of Elastic and Inelastic Electron and Positron Scattering from Metastable Hydrogen in the Glauber and Wallace Approximations

by

Zongchao Yan, M.Sc. (Tong Ji Univ.)

©A thesis submitted to the School of Graduate
Studies in partial fulfillment of the
requirements for the degree of
Master of Science

Department of Physics
Memorial University of Newfoundland

August 19[illegible]

St. John's Newfoundland

ISBN 0-315-61845-0

To My Wife Wenying

Abstract

The differential cross sections for the elastic and inelastic scattering of electron and positron from hydrogen in the metastable 2s state (2s-2s, 2s-2p, 2s-3s, and 2s-3p) are calculated by using the Glauber and Wallace approximations, at several intermediate energies (from 50 eV to 400 eV). For the correction term of the Wallace amplitude the three-dimensional integral expression is adopted in the calculation. We also make some comparison between electron and positron scattering processes from the metastable 2s state of hydrogen and processes from the ground state (1s-1s, 1s-2s, 1s-2p, 1s-3s, and 1s-3p), revealing some significant difference in their relative behaviors.

Acknowledgements

I acknowledge my deep indebtedness to my supervisor Dr. T.T. Gien for his supervision throughout the course of this work. I wish to thank the staff of the Computing Service of the University for the assistance. Thanks are also due to the School of Graduate Studies, Memorial University of Newfoundland for providing me with University Fellowship, to the Department of Physics and to Dr. T.T. Gien for providing me with teaching and research assistantships. Finally, and most of all, my thanks go to my parents for their constant spiritual support and unfailing encouragement.

Contents

List of Tables

List of Figures

Chapter 1

Introduction

Study of the scattering of electrons by atoms in the excited states is of great importance. Much new dynamics can be expected to come from the comparisons with electron and positron scattering processes by atoms in the ground state; indeed excited atoms have larger spatial extension and have closer coupling with other states, thus producing much larger polarization effects. Also, these scattering processes play an important role in plasma physics, astrophysics and various gaseous phenomena.

On the theoretical side some calculations have been carried out in the past decade, most of the work being for the 2s-2s process. Joachain *et al.* [1] studied the elastic scattering of electrons from the 2s state of hydrogen by using the eikonal-Born series (EBS) approximation, together with the static and corrected static approximations. Ho and Chan *et al.* [2] studied the e-H(2s) elastic scattering in the framework of the Glauber approximation. Joachain *et al.* [3] also studied the e-H(2s) elastic scattering by means of the second order optical potential method. Recently, they [4] calculated the $e^{\pm}$-H(2s) differential cross section in the third order optical potential model formalism. Pundir *et al.* [5]

studied electron scattering by hydrogen in the 2s state by using the Coulomb-projected Born approximation. Saxena *et al.* [6] calculated the differential and integral cross sections for 2s-*ns* ($n = 3, 4$) of the hydrogen atom by positron impact in a similar Coulomb-projected Born approximation formalism. Rao *et al.* [7] performed the calculation on e-H(2s) elastic scattering by using the so-called high-energy high-order Born (HHOB) approximation of Yates [8] which can be viewed as an approximate version of the EBS one. Tayal [9] used an improved corrected static approximation to study the e-H(2s) elastic scattering. Das *et al.* [10] did the work on e-H(2s) process by using Das' calculation method which is similar to the Schwinger variational principle. Chandra Prahba *et al.* [11] [12] used eikonal approach to study e-H(2s) process.

On the experimental side only one experiment [13] has been carried out to measure the electron-impact ionization cross section of hydrogen in the metastable 2s state. However, more experimental results on electron scattering (elastic and inelastic) from metastable hydrogen are expected to come in the near future.

In this work, we have calculated the elastic and inelastic differential cross sections of electron and positron scattering from metastable hydrogen H(2s) (2s-2s, 2s-2p, 2s-3s, and 2s-3p) by using the Glauber and Wallace approximations, at several intermediate energies. The many-body Glauber and Wallace amplitudes have some deficiencies which are rooted in the frozen target approximation used in the derivation of these amplitudes. Nevertheless, for scattering from 2s metastable state of hydrogen, the intermediate excitation energy effect is less important compared to the scattering from the ground state of hydrogen, especially at intermediate and high incident energies because in the case of scattering from 2s metastable state, the excitation energies of the intermediate states are either much smaller or zero. In

other words the effect due to the distortion of the target wave function would be expected to be of less significance. We have carried out some comparative studies between the Wallace and Glauber approximations, trying to see the effects due to the straight line and weak-coupling approximations which are inherent in the Glauber approximation and are improved in the Wallace one. We also have made the comparison between electron and positron scattering processes from metastable 2s state of hydrogen and the processes from the ground state (1s-1s, 1s-2s, 1s-2p, 1s-3s, and 1s-3p), trying to reveal some significant difference in their relative behaviors. For the correction term of the Wallace amplitude, the three-dimensional integral expressions have been employed in the calculation; and the self-consistent check on the reduction procedures has been made by resorting to the four-dimensional integral expressions.

Chapter 2

The Glauber and Wallace approximations

2.1 The Glauber potential scattering amplitude and its properties

2.1.1 The Glauber amplitude

In this thesis atomic units (a.u.) will be used. Before discussing the many-body eikonal approximations, we shall discuss eikonal approximations within the potential scattering formalism. This is because potential scattering is easier to deal with than the many-body scattering; on the other hand, since at high energies, the large momentum transfer behaviors are dominated by the static potential which is central for atomic targets such as hydrogen, helium ,*etc*. We first consider the Glauber amplitude [14]. We assume that the

short wavelength condition

$$ka \gg 1 \tag{2.1}$$

is satisfied, along with the high energy requirement:

$$\frac{|V_0|}{E} \ll 1, \tag{2.2}$$

where $k = |\vec{k}_i|$, the magnitude of incident momentum, a is the 'range' of the potential, E is the incident energy, and V_0 is a typical strength of the potential $V(\vec{r})$. The Lippmann-Schwinger equation is

$$|\Psi^{(+)}\rangle = |\vec{k}_i\rangle + G_0^{(+)} V |\Psi^{(+)}\rangle, \tag{2.3}$$

where $|\Psi^{(+)}\rangle$ is the state vector of the collision system, and $G_0^{(+)}$ is the free Green's function. If we write eq. (2.3) in the coordinate representation, we have

$$\Psi^{(+)}(\vec{r}) = \exp(i\vec{k}_i \cdot \vec{r}) + \int G_0^{(+)}(\vec{r}, \vec{r'}) U(\vec{r'}) \Psi^{(+)}(\vec{r'}) d\vec{r'}, \tag{2.4}$$

where $U(\vec{r}) = 2V(\vec{r})$ is the reduced potential, and the Green's function $G_0^{(+)}$ is

$$G_0^{(+)}(\vec{r}, \vec{r'}) = -\lim_{\epsilon_0 \to 0^+} \int d\vec{\kappa} \frac{\exp(i\vec{\kappa} \cdot (\vec{r} - \vec{r'}))}{\kappa^2 - k^2 - i\epsilon_0}. \tag{2.5}$$

If the short wavelength and high energy conditions (2.1) and (2.2) are applied to (2.5), the Green's function will reduce to

$$G_0^{(+)}(\vec{r}, \vec{r'}) \approx -\exp(i\vec{k}_i \cdot (\vec{r} - \vec{r'})) \int \frac{\exp(i\vec{Q} \cdot (\vec{r} - \vec{r'}))}{2\vec{k}_i \cdot \vec{Q} - i\epsilon_0} d\vec{Q}, \tag{2.6}$$

where $\vec{Q} = \vec{\kappa} - \vec{k}_i$, and the denominator of the integrand of eq. (2.5) has been linearized by ignoring the Q^2 term. The integral can be performed by using the residual theorem, thus

$$G_0^{(+)}(\vec{r}, \vec{r'}) = (-\frac{4\pi^3 i}{k}) \exp(ik(z - z')) \delta^2(\vec{b} - \vec{b'}) \theta(z - z'), \tag{2.7}$$

where a cylindrical coordinate system has been used in such a way that $\vec{r} = \vec{b} + z\hat{k}_i$, and $\vec{r}' = \vec{b}' + z'\hat{k}_i$; namely we have chosen the z axis along the incident momentum. The $\theta(x)$ is the step function:

$$\begin{aligned} \theta(x) &= 1, \text{if } x > 0 \\ &= 0, \text{if } x < 0. \end{aligned} \tag{2.8}$$

From eq. (2.7) one can see that the linearized Green's function propagates the scattering information along the forward direction. Such a propagator must have lost some scattering information. Putting eq. (2.7) back to eq. (2.4) leads to the so-called eikonal scattering wave function:

$$\Psi_E^{(+)}(\vec{r}) = \exp[i\vec{k}_i \cdot \vec{r} - \frac{i}{k}\int_{-\infty}^{z} V(\vec{b}, z')dz'], \tag{2.9}$$

where the integral is performed along the direction of $\vec{k}_i$.

We should stress that the eikonal wave function $\Psi_E^{(+)}$ does not have the correct asymptotic form appropriate for an incident wave plus a spherical outgoing wave, but only satisfies the incoming boundary condition, that is,

$$\Psi_E^{(+)} \overset{z\to-\infty}{\longrightarrow} \exp(i\vec{k}_i \cdot \vec{r}). \tag{2.10}$$

Indeed, $\Psi_E^{(+)}$ describes the motion only along the original incident direction. It is nevertheless still used to obtain an approximate scattering amplitude, the eikonal scattering one (see p193 of ref. [15]):

$$f = -\frac{1}{2\pi}\int \exp(i\vec{q}\cdot\vec{r})V(\vec{r})\exp[-\frac{i}{k}\int_{-\infty}^{z} V(\vec{b}, z')dz']d\vec{r}, \tag{2.11}$$

where $\vec{q} = \vec{k}_i - \vec{k}_f$, the momentum transfer.

One can see that the eikonal approximation is actually a high energy semi-classical one. The semi-classical wave function should be [16]

$$\Psi^{(+)} \sim \exp(iS(x)), \tag{2.12}$$

which leads to the Hamilton-Jacobi equation for $S(x)$ ($S(x)$ is called the Hamilton's characteristic function in classical mechanics):

$$\frac{(\nabla S)^2}{2} + V = E. \tag{2.13}$$

Thus, the actual phase of the scattering wave should be calculated along a curved trajectory determined by the eq. (2.13). Needless to say, solving eq. (2.13) to determine the trajectory would be a forbidding task in general. It is thus acceptable to make a compromise, by which the z direction is rotated to a new position perpendicular to the momentum transfer $\vec{q}$, as proposed first by Glauber [14]. This compromise may perhaps improve the forward scattering amplitude (eq. (2.11)). If we use this critical assumption of $\vec{q} \cdot \vec{r} = \vec{q} \cdot \vec{b}$ (which is valid near the forward direction; see Fig.9.2. of p194 of ref. [15]), the amplitude can be reduced to a new form:

$$f_G = \frac{k}{2\pi i} \int \exp(i\vec{q} \cdot \vec{b})[\exp(\frac{i}{k}\chi_0(\vec{b})) - 1]d^2b, \tag{2.14}$$

where

$$\chi_0(\vec{b}) = -\int_{-\infty}^{\infty} V(\vec{b}, z)dz. \tag{2.15}$$

The expression of f_G is called the Glauber amplitude for potential scattering.

2.1.2 The properties of the Glauber potential scattering amplitude

Although the Glauber amplitude is constructed from the scattering wave function which lacks the correct asymptotic form (i.e., an incident wave plus a spherical outgoing wave), a

number of generally desirable properties are still contained in it.

The first intriguing virtue of the Glauber amplitude is that it can yield an exact result for scattering by a Coulomb potential. Glauber [14] has shown that if one uses the sequence

$$V(r) = \begin{cases} Q/r & \text{if } r \leq a \\ 0 & \text{if } r > a, \end{cases}$$

where Q is the charge of projectile, one can obtain the Glauber amplitude $f_G^{(a)}(\theta)$ as a function of parameter a (the adoption of the cutoff is to avoid the divergence of the phase χ_0 for the pure Coulomb potential). After taking the limit of $a \to \infty$, $f_G^{(a)}(\theta)$ becomes

$$f_G(\theta) = -\frac{Q}{2k^2 \sin^2 \frac{\theta}{2}} \exp[-2i(\frac{Q}{k} \ln(\sin \frac{\theta}{2}) - \eta_0)] \exp(-\frac{2Qi}{k} \ln(2ka)), \tag{2.16}$$

where

$$\eta_0 = \arg \Gamma(1 + \frac{Qi}{k}). \tag{2.17}$$

Except for a constant phase factor $\exp(-\frac{2Qi}{k} \ln(2ka))$ which is independent of the scattering angle θ, the result is identical with the exact Coulomb scattering amplitude [17] at all scattering angles. As was known, the Coulomb force is the unique one that determines atomic collision dynamics. Although the interaction potential between incident particle and atom is not purely Coulombic, the $e^{\pm}$-nucleus interaction, which is a pure Coulomb one, dominates the scattering at large momentum transfer (high energies and large angles). So long as the target wavefunction is not very effective enough at screening the nucleus, the Glauber amplitude can give rise to quite satisfactory results at large momentum transfers. Since the property that the Glauber amplitude reproduces exactly the Coulomb scattering amplitude is an 'all angles' one, we should not judge the angular validity of the Glauber amplitude simply from the semi-classical point of view. As a matter of fact, Glauber's

proposal of making the path integral along a special direction which is perpendicular to the momentum transfer vector distorts the amplitude from a purely semi-classical one, thus bringing about a considerably complicated situation.

Another important virtue of the Glauber amplitude is that it is unitary at high energies [14], thus reflecting the conservation of the probability of scattering process.

It is worth pointing out that the unitarity through the optical theorem can be satisfied by any amplitude which has a structure of the Glauber form [14] [18]

$$f = \frac{k}{2\pi i}\int \exp(i\vec{q}\cdot\vec{b})[\exp(i\chi(\vec{b},\vec{k})) - 1]d^2\vec{b}, \tag{2.18}$$

regardless of the form of $\chi(\vec{b},\vec{k})$, even if $\chi(\vec{b},\vec{k})$ is complex, provided that the integral (2.18) converges.

The third favorable virtue of the Glauber amplitude is that at sufficiently high incident energy, the Glauber amplitude reduces to the first Born one for all interaction potentials and all momentum transfers (see, for example, p241 of ref. [18]). Since the first Born term dominates potential scattering processes at high energies and at all momentum transfers, it is expected that the Glauber amplitude will work well at sufficiently high incident energies.

Furthermore, if we expand f_G into a multiple scattering form in powers of the potential, we obtain

$$f_G = \sum_{n=1}^{\infty} f_{Gn}, \tag{2.19}$$

where

$$f_{Gn} = \frac{1}{2\pi}(\frac{i}{k})^{n-1}\frac{1}{n!}\int \exp(i\vec{q}\cdot\vec{b})[\chi_0(\vec{b})]^n d^2\vec{b}. \tag{2.20}$$

It is well established that for a short-range potential which takes the form of a superposition

of the Yukawa type [19] [20]

$$V(r) = V_0 \int_{\alpha_1}^{\infty} \rho(\alpha) \frac{\exp(-\alpha r)}{r} d\alpha, \tag{2.21}$$

the Glauber amplitude can be written as

$$\begin{aligned} f_G(k,q) &= f_{B1}(q) + i\frac{B(q)}{k} + \frac{C(q)}{k^2} + \cdots \\ &= f_{B1} + f_{G2} + f_{G3} + \cdots, \end{aligned} \tag{2.22}$$

where the coefficients $B(q)$, $C(q)$ also appear in the corresponding Born series:

$$\begin{aligned} f(k,q) &= f_{B1}(q) + [\frac{A(q)}{k^2} + i\frac{B(q)}{k}] + [\frac{C(q)}{k^2} + i\frac{D(q)}{k^3}] + \cdots \\ &= f_{B1} + f_{B2} + f_{B3} + \cdots \end{aligned} \tag{2.23}$$

at all momentum transfers provided that the semi-classical condition $ka \gg 1$, the high energy condition $|V_0|/k^2 \ll 1$ as well as the weak coupling condition $(|V_0|/k^2)(ka) \ll 1$, which guarantees the convergence of the Born series, are all satisfied. Thus the Glauber approximation is one which just selects in each term of the Born series the dominant contribution (to order k^{-1}) under the above conditions. This property makes it possible to use the higher order Glauber terms to approximate the corresponding Born terms which are extremely difficult to deal with. In addition, the Glauber terms are alternately real and imaginary.

2.2 The Wallace potential scattering amplitude and its properties

2.2.1 The Wallace amplitude

The Glauber amplitude is constructed from the linearization of the Green's function. Thus it only chooses in each term of the Born series the dominant contribution to order k^{-1} in some cases. It is interesting to look for an improvement beyond the conventional Glauber amplitude towards an understanding of the large angle corrections. This has been done by Wallace [21] who obtained in a systematic way the leading correction to the Glauber amplitude by using a technique originally adopted by Abarbanel and Itzykson [22]. Let us discuss his work in some detail.

In potential scattering theory, what we should do is to calculate the T matrix:

$$T = \langle \vec{k_f} | V + VGV | \vec{k_i} \rangle, \tag{2.24}$$

where $|\vec{k_i}\rangle$ and $|\vec{k_f}\rangle$ are initial and final states of the incident particle respectively, $|\vec{k_i}| = |\vec{k_f}|$, V is the potential, and G is the full Green's function defined by:

$$G^{-1} = \frac{k_i^2}{2} - \frac{P^2}{2} - V + i\epsilon_0, \epsilon_0 \to 0^+ \tag{2.25}$$

where P is the momentum operator.

Sugar and Blankenbecler [23] suggested that P^2 could be expanded about a vector $\vec{k_n}$ in order to eikonalize the Green's function:

$$k_i^2 - P^2 = k_i^2 - (\vec{P} - \vec{k_n})^2 - 2\vec{k_n} \cdot (\vec{P} - \vec{k_n}) - k_n^2. \tag{2.26}$$

The eikonal approximation is achieved by dropping the quadratic term $(\vec{P} - \vec{k_n})^2$. If we

choose $\vec{k}_n$ to be

$$\vec{k} = \frac{1}{2}(\vec{k}_i + \vec{k}_f), \tag{2.27}$$

then

$$G^{-1} \approx \frac{1}{2}k_i^2 \sin^2\frac{\theta}{2} + k_i \cos\frac{\theta}{2}\hat{k}\cdot(\vec{k} - \vec{P}) - V + i\epsilon_0 \tag{2.28}$$

where θ is the angle between $\vec{k}_i$ and $\vec{k}_f$. In the Abarbanel and Itzykson formalism, the first term $\frac{1}{2}k_i^2 \sin^2\frac{\theta}{2}$ is ignored and the resulting Green's function is thus

$$g_{AI}^{-1} = k_i \cos\frac{\theta}{2}\hat{k}\cdot(\vec{k} - \vec{P}) - V + i\epsilon_0, \tag{2.29}$$

whereas in the conventional Glauber approximation, the condition $\theta \approx 0$ is assumed and the resulting Green's function is taken as

$$g^{-1} = k_i\hat{k}\cdot(\vec{k} - \vec{P}) - V + i\epsilon_0. \tag{2.30}$$

Thus either g_{AI} or g approximate the exact Green's function under the condition of small scattering angles. In the work of Abarbanel and Itzykson, the exact Green's function can be recast into

$$G^{-1} = g_{AI}^{-1} - N_\tau, \tag{2.31}$$

where g_{AI} is the eikonal part, the remaining part N_τ is the correction caused by momentum deviations from both the initial and final directions, i.e.

$$N_\tau = \frac{1}{2}(\vec{P} - \vec{k}_f)\cdot(\vec{P} - \vec{k}_i). \tag{2.32}$$

The eq. (2.31) can easily be inverted into the form as

$$G = g_{AI} + g_{AI}N_\tau G. \tag{2.33}$$

Eq. (2.33) can be iterated and the T matrix expanded as a perturbation series of N_τ as

$$\begin{aligned} T &= \langle \vec{k_f}|V + VGV|\vec{k_i}\rangle \\ &= \langle \vec{k_f}|V + Vg_{AI}V + Vg_{AI}N_\tau g_{AI}V + \cdots|\vec{k_i}\rangle \\ &= \langle \vec{k_f}|V|\vec{k_i}\rangle + \langle \vec{k_f}|Vg_{AI}V|\vec{k_i}\rangle + \langle \vec{k_f}|Vg_{AI}N_\tau g_{AI}V|\vec{k_i}\rangle + \cdots. \end{aligned} \tag{2.34}$$

It can be shown that the first two terms give a scattering amplitude similar to the Glauber one, i.e. if we adopt two dimensional Fourier-like transform of the T matrix as

$$T(\vec{q}) = -k_i \int d^2\vec{b} \exp(i\vec{q}\cdot\vec{b})T(\vec{b},\vec{q}), \tag{2.35}$$

then for the first two terms of eq. (2.34), the Fourier component of eq. (2.35) is

$$T_{AI}(\vec{b},\vec{q}) = -i\cos\frac{\theta}{2}\{\exp[i\tau_0(\vec{b})/\cos\frac{\theta}{2}] - 1\}, \tag{2.36}$$

where

$$\cos\frac{\theta}{2} = (1 - \frac{q^2}{4k_i^2})^{1/2}, \tag{2.37}$$

and $\tau_0(\vec{b})$ is the conventional Glauber phase:

$$\tau_0(\vec{b}) = -\frac{1}{k_i}\int_{-\infty}^{\infty} V dz. \tag{2.38}$$

Comparing eq. (2.36) to the Glauber approximation which has the form

$$T^0(\vec{b}) = -i[\exp(i\tau_0(\vec{b})) - 1], \tag{2.39}$$

one can see that $T_{AI}(\vec{b},\vec{q})$ is not a true Fourier transform of the T matrix because $T_{AI}(\vec{b},\vec{q})$ depends on both $\vec{b}$ and $\vec{q}$; whereas $T^0(\vec{b})$ depends only on the impact parameter $\vec{b}$. Of course at small θ, these two forms make no difference. However $T_{AI}(\vec{b},\vec{q})$ is inferior to the Glauber one at large angles. As an example, for Coulomb potential, $T_{AI}(\vec{b},\vec{q})$ will lead to

an incorrect scattering phase. This led Wallace to choose the Glauber amplitude, rather than the Abarbanel and Itzykson one, as the leading term of his eikonal approximation, the one that is the correct zeroth order high energy approximation for all scattering angles. This can be achieved by simply linking g^{-1} with g_{AI}^{-1}:

$$g^{-1} = g_{AI}^{-1} + \lambda(g^{-1} + V), \tag{2.40}$$

whe. the parameter λ is defined as

$$\lambda = 1 - \cos\frac{\theta}{2}. \tag{2.41}$$

From eq. (2.31) and eq. (2.40) one arrives at

$$\begin{aligned} G^{-1} &= g^{-1} - N \\ N &= \lambda(g^{-1} + V) + N_r. \end{aligned} \tag{2.42}$$

Inverting eq. (2.42) for G^{-1}, an expression for G is obtained as

$$G = g + gNG = g + GNg. \tag{2.43}$$

By resorting to the iteration method, we obtain a perturbation expansion in powers of N (not in powers of potential V!):

$$G = g + (gN)g + (gN)^2 g + \cdots. \tag{2.44}$$

Substituting the eq. (2.44) into eq. (2.24), we obtain the T matrix as a perturbation series in powers of N:

$$\begin{aligned} T &= \langle \vec{k_f} | (V + VgV) + VgNgV + V(gN)^2 gV + V(gN)^3 gV + \cdots | \vec{k_i} \rangle \\ &= T^0 + T^1 + T^2 + T^3 + \cdots. \end{aligned} \tag{2.45}$$

The first term T^0 is the Glauber approximation, and the term T^n is the nth-order correction to T^0 due to the inclusion of momentum transfer effect. It can be shown that the complete eikonal series (2.45) can be written as a Fourier-like transform integral [21]:

$$T(q) = -k_i \int d^2\vec{b} \exp(i\vec{q}\cdot\vec{b}) T_E(\vec{b}; q^2), \tag{2.46}$$

where

$$T_E(\vec{b}; q^2) = \sum_{n=0}^{\infty} (1-\lambda)^{1-n} T^n(\vec{b}; \lambda) \tag{2.47}$$

with $\lambda = 1 - \cos\theta/2$. Since $T^n(\vec{b};\lambda)$ are very complicated, we do not want to write them explicitly.

Wallace first investigated $T(q)$ in the forward scattering situation; this is because the results obtained in this situation may be extended to the general case; on the other hand, the forward scattering is directly related to the total cross section via the optical theorem. Thus by setting $q = 0$ into eq. (2.47), one gets

$$T_E(b;0) = \sum_{n=0}^{\infty} T^n(b;0), \tag{2.48}$$

where the leading terms in the sum are summarized by

$$\begin{aligned}
T^0(b;0) &= -i[\exp(i\tau_0(b)) - 1] \\
T^1(b;0) &= -i\exp(i\tau_0(b))[i\tau_1(b)] \\
T^2(b;0) &= -i\exp(i\tau_0(b))\{[i\tau_1(b)]^2/2! + i\tau_2(b) - \omega_2(b)\} \\
T^3(b;0) &= -i\exp(i\tau_0(b))\{[i\tau_1(b)]^3/3! + i\tau_1(b)[i\tau_2(b) - \omega_2(b)] + i[\tau_3(b) + \phi_3(b)] - \omega_3(b)\}
\end{aligned}$$

$$T^n(b;0) = -i\exp(i\tau_0(b))\{[i\tau_1(b)]^n/n! + [i\tau_1(b)]^{n-2}[i\tau_2(b)]/(n-2)! + \cdots\}, \quad (2.49)$$

where some quantities are listed below:

$$\tau_0(b) = -\frac{1}{k_i}\int_{-\infty}^{\infty} dz V(r), \quad (2.50)$$

$$\tau_1(b) = \frac{1}{2k_i}\int_{-\infty}^{\infty} dz \nabla\chi_-(\vec{r})\cdot\nabla\chi_+(\vec{r}), \quad (2.51)$$

and

$$\nabla\chi_+(\vec{r}) = -\frac{1}{k_i}\int_{-\infty}^{z} dz'\nabla' V(\vec{r'}), \quad (2.52)$$

$$\nabla\chi_-(\vec{r}) = -\frac{1}{k_i}\int_{z}^{\infty} dz'\nabla' V(\vec{r'}). \quad (2.53)$$

These equations demonstrate the exponential feature of the eikonal series. If we only keep $\tau_0(b)$ and $\tau_1(b)$ and ignore all the others, we obtain a phase corrected eikonal amplitude:

$$T^I(b) = -i\{e^{i[\tau_0(b)+\tau_1(b)]} - 1\}. \quad (2.54)$$

Since the Glauber phase is proportional to k_i^{-1}, whereas the phase correction term is proportional to k_i^{-3}, then $\tau_1(b)$ corrects the Glauber phase to the relative order of k_i^{-2}.

The new phase can be written explicitly as

$$\tau_0(b) + \tau_1(b) = k_i\int_0^{\infty} dz[-2\epsilon U(r) - \epsilon^2(1 + b\frac{d}{db})U^2(r)], \quad (2.55)$$

where $V(r) = V_0U(r)$, and $\epsilon = V_0/k_i^2$. On the other hand, the WKB phase is [24]

$$\chi^{WKB}(b) = k_i\int_0^{\infty} dz[-2\epsilon U(r) - \epsilon^2U^2(r) - \epsilon^3U^3(r) - \frac{5}{4}\epsilon^4U^4(r) + \cdots]. \quad (2.56)$$

Comparing these two phases, one can see that the phase in Wallace approximation contains the WKB correction up to ϵ^2 together with a new type of correction involving a transverse derivative $b\frac{d}{db}$ which comes from corrections to either the linearization of the Green's function which has been adopted in deriving the Glauber amplitude, or equivalently, the straight line path which has been inherent in the WKB phase (2.56). In addition, it is worth mentioning that $\tau_1(b)$ is zero for a Coulomb potential.

Now let us turn to discuss large momentum transfer behaviors. In this case T_E is not only a function of $\vec{b}$ but also a function of q^2 through the parameter λ:

$$\lambda = 1 - \cos\frac{\theta}{2} = 1 - (1 - \frac{q^2}{4k_i^2})^{1/2}. \tag{2.57}$$

Wallace developed T_E into a power series of k_i^{-1} and q^2, namely,

$$T_E(b;q^2) = \sum_{n=0}^{\infty} k_i^{-n}[\sum_{l=0}^{n/2} q^{2l} t_{l,n-2l}(b)]. \tag{2.58}$$

The leading terms in eq. (2.58) were found through k_i^{-3} by Wallace [21]:

$$\begin{aligned}
1 &: T^0(b;0) \\
k_i^{-1} &: T^1(b;0) \\
k_i^{-2} &: T^2(b;0) + i[(\nabla^2 + q^2)/8k_i^2]\{[1 - i\tau_0(b)]\exp(i\tau_0(b))\} \\
k_i^{-3} &: T^3(b;0) - i[(\nabla^2 + q^2)/8k_i^2]\{[2 + i\tau_0(b)]i\tau_1(b)\exp(i\tau_0(b))\}.
\end{aligned} \tag{2.59}$$

The higher order terms were not displayed by Wallace because they are too complicated to be calculated. From the above sequence, we can see that (2.59) contains the sequence (2.49) for the forward scattering together with the terms having the structure of $(\nabla^2 + q^2)f(b)$. In fact $\nabla^2 + q^2$ is a null operator under the Fourier transform, that is:

$$\int d^2\vec{b}\exp(i\vec{q}\cdot\vec{b})(\nabla^2 + q^2)f(b) = 0 \tag{2.60}$$

It is this very important feature that leads Wallace to propose the following conjecture for scattering by spherically symmetric potentials:

$$T_E(b;q^2) \overset{conjecture}{\Longrightarrow} T(b) + \sum_{l=1}^{\infty}[(\nabla^2 + q^2)/k_i^2]^l t_l(b). \tag{2.61}$$

That is: the dependence on q^2 of $T_E(b;q^2)$ due to the parameter λ could be systematically canceled by terms involving $\nabla^2 + q^2$. Thus the formula (2.54) derived for the forward scattering case is conjectured to correct the Glauber phase function to the relative order of k_i^{-2} at any momentum transfer. An example of the conjectured cancellation is given by Wallace for all orders in q^2 based on the known result for Yukawa potential scattering through the second Born approximation.

In conclusion, we write out the explicit form of the Wallace amplitude corresponding to $T^I(b)$ as

$$f_W = \frac{k_i}{2\pi i}\int \exp(i\vec{q}\cdot\vec{b})\{\exp[i(k_i^{-1}\chi_0(\vec{b}) + k_i^{-3}\chi_1(\vec{b}))] - 1\}d^2\vec{b}, \tag{2.62}$$

where

$$\chi_1(\vec{b}) = \frac{1}{2}\int_{-\infty}^{\infty}(\nabla\chi_+)(\nabla\chi_-)dz \tag{2.63}$$

and

$$\chi_+(\vec{b},z) = -\int_{-\infty}^{z} V(\vec{b},z')dz' \tag{2.64}$$

$$\chi_-(\vec{b},z) = -\int_{z}^{\infty} V(\vec{b},z')dz' \tag{2.65}$$

$$\chi_0(\vec{b}) = -\int_{-\infty}^{\infty} V(\vec{b},z)dz \tag{2.66}$$

We should note that $\chi_0(\vec{b})$ is the first order in V whereas $\chi_1(\vec{b})$, the second order.

2.2.2 The properties of the Wallace potential scattering amplitude

The Wallace amplitude possesses the properties of the Glauber one. For example, the Wallace amplitude will reproduce the correct form of the Rutherford type for a Coulomb potential since the correction term χ_1 is zero for such a potential. The Wallace amplitude is unitary at high energy [25]; this is because this amplitude has a structure of the Glauber type. Also the Wallace amplitude has the correct high energy behavior, namely,

$$f_W \stackrel{k\to\infty}{\longrightarrow} f_{B1} \tag{2.67}$$

for any scattering angle, where $k = |\vec{k}_i|$. Furthermore, in order to study perturbation features of the Wallace amplitude, we can make the following expansion in powers of the interaction potential:

$$f_W = \sum_{n=1}^{\infty} f_{Wn} \tag{2.68}$$

where

$$f_{Wn} = (\frac{i}{k})^{n-1}\frac{1}{2\pi n!}\int d^2\vec{b}\exp(i\vec{q}\cdot\vec{b})(\chi_0^n(\vec{b}) - n(n-1)\frac{i}{k}\chi_0^{n-2}(\vec{b})\chi_1(\vec{b}) + \cdots). \tag{2.69}$$

One can see that f_{Wn} are complex when $n \geq 2$ in contrast to the term f_{Gn} which are alternately purely real and purely imaginary. Thus f_{Wn} has a tendency to reproduce the corresponding Born term f_{Bn}. It should be recalled that in the derivation of the Wallace amplitude, the first step is to expand the T matrix as a perturbation series of N which directly includes the corrections to the straight line path, see eq. (2.45); the second step is to sum all leading contributions from each term of the perturbation series, see eq. (2.49). It is thus expected that when we expand the Wallace amplitude as a perturbation series in potential V, each term should be closer to its exact one: the corresponding Born term,

although the justification strongly depends on the possible cancellation of parameter λ. The case studies on the Wallace amplitude have been made by Byron *et al.* for various types of central potentials, and in particular for the Yukawa-type potential which takes the form [26]:

$$V(r) = V_0 \int_{\alpha_0}^{\infty} \rho(\alpha) \frac{\exp(-\alpha r)}{r} d\alpha, \tag{2.70}$$

where V_0 is a strength of the potential. For such a potential the Born term $f_{Bn}(n \geq 2)$ can be written as

$$f_{Bn}(k,q) = i^{n-1} V_0^n \left(\frac{A_{Bn}(q)}{k^{n-1}} + i\frac{B_{Bn}(q)}{k^n} + O(k^{-1-n})\right) \tag{2.71}$$

for all momentum transfers. Based on the work of Wallace [21] and of Byron *et al.* [26] it is strongly suggested that for the Yukawa-type potential of the form (2.70), the corresponding Glauber terms and Wallace terms could be expressed as

$$f_{Gn}(k,q) = i^{n-1} V_0^n \frac{A_{Bn}(q)}{k^{n-1}}, (n \geq 2) \tag{2.72}$$

and

$$f_{Wn}(k,q) = i^{n-1} V_0^n \left(\frac{A_{Bn}(q)}{k^{n-1}} + i\frac{B_{Bn}(q)}{k^n}\right), (n \geq 2) \tag{2.73}$$

for all momentum transfers, although a rigorous proof is still lacking. From the expressions we can see that the Wallace amplitude presents in each order of perturbation of potential V not only the leading contribution but also the next one of the corresponding Born term. In contrast to the Glauber case only the leading terms exist.

2.3 The many-body generalization

2.3.1 The frozen target approximation

Compared with pure potential scattering, many-body scattering is much more difficult to deal with. This is because there are extra degrees of freedom associated with target. Thus some approximation should be used concerning the target coordinates. The most commonly adopted method is the so-called frozen target approximation in which the aggregate of all degrees of freedom of the target are fixed during a collision process, thus possible virtual transitions of the target being not permitted. The frozen target approximation, however, should be expected to work well for high incident energy scattering. There are many methods to realize this approximation, one of them being proposed by Chase [27] which clearly embodies the physical picture. We would like to introduce Chase's method here.

As we know, the general formula for calculating the scattering amplitude is given by (see p263 of ref. [18])

$$f_{f0}(\vec{k}_f, \vec{k}_0) = -\frac{1}{2\pi}\langle \vec{k}_f \Psi_f | \sum_{n=0}^{\infty} V(G_0^{(+)}V)^n | \vec{k}_0 \Psi_0 \rangle, \tag{2.74}$$

where $G_0^{(+)}$ is the free Green's function defined by

$$\begin{aligned} G_0^{(+)} &= (E - H_0 + i\epsilon_0)^{-1}, \\ H_0 &= H_a + K_0. \end{aligned} \tag{2.75}$$

In these expressions, H_a is the target Hamiltonian, K_0 is the kinetic energy operator of the projectile, Ψ_0 and Ψ_f are the initial and final target energy eigenstates respectively, and $\vec{k}_0$ and $\vec{k}_f$ are the initial and final momentums of the projectile respectively. If we take the coordinate representation $\{|\vec{r}_0, X\rangle\}$, here $\vec{r}_0$ is the coordinate of the incident particle and

X stands for the aggregate of the coordinates of the target, then it is well-known [28] that

$$G_0^{(+)}(\vec{r}_0, X; \vec{r}_0', X') = -\frac{1}{4\pi}\sum_n \frac{\exp\{ik_n|\vec{r}_0 - \vec{r}_0'|\}}{|\vec{r}_0 - \vec{r}_0'|}\Psi_n(X)\Psi_n^*(X'), \tag{2.76}$$

where

$$k_n = [k_0^2 - 2(\epsilon_n - \epsilon_0)]^{1/2}, \tag{2.77}$$

and

$$H_a\Psi_n(X) = \epsilon_n\Psi_n(X). \tag{2.78}$$

It is understood that the summation over n runs over the complete set of target energy eigenstates (i.e. the discrete states and the continuum), which is a difficult task. There is, however, a simple way to avoid this difficulty. If we look at the expression for k_n, we can see that for sufficiently high energy k_0, the energy difference between the initial state and intermediate states could be approximated by a single average excitation energy $\bar{\epsilon}$. Thus k_n becomes $\bar{k}$, or

$$k_n \approx \bar{k} = (k_0^2 - 2\bar{\epsilon})^{1/2}, \tag{2.79}$$

which is independent of n. Therefore the summation in eq. (2.76) can now be trivially performed by using the closure relation of the target:

$$G_0^{(+)}(\vec{r}_0, X; \vec{r}_0', X') \simeq -\frac{1}{4\pi}\frac{\exp\{i\bar{k}|\vec{r}_0 - \vec{r}_0'|\}}{|\vec{r}_0 - \vec{r}_0'|}\delta(X - X'). \tag{2.80}$$

In eq. (2.80), the existence of the delta function $\delta(X - X')$ reflects the fact that the target coordinates have been frozen. Furthermore if the average excitation energy $\bar{\epsilon}$ is chosen to be zero (i.e., if the target states are assumed to be frozen during the collision), then eq. (2.80) can be reduced to

$$G_0^{(+)}(\vec{r}_0, X; \vec{r}_0', X') \simeq G_0^{(+)}(\vec{r}_0, \vec{r}_0')\delta(X - X'), \tag{2.81}$$

where $G_0^{(+)}(\vec{r}_0, \vec{r}_0')$ is simply the free Green's function which can be used to describe a scattering process between the incident particle with the momentum $\vec{k}_0$ and the potential V. When we substitute eq. (2.81) into eq. (2.74), the many-body scattering amplitude is reduced to a potential scattering one averaged by target states, i.e.

$$f_{f0}(\vec{k}_f, \vec{k}_0) = \langle \Psi_f | f(\vec{k}_0, \theta) | \Psi_0 \rangle, \tag{2.82}$$

where $f(\vec{k}_0, \theta)$ is the potential scattering amplitude. In this way, if we treat the scattering by $V(\vec{r}_0, X)$ by using the Glauber approximation, we obtain the many-body Glauber amplitude:

$$f_{f0}^G(\vec{k}_f, \vec{k}_0) = \frac{ik_0}{2\pi} \int d^2\vec{b}_0 dX \exp(i\vec{q}\cdot\vec{b}_0)\Psi_f^*(X)[1 - \exp(\frac{i}{k_0}\chi_0(\vec{b}_0, X))]\Psi_0(X), \tag{2.83}$$

with

$$\chi_0(\vec{b}_0, X) = -\int_{-\infty}^{\infty} V(x_0, y_0, z_0; X) dz_0. \tag{2.84}$$

In the similar way, we can obtain the many-body Wallace amplitude as

$$\begin{aligned} f_{f0}^W(\vec{k}_f, \vec{k}_0) &= \frac{ik_0}{2\pi} \int d^2\vec{b}_0 dX \exp(i\vec{q}\cdot\vec{b}_0)\Psi_f^*(X)\{1 - \exp[i(\frac{1}{k_0}\chi_0(\vec{b}_0, X) \\ &\quad + \frac{1}{k_0^3}\chi_1(\vec{b}_0, X))]\}\Psi_0(X), \end{aligned} \tag{2.85}$$

with

$$\chi_1(\vec{b}_0, X) = \frac{1}{2}\int_{-\infty}^{\infty} (\nabla_0\chi_+)(\nabla_0\chi_-) dz_0, \tag{2.86}$$

$$\chi_+(\vec{b}_0, z_0; X) = -\int_{-\infty}^{z_0} V(x_0, y_0, z_0'; X) dz_0', \tag{2.87}$$

$$\chi_-(\vec{b}_0, z_0; X) = -\int_{z_0}^{\infty} V(x_0, y_0, z_0'; X) dz_0'. \tag{2.88}$$

It should be pointed out that in f_{f0}^G and f_{f0}^W, the frozen target approximation has been used in which not only the target coordinates are fixed but also the average excitation energy $\bar{\epsilon}$ is taken to be zero during a collision. It is therefore expected that both f_{f0}^G and f_{f0}^W will suffer from some deficiencies in general.

2.3.2 The properties of the Glauber many-body amplitude

In order to study high energy behaviors of the Glauber many-body amplitude, it is more instructive to expand the Glauber amplitude into a perturbation series in potential V, namely,

$$f_{f0}^{G} = \sum_{n=1}^{\infty} f_{f0}^{Gn}, \tag{2.89}$$

where

$$f_{f0}^{Gn} = \frac{1}{2\pi}(\frac{i}{k_0})^{n-1}\frac{1}{n!}\int \exp(i\vec{q}\cdot\vec{b_0})\Psi_f^*(X)[\chi_0(\vec{b_0},X)]^n\Psi_0(X)d^2\vec{b_0}dX, \tag{2.90}$$

$$\chi_0(\vec{b_0},X) = -\int_{-\infty}^{\infty} V(x_0,y_0,z_0;X)dz_0. \tag{2.91}$$

The term f^{Gn} is of course nth order in V. The series (2.89) is called the many-body Glauber series. The corresponding Born series is

$$f_{f0} = \sum_{n=1}^{\infty} f_{f0}^{Bn}, \tag{2.92}$$

where

$$f_{f0}^{Bn} = -\frac{1}{2\pi}\langle\vec{k}_f\Psi_f|V(G_0^{(+)}V)^{n-1}|\hat{k}_0\Psi_0\rangle. \tag{2.93}$$

By remembering that the momentum transfer $\vec{q}$ is perpendicular to the z-direction, one has

$$\vec{q}\cdot\vec{b_0} = \vec{q}\cdot\vec{r}_0. \tag{2.94}$$

This results the following identity

$$f_{f0}^{G1} = f_{f0}^{B1} \tag{2.95}$$

at all incident energies and all momentum transfers. Thus for elastic scattering, the first Glauber term contains the first-order treatment of the static potential of the state Ψ_0.

Let us go on to consider the second order Glauber term f_{f0}^{G2} :

$$f_{f0}^{G2} = \frac{i}{4\pi k_0} \int \exp(i\vec{q}\cdot\vec{b_0})\Psi_f^*(X)[\chi_0(\vec{b},X)]^2\Psi_0(X)d^2\vec{b}dX \tag{2.96}$$

It is well-known that the real part of the second Born term contains the dipole polarization effect of the target, that is for s-s transition we have [29]

$$\Re f_{f0}^{B2} \xrightarrow{k_0 \text{ large}, q \text{ small}} \pi \sum_n \frac{1}{k_n}\langle\Psi_f|Z|\Psi_n\rangle\langle\Psi_n|Z|\Psi_0\rangle \times \{1 - \frac{k_n q}{[k_n^2 q^2 + 4(\epsilon_0 - \epsilon_n)(\epsilon_f - \epsilon_n)]^{1/2}}\}, \tag{2.97}$$

where Z denotes the sum of the z-coordinates of the atomic electrons. It is obviously that if we use the frozen target approximation and set $\epsilon_n = \epsilon_0$ for all n, we have

$$\Re f_{f0}^{B2} \xrightarrow{k_0 \text{ large}, q \text{ small}} 0. \tag{2.98}$$

Thus the leading polarization effect is missing from the Glauber amplitude. In fact f_{f0}^{G2} is purely imaginary for s-s scattering. The disappearance of the real part of f_{f0}^{G2} is caused by the adoption of the straight line approximation or the linearization of the Green's function. In fact if some correction is made to the straight line approximation, the real part of the second order term can be reinstated, as in the case of the Wallace approximation. However, it does not mean that the polarization effect is recovered. For example, although the real part of the second Wallace term exists and behaves like k_0^{-2}, it does not have the correct asymptotic form (2.97) which has the k_0^{-1} decay law. Thus the polarization effect is still missing from the Wallace amplitude.

As for the imaginary part of f_{f0}^{G2}, it can be shown that [30] [31]

$$\Im f_{f0}^{G2} \xrightarrow{q\to 0} \ln q \tag{2.99}$$

for $e^{\pm}$-H or $e^{\pm}$-He s-s scattering. On the other hand [31],

$$f_{f0}^{G}(1s-ns) \xrightarrow{q\to 0} \ln q \tag{2.100}$$

$$f_{f0}^{G}(1s-np) \xrightarrow{q\to 0} 1/q \tag{2.101}$$

for $e^{\pm}$-H scattering. These singular behaviors lie outside the physical region for inelastic scattering. For elastic scattering, however, especially for 1s-1s case, the divergence is really disastrous. The direct consequence of this divergence is that the optical theorem

$$\Im f_{00}(\theta=0) = \frac{k_0}{4\pi}\sigma_{tot}, \tag{2.102}$$

which reflects the conservation of the probability of the quantum mechanical process, will no longer exist (here σ_{tot} denotes the total cross section). The breakdown of the unitarity could be traced back to the divergence of the imaginary part of the second Glauber term, see (2.99). Furthermore, the divergence of $\Im f_{00}^{G2}$ comes directly from the adoption of the frozen target approximation. As a matter of fact, it can be shown that [32] [33] [34] if the frozen target approximation is used in the calculation of f_{00}^{B2}, $\Im f_{00}^{B2}$ behaves likes $\ln q$, the same type of divergence as $\Im f_{00}^{G2}$. It is therefore not surprising to find that the divergence in f_{00}^{G} is associated with, and only with, f_{00}^{G2}

In brief, in the Glauber amplitude there are two serious deficiencies, one is the disappearance of the polarization effect, the other is the spurious behavior of the absorption effect. These two deficiencies are rooted in the second Glauber term. It is also worth noticing that the Glauber amplitude gives the same predictions between the electron and the positron differential cross sections.

However, the Glauber amplitude still contains some favourable features. It is conjectured

that for s-s processes,

$$f_{f0}^{Gn} \approx \Re f_{f0}^{Bn}, \text{if } n \text{ is odd}$$

$$\approx i\Im f_{f0}^{Bn}, \text{if } n \text{ is even.} \tag{2.103}$$

In fact these relations were first brought to light in a study of scattering by Yukawa type potential [19] [20] [26] [35] where it was shown that these relations are exact for all q at asymptotically large k_0. Thus the Glauber amplitude seems to give fairly accurate information on half of the Born series.

2.3.3 The properties of the Wallace many-body amplitude

Parallel to the discussion of the many-body Glauber amplitude, let us first expand the Wallace amplitude (2.85) into a perturbation series in potential V:

$$f_{f0}^{W} = \sum_{n=1}^{\infty} f_{f0}^{Wn}, \tag{2.104}$$

where the first Wallace term f_{f0}^{W1} is identical to the first Born term f_{f0}^{B1}, i.e.

$$f_{f0}^{W1} = f_{f0}^{B1}, \tag{2.105}$$

and for $n \geq 2$,

$$f_{f0}^{Wn} = \frac{1}{2\pi}(\frac{i}{k_0})^{n-1}\frac{1}{n!}\int \exp(i\vec{q}\cdot\vec{b_0})\Psi_f^*(X)\{\chi_0^n(\vec{b_0},X) - n(n-1)\frac{i}{k_0}\chi_0^{n-2}(\vec{b_0},X)\chi_1(\vec{b_0},X)$$
$$+ \text{ terms containing higher powers of } \chi_1 \text{ if } n \geq 4\}\Psi_0(X)d^2\vec{b_0}dX. \tag{2.106}$$

From eq. (2.105) one can see that for elastic scattering the first Wallace term contains the first-order treatment of the static potential of the state Ψ_0. For the higher order terms, the existence of the extra phase χ_1 makes them no longer purely real and imaginary. Let us

now consider these higher order terms. For simplicity we assume that both Ψ_0 and Ψ_f are s-states and therefore they are real. It is easy to see that:

$$\Im f_{f0}^{W2} = \Im f_{f0}^{G2} \tag{2.107}$$

$$\Re f_{f0}^{W3} = \Re f_{f0}^{G3}. \tag{2.108}$$

By recalling that f_{f0}^{G2} has the $\ln q$ divergence for small q, the Wallace amplitude f_{f0}^{W} thus has the same kind of divergence which comes from the imaginary part of the second order term. This divergence is diagnosed to be associated with the adoption of the frozen target approximation in which the average excitation energy is set to be zero. Therefore the optical theorem, which is a consequence of the conservation of the probability, will be broken down. As for the real part of the second Wallace term,

$$\Re f_{f0}^{W2} = \frac{1}{2\pi k_0^2} \int \exp(i\vec{q}\cdot\vec{b_0}) \Psi_f^*(X) \chi_1(\vec{b_0}, X) \Psi_0(X) d^2\vec{b_0} dX. \tag{2.109}$$

From eq. (2.109) we can see that the long-range dipole dynamic polarization effects have been omitted by f_{f0}^{W2}; this is because $\Re f_{f0}^{W2}$ varies as k_0^{-2} whereas the correct dipole polarization effects should have the k_0^{-1} decay law as expressed in (2.97). In other words, $\Re f_{f0}^{W2}$ falls off more rapidly with increasing energy, at small q, than it ought to. The lack of the polarization effects in the Wallace amplitude also comes from the adoption of the frozen target approximation with average excitation energy set to be zero. The Wallace amplitude still suffers the same kinds of deficiencies as the Glauber amplitude.

On the other hand, unlike the Glauber amplitude, $\Re f_{f0}^{W2}$ and $\Im f_{f0}^{W3}$ are no longer missing from the amplitude. In fact, Byron *et al.* [36] have studied the large momentum transfer behaviors of the first three Wallace terms. As expected, the terms f_{f0}^{W1}, $\Im f_{f0}^{W2}$ and $\Re f_{f0}^{W3}$

duplicate the large q behaviors of the corresponding Glauber terms. The large q behavior of $\Re f_{fi}^{W2}$ which is missing from the Glauber series agrees precisely with the large q expression for real part of the second Born term calculated in the frozen target approximation with the zero average excitation energy. As for $\Im f_{fi}^{W3}$, which is also missing from the Glauber series, it does not, however, seem to contain exactly the same component as the imaginary part of the third Born term calculated by unitarity-by-order relation. In short, the Wallace terms at most up to the third only do seem to better represent the asymptotic behaviors of the corresponding Born terms than those of the Glauber amplitude.

Going to the higher orders of the Wallace expansion, one can show that the Wallace terms $f_{fi}^{Wn}(n \geq 4)$ are all divergent [36]. This means that the perturbation expansion of the Wallace amplitude does not exist at all; in other words, the attempt to analyse the Wallace amplitude perturbatively would perhaps be meaningless. However, the Wallace amplitude itself converges; this is because the correction term χ_1 appears to be in a phase factor. Finally we want to point out that because of the existence of the extra phase χ_1 in the amplitude which does not change sign when the negative charge is replaced by a positive one, the Wallace amplitude is able to predict the desired difference between positron and electron differential cross sections [37].

The Wallace amplitude was first used to $e^{\pm}$-hydrogen scattering process by Unnikrishnan *et al.* [38] who succeeded in reducing the scattering amplitude to a triple integral form which can be evaluated numerically. Subsequently, Franco *et al.* [37] also independently applied the Wallace amplitude to study $e^{\pm}$-H elastic scattering and with a similar procedure of reduction they also put the scattering amplitude into a triple integral form. In addition Byron *et al.* [36] [39] also performed the calculations in the Wallace approximation for $e^{\pm}$-H

elastic and inelastic scattering. Comparisons with experiments on electron scattering from hydrogen in its ground state have been made which suggest that the Wallace amplitude is an improvement over the Glauber one (see ref. [36] [37] [38] [39] for details).

2.3.4 The other related approximation methods (EBS, MGA and UEBS)

Based on the systematic study made by Byron *et al.*, it is seen that in order to construct in a consistent way a perturbation expansion of scattering amplitude up to k_0^{-2}, it is necessary to include not only f_{f0}^{B1} and f_{f0}^{B2}, but also $\Re f_{f0}^{B3}$. In view of the relationships between the Glauber terms and the Born terms [40], it is probably reasonable to replace $\Re f_{f0}^{B3}$ by f_{f0}^{G3} which is much easier to calculate than $\Re f_{f0}^{B3}$. Byron *et al.* [41] thus have suggested the following practical approximation which is correct to the order of k_0^{-2}:

$$f_{f0}^{EBS} = f_{f0}^{B1} + f_{f0}^{B2} + f_{f0}^{G3}. \tag{2.110}$$

This formula is called the eikonal-Born series (EBS).

On the other hand, it was Gien [42] who considered to improve the conventional Glauber amplitude from another point of view. As Gien proposed, since the Glauber amplitude has many features which are quite attractive for the application to atomic collision, this amplitude could be retained as a good approximation for $e^{\pm}$ scattering off atomic targets at intermediate energies provided that the serious deficiencies of the scattering amplitude due to its eikonalization are corrected properly. The most serious deficiencies of the conventional Glauber amplitude are identified to be with its second order perturbation term. The conventional Glauber amplitude could, therefore, be improved very much by simply correcting its second order term with its counterpart prior to eikonalization, i.e. the second

Born term. The modified Glauber amplitude is then established as (see ref. [43] for detail)

$$f_{f0}^{MG} = f_{f0}^{G} - f_{f0}^{G2} + f_{f0}^{B2}. \tag{2.111}$$

It is clear that the modified Glauber amplitude of electron-atom scattering is no longer divergent in the forward direction and thus the unitarity is recovered. Besides, the polarization effect of the atomic target which is missing from the conventional Glauber amplitude is reinstated. Furthermore the modified Glauber amplitude f_{f0}^{MG} can be recast as

$$f_{f0}^{MG} = f_{f0}^{B1} + f_{f0}^{B2} + f_{f0}^{G3} + \sum_{n\geq 4}^{\infty} f_{f0}^{Gn} \tag{2.112}$$

by bearing in mind that the first Glauber term is identical to the first Born term. Comparing with the second Born approximation and the EBS approximation, one can see that the modified Glauber approximation incorporates the contribution from the higher order perturbation terms which are nothing else but the eikonalized Born terms, i.e. the Glauber terms. The adoption of these terms to approximate the high order Born terms might not be too bad at all since the possible mutual cancellation among these higher order scattering terms of an infinite series may make the value of the sum of these terms become not very far apart from that of the Born terms, as pointed out by Gien (see p145 of ref. [42]). It is well known that the $e^{\pm}$-nucleus interaction could slow the convergence of the perturbation series at large momentum transfer due to the singularity behavior of the Coulomb interaction. Thus the inclusion of the higher order terms in the perturbation series is of critical importance. In this connection, the modified Glauber approximation has taken these terms in an ingenious way.

The third related approximation is the so called unitarized eikonal-Born series (UEBS) one. It is known that the Wallace amplitude is designed to relax the straight-line assump-

tion of the Glauber approximation. However, it still retains the zero excitation energy assumption in its many-body generalization. Thus the Wallace approximation still suffers serious deficiencies which are believed to be associated with the poor behavior of the second Wallace term f_{fi}^{W2}. In order to avoid these deficiencies, while keeping the advantages of f_{fi}^{W}, Byron *et al.* [44] have constructed a modified Wallace amplitude, called the unitarized eikonal-Born series (UEBS), by simply replacing f_{fi}^{W2} by its exact counterpart; i.e. the second Born term, namely:

$$f_{fi}^{UEBS} = f_{fi}^{W} + (f_{fi}^{B2} - f_{fi}^{W2}). \tag{2.113}$$

The adjective 'unitarized' as appeared in eq. (2.113) should be discussed a little bit (see p62 of ref. [34]). We can say that f_{fi}^{W} is unitary in such a sense that since the interaction potential V occurs in a phase, the amplitude can not grow indefinitely in size as the strength of V becomes large. As for the EBS amplitude, since the potential V does not appear in any phase factor, this amplitude is definitely not unitary any more. On the other hand, when the f_{fi}^{B2} and f_{fi}^{W2} are added to the Wallace amplitude f_{fi}^{W}, the unitarity of f_{fi}^{W} is disturbed. The degree to which the unitarity is lost depends on the balance between f_{fi}^{B2} and f_{fi}^{W2}. Since both f_{fi}^{B2} and f_{fi}^{W2} have real and imaginary parts, the f_{fi}^{B2} and f_{fi}^{W2} could be partially balanced and the unitarity in f_{fi}^{W} could not be destroyed very much. Compared to the EBS amplitude which is of no unitarity, the modified Wallace amplitude contains much more unitarity.

Chapter 3

The study of $e^{\pm}$-scattering off the metastable 2s state of hydrogen in the Glauber and Wallace approximations

3.1 The scattering amplitudes in the Glauber approximation

The many-body Glauber amplitude is given by [31]

$$f^G(\vec{k}_f, \vec{k}_0) = \frac{ik_0}{2\pi} \int d^2\vec{b}_0 dX \exp(i\vec{q}\cdot\vec{b}_0)\Psi_f^*(X)[1 - \exp(\frac{i}{k_0}\chi_0(\vec{b}_0, X))]\Psi_0(X), \qquad (3.1)$$

where

$$\chi_0(\vec{b}_0, X) = -\int_{-\infty}^{\infty} V(x_0, y_0, z_0; X) dz_0. \tag{3.2}$$

For electron or positron scattering off hydrogen, the Glauber amplitude can be reduced into a closed form in terms of a generating function [31]. For 1s-ns processes, we have the formula:

$$f^G(1s \to ns; \vec{q}) = 2ik_0 n^{-3/2} \sum_{j=0}^{n-1} \alpha_j(n)(-1)^{j+1} \frac{\partial^{j+1}}{\partial \lambda^{j+1}} I_0(\lambda; q)|_{\lambda=1+1/n}, \tag{3.3}$$

where

$$\alpha_j(n) = \frac{(-n+1)_j}{(2)_j j!} (\frac{2}{n})^j, \tag{3.4}$$

$$(n)_j = \frac{\Gamma(n+j)}{\Gamma(n)}; \tag{3.5}$$

and $I_0(\lambda; q)$ is the generating function defined by

$$I_0(\lambda; q) = -4i\eta\Gamma(1+i\eta)\Gamma(1-i\eta)\lambda^{-2-2i\eta} q^{-2+2i\eta} F(1-i\eta, 1-i\eta; 1; -\frac{\lambda^2}{q^2}). \tag{3.6}$$

In eq. (3.6), the parameter $\eta = -Q/k_0 (Q = \pm$ for positron and electron respectively), the function F is the usual hypergeometric one.

For 1s-np processes, we have

$$\begin{aligned} f^G(1s \to np_\pm; \vec{q}) \;=\; & \exp(\mp i\phi_q) \frac{4}{3} (\frac{3}{2})^{1/2} ik_0 \frac{1}{n^3} [\frac{(n+1)!}{(n-2)!}]^{1/2} \times \\ & \sum_{j=0}^{n-2} \beta_j(n)(-1)^{j+1} \frac{\partial^{j+1}}{\partial \lambda^{j+1}} I_1(\lambda; q)|_{\lambda=1+1/n}, \end{aligned} \tag{3.7}$$

where ϕ_q is the polar angle of $\vec{q}$,

$$\beta_j(n) = \frac{(-n+2)_j}{j!(4)_j} (\frac{2}{n})^j, \tag{3.8}$$

and $I_1(\lambda;q)$ is the another generating function defined by

$$I_1(\lambda;q) = - 4\Gamma(1+i\eta)\Gamma(2-i\eta)\eta\lambda^{-2-2i\eta}q^{-3+2i\eta}[-F(2-i\eta,1-i\eta;1;-\frac{\lambda^2}{q^2}) + (1+i\eta)F(2-i\eta,1-i\eta;2;-\frac{\lambda^2}{q^2})]. \tag{3.9}$$

From eq. (3.3) and eq. (3.7), it is a straightforward matter to obtain the following scattering amplitudes

$$f^G(1s \to 1s;\vec{q}) = -8k_0\eta\frac{\pi\eta}{\sinh\pi\eta}q^{-2+2i\eta}\frac{\partial}{\partial\lambda}\Pi_0(\lambda)|_{\lambda=2}, \tag{3.10}$$

$$f^G(1s \to 2s;\vec{q}) = -2^{3/2}k_0\eta\frac{\pi\eta}{\sinh\pi\eta}q^{-2+2i\eta}(\frac{\partial}{\partial\lambda}+\frac{1}{2}\frac{\partial^2}{\partial\lambda^2})\Pi_0(\lambda)|_{\lambda=3/2}, \tag{3.11}$$

$$f^G(1s \to 2p_\pm;\vec{q}) = \exp(\mp i\phi_q)2ik_0\eta(1-i\eta)\frac{\pi\eta}{\sinh\pi\eta}q^{-3+2i\eta}\frac{\partial}{\partial\lambda}\Pi_1(\lambda)|_{\lambda=3/2}, \tag{3.12}$$

$$f^G(1s \to 3s;\vec{q}) = -\frac{8}{3^{3/2}}k_0\eta\frac{\pi\eta}{\sinh\pi\eta}q^{-2+2i\eta}(\frac{\partial}{\partial\lambda}+\frac{2}{3}\frac{\partial^2}{\partial\lambda^2}+\frac{2}{27}\frac{\partial^3}{\partial\lambda^3})\Pi_0(\lambda)|_{\lambda=4/3}, \tag{3.13}$$

$$f^G(1s \to 3p_\pm;\vec{q}) = \exp(\mp i\phi_q)\frac{32i}{27}k_0\eta(1-i\eta)\frac{\pi\eta}{\sinh\pi\eta}q^{-3+2i\eta}\times (\frac{\partial}{\partial\lambda}+\frac{1}{6}\frac{\partial^2}{\partial\lambda^2})\Pi_1(\lambda)|_{\lambda=4/3}, \tag{3.14}$$

where

$$\Pi_0(\lambda) = \lambda^{-2-2i\eta}F(1-i\eta,1-i\eta;1;-\frac{\lambda^2}{q^2}), \tag{3.15}$$

and

$$\Pi_1(\lambda) = \lambda^{-2-2i\eta}[-F(2-i\eta, 1-i\eta; 1; -\frac{\lambda^2}{q^2}) + (1+i\eta)F(2-i\eta, 1-i\eta; 2; -\frac{\lambda^2}{q^2})]. \quad (3.16)$$

As for transitions from the 2s state of hydrogen, since

$$\Psi_{1s}(r) = \frac{1}{\sqrt{\pi}}\exp(-r), \quad (3.17)$$

$$\Psi_{2s}(r) = \frac{1}{\sqrt{8\pi}}(1-\frac{r}{2})\exp(-r/2), \quad (3.18)$$

we have

$$\Psi_{2s}(r) = [\mathcal{D}(\frac{\partial}{\partial\mu})\Psi_{1s}(\mu r)]|_{\mu=1/2}, \quad (3.19)$$

where the differential operator $\mathcal{D}$ is given by

$$\mathcal{D}(\frac{\partial}{\partial\mu}) = \frac{1}{\sqrt{8}}(1+\frac{1}{2}\frac{\partial}{\partial\mu}); \quad (3.20)$$

therefore the scattering amplitudes for transitions from 2s state can be expressed as

$$f^G(2s \to ns; \vec{q}) = 2ik_0 n^{-3/2}\sum_{j=0}^{n-1}\alpha_j(n)(-1)^{j+1}\mathcal{D}(\frac{\partial}{\partial\lambda})\frac{\partial^{j+1}}{\partial\lambda^{j+1}}I_0(\lambda;q)|_{\lambda=1/2+1/n}, \quad (3.21)$$

and

$$\begin{aligned} f^G(2s \to np_\pm; \vec{q}) &= \exp(\mp i\phi_q)\frac{4}{3}(\frac{3}{2})^{1/2}ik_0\frac{1}{n^3}[\frac{(n+1)!}{(n-2)!}]^{1/2}\times \\ &\sum_{j=0}^{n-2}\mathcal{D}(\frac{\partial}{\partial\lambda})\beta_j(n)(-1)^{j+1}\frac{\partial^{j+1}}{\partial\lambda^{j+1}}I_1(\lambda;q)|_{\lambda=1/2+1/n}. \end{aligned} \quad (3.22)$$

In particular, we have

$$f^G(2s \to 2s; \vec{q}) = -k_0\eta\frac{\pi\eta}{\sinh\pi\eta}q^{-2+2i\eta}(\frac{\partial}{\partial\lambda}+\frac{\partial^2}{\partial\lambda^2}+\frac{1}{4}\frac{\partial^3}{\partial\lambda^3})\Pi_0(\lambda)|_{\lambda=1}, \quad (3.23)$$

$$\begin{aligned} f^G(2s \to 2p_\pm; \vec{q}) &= \exp(\mp i\phi_q)\frac{1}{\sqrt{2}}ik_0\eta(1-i\eta)\frac{\pi\eta}{\sinh\pi\eta}q^{-3+2i\eta}\times \\ &(\frac{\partial}{\partial\lambda}+\frac{1}{2}\frac{\partial^2}{\partial\lambda^2})\Pi_1(\lambda)|_{\lambda=1}, \end{aligned} \quad (3.24)$$

$$f^G(2s \to 3s;\vec{q}) = -\frac{4}{3\sqrt{6}}k_0\eta\frac{\pi\eta}{\sinh\pi\eta}q^{-2+2i\eta}(\frac{\partial}{\partial\lambda}+\frac{7}{6}\frac{\partial^2}{\partial\lambda^2} + \frac{11}{27}\frac{\partial^3}{\partial\lambda^3}+\frac{1}{27}\frac{\partial^4}{\partial\lambda^4})\Pi_0(\lambda)|_{\lambda=5/6}, \tag{3.25}$$

$$f^G(2s \to 3p_\pm;\vec{q}) = \exp(\mp i\phi_q)\frac{8\sqrt{2}}{27}ik_0\eta(1-i\eta)\frac{\pi\eta}{\sinh\pi\eta}q^{-3+2i\eta}\times (\frac{\partial}{\partial\lambda}+\frac{2}{3}\frac{\partial^2}{\partial\lambda^2}+\frac{1}{12}\frac{\partial^3}{\partial\lambda^3})\Pi_1(\lambda)|_{\lambda=5/6}, \tag{3.26}$$

where the functions $\Pi_0(\lambda)$ and $\Pi_1(\lambda)$ are defined by eq. (3.15) and eq. (3.16), and their derivatives are presented in Appendix.

The differential cross sections are given by

$$\frac{d\sigma^G}{d\Omega}(ns \to ms;\vec{q}) = \frac{k_f}{k_0}|f^G(ns \to ms;\vec{q})|^2, \tag{3.27}$$

$$\frac{d\sigma^G}{d\Omega}(ns \to mp;\vec{q}) = 2\frac{k_f}{k_0}|f^G(ns \to mp;\vec{q})|^2, \tag{3.28}$$

where

$$k_f = [k_0^2 - (\frac{1}{n^2}-\frac{1}{m^2})]^{1/2}. \tag{3.29}$$

3.2 The scattering amplitudes in the Wallace approximation

The many-body Wallace amplitude is given by [36]

$$f^W(\vec{k}_f,\vec{k}_0) = \frac{ik_0}{2\pi}\int d^2\vec{b}_0 dX \exp(i\vec{q}\cdot\vec{b}_0)\Psi_f^*(X)\times \{1-\exp[i(\frac{1}{k_0}\chi_0(\vec{b}_0,X)+\frac{1}{k_0^3}\chi_1(\vec{b}_0,X))]\}\Psi_0(X), \tag{3.30}$$

where

$$\chi_0(\vec{b}_0, X) = -\int_{-\infty}^{\infty} V(x_0, y_0, z_0; X) dz_0, \tag{3.31}$$

$$\chi_1(\vec{b}_0, X) = \frac{1}{2}\int_{-\infty}^{\infty} (\nabla_0 \chi_+)(\nabla_0 \chi_-) dz_0, \tag{3.32}$$

$$\chi_+(\vec{b}_0, z_0; X) = -\int_{-\infty}^{z_0} V(x_0, y_0, z_0'; X) dz_0', \tag{3.33}$$

$$\chi_-(\vec{b}_0, z_0; X) = -\int_{z_0}^{\infty} V(x_0, y_0, z_0'; X) dz_0'. \tag{3.34}$$

Since the Glauber amplitude can be put into a closed form for $e^{\pm}$-H scattering, it is advantageous for numerical work to split the Wallace amplitude into two parts:

$$f^W(\vec{k}_f, \vec{k}_0) = f^G(\vec{k}_f, \vec{k}_0) + W(\vec{k}_f, \vec{k}_0), \tag{3.35}$$

where f^G is the Glauber amplitude and $W(\vec{k}_f, \vec{k}_0)$ is defined by

$$\begin{aligned} W(\vec{k}_f, \vec{k}_0) &= \frac{ik_0}{2\pi}\int d^2\vec{b}_0 dX \exp(i\vec{q}\cdot\vec{b}_0)\Psi_f^*(X)\exp(\frac{i}{k_0}\chi_0(\vec{b}_0, X)) \times \\ &\quad [1 - \exp(\frac{i}{k_0^3}\chi_1(\vec{b}_0, X))]\Psi_0(X). \end{aligned} \tag{3.36}$$

The derivations of the Wallace amplitudes for the processes listed in the preceding section are shown in the Appendix. Before writing down these formulas we need to define some quantities.

$$X = X(\alpha, \delta, q) = \alpha(\sqrt{\delta^2 + q^2} - \delta)^{1/2}, \tag{3.37}$$

$$Y = Y(\alpha, \delta, q) = \alpha(\sqrt{\delta^2 + q^2} + \delta)^{1/2}, \tag{3.38}$$

$$C_n^{(0)} = \frac{\partial^n}{\partial \delta^n}[J_0(X)K_0(Y)], \tag{3.39}$$

$$C_n^{(1)} = \frac{\partial^n}{\partial \delta^n}[J_1(X)K_1(Y)], \tag{3.40}$$

$$M = -\frac{i}{k_0^3}(I_1 + \frac{\cos\phi}{a}I_2), \tag{3.41}$$

$$\alpha = \sqrt{2M}. \tag{3.42}$$

In eq. (3.41), I_1 and I_2 are further defined by

$$I_1 = 2gK(\nu), \tag{3.43}$$

$$I_2 = 2g^{-1}E(\nu), \tag{3.44}$$

where

$$\nu = \frac{2}{A+B}\sqrt{AB}, \tag{3.45}$$

$$g = \frac{2}{A+B}, \tag{3.46}$$

$$A = [\gamma^2 + (1+a)^2]^{1/2}, \tag{3.47}$$

$$B = [\gamma^2 + (1-a)^2]^{1/2}; \tag{3.48}$$

and $K(\nu)$ and $E(\nu)$ are the complete elliptic integrals of the first and second kinds:

$$K(\nu) = \int_0^{\pi/2} \frac{dx}{\sqrt{1-\nu^2\sin^2 x}}, \tag{3.49}$$

$$E(\nu) = \int_0^{\pi/2} \sqrt{1-\nu^2\sin^2 x}\,dx. \tag{3.50}$$

In all these expressions, the variables a, γ and ϕ will be considered to be the variables of integrals in the formulas below.

For transitions from the ground state of hydrogen, we have:

$$W(1s \to 1s;\vec{q}) = \frac{4ik_0}{\pi}\int_0^\infty da a^{1+2i\eta}\int_0^\infty d\gamma \int_0^\pi d\phi (P_4 + 2C_5^{(0)})|_{\lambda=2}, \tag{3.51}$$

$$\begin{aligned} W(1s \to 2s;\vec{q}) \;=\; & \frac{ik_0}{\sqrt{2}\pi}\int_0^\infty da a^{1+2i\eta}\int_0^\infty d\gamma \int_0^\pi d\phi \times \\ & (2P_4 - \frac{2}{3}\delta P_5 + 4C_5^{(0)} + \frac{4}{3}\delta C_6^{(0)})|_{\lambda=3/2}, \end{aligned} \tag{3.52}$$

$$W(1s \to 2p_{\pm};\vec{q}) = \exp(\mp i\phi_q)(-\frac{k_0}{2\pi})\int_0^\infty daa^{1+2i\eta}\int_0^\infty d\gamma\int_0^\pi d\phi \times$$
$$(1+a\cos\phi)(E_5 - 2C_6^{(1)})|_{\lambda=3/2}, \tag{3.53}$$

$$W(1s \to 3s;\vec{q}) = \frac{4ik_0}{3\sqrt{3}\pi}\int_0^\infty daa^{1+2i\eta}\int_0^\infty d\gamma\int_0^\pi d\phi(P_4 - \frac{1}{2}\delta P_5 + \frac{1}{24}\delta^2 P_6 + 2C_5^{(0)}$$
$$+\delta C_6^{(0)} + \frac{1}{12}\delta^2 C_7^{(0)})|_{\lambda=4/3}, \tag{3.54}$$

$$W(1s \to 3p_{\pm};\vec{q}) = \exp(\mp i\phi_q)(-\frac{8k_0}{27\pi})\int_0^\infty daa^{1+2i\eta}\int_0^\infty d\gamma\int_0^\pi d\phi(1+a\cos\phi)\times$$
$$(E_5 - \frac{1}{8}\delta E_6 - 2C_6^{(1)} - \frac{1}{4}\delta C_7^{(1)})|_{\lambda=4/3}. \tag{3.55}$$

For transitions from the 2s hydrogen, we have:

$$W(2s \to 2s;\vec{q}) = \frac{ik_0}{8\pi}\int_0^\infty daa^{1+2i\eta}\int_0^\infty d\gamma\int_0^\pi d\phi \times$$
$$(4P_4 - 4\delta P_5 + \delta^2 P_6 + 8C_5^{(0)} + 8\delta C_6^{(0)} + 2\delta^2 C_7^{(0)})|_{\lambda=1}, \tag{3.56}$$

$$W(2s \to 2p_{\pm};\vec{q}) = \exp(\mp i\phi_q)(-\frac{k_0}{4\sqrt{2}\pi})\int_0^\infty daa^{1+2i\eta}\int_0^\infty d\gamma\int_0^\pi d\phi(1+a\cos\phi)\times$$
$$(E_5 - \frac{1}{2}\delta E_6 - 2C_6^{(1)} - \delta C_7^{(1)})|_{\lambda=1}, \tag{3.57}$$

$$W(2s \to 3s;\vec{q}) = \frac{2ik_0}{3\sqrt{6}\pi}\int_0^\infty daa^{1+2i\eta}\int_0^\infty d\gamma\int_0^\pi d\phi(P_4 - \frac{7}{5}\delta P_5 + \frac{44}{75}\delta^2 P_6$$
$$- \frac{8}{125}\delta^3 P_7 + 2C_5^{(0)} + \frac{14}{5}\delta C_6^{(0)} + \frac{88}{75}\delta^2 C_7^{(0)} + \frac{16}{125}\delta^3 C_8^{(0)})|_{\lambda=5/6} \tag{3.58}$$

$$W(2s \to 3p_{\pm};\vec{q}) = \exp(\mp i\phi_q)(-\frac{4k_0}{27\sqrt{2\pi}})\int_0^\infty daa^{1+2i\eta}\int_0^\infty d\gamma\int_0^\pi d\phi(1+a\cos\phi)\times$$
$$(E_5 - \frac{4}{5}\delta E_6 + \frac{3}{25}\delta^2 E_7 - 2C_6^{(1)} - \frac{8}{5}\delta C_7^{(1)} - \frac{6}{25}\delta^2 C_8^{(1)})|_{\lambda=5/6}. \quad (3.59)$$

From eq. (3.52) to eq. (3.59), the quantities δ, P_i and E_i are defined as follows:

$$\delta = \lambda(1+a^2+\gamma^2+2a\cos\phi)^{1/2}, \quad (3.60)$$

$$P_4 = \frac{24}{(q^2+\delta^2)^{5/2}}[1-5(\frac{q^2}{q^2+\delta^2})+\frac{35}{8}(\frac{q^2}{q^2+\delta^2})^2], \quad (3.61)$$

$$P_5 = \frac{120\delta}{(q^2+\delta^2)^{7/2}}[1-7(\frac{q^2}{q^2+\delta^2})+\frac{63}{8}(\frac{q^2}{q^2+\delta^2})^2], \quad (3.62)$$

$$P_6 = \frac{720}{(q^2+\delta^2)^{7/2}}[1-\frac{21}{2}(\frac{q^2}{q^2+\delta^2})+\frac{189}{8}(\frac{q^2}{q^2+\delta^2})^2-\frac{231}{16}(\frac{q^2}{q^2+\delta^2})^3], \quad (3.63)$$

$$P_7 = \frac{5040\delta}{(q^2+\delta^2)^{9/2}}[1-\frac{27}{2}(\frac{q^2}{q^2+\delta^2})+\frac{297}{8}(\frac{q^2}{q^2+\delta^2})^2-\frac{429}{16}(\frac{q^2}{q^2+\delta^2})^3], \quad (3.64)$$

$$E_5 = \frac{360q}{(q^2+\delta^2)^{7/2}}[1-\frac{7}{2}(\frac{q^2}{q^2+\delta^2})+\frac{21}{8}(\frac{q^2}{q^2+\delta^2})^2], \quad (3.65)$$

$$E_6 = \frac{2520q\delta}{(q^2+\delta^2)^{9/2}}[1-\frac{9}{2}(\frac{q^2}{q^2+\delta^2})+\frac{33}{8}(\frac{q^2}{q^2+\delta^2})^2], \quad (3.66)$$

$$E_7 = \frac{20160q}{(q^2+\delta^2)^{9/2}}[1-\frac{27}{4}(\frac{q^2}{q^2+\delta^2})+\frac{99}{8}(\frac{q^2}{q^2+\delta^2})^2-\frac{429}{64}(\frac{q^2}{q^2+\delta^2})^3]. \quad (3.67)$$

The differential cross sections are given by

$$\frac{d\sigma^W}{d\Omega}(ns \to ms;\vec{q}) = \frac{k_f}{k_0}|f^G(ns \to ms;\vec{q}) + W(ns \to ms;\vec{q})|^2, \quad (3.68)$$

and

$$\frac{d\sigma^W}{d\Omega}(ns \to mp;\vec{q}) = 2\frac{k_f}{k_0}|f^G(ns \to mp;\vec{q}) + W(ns \to mp;\vec{q})|^2. \quad (3.69)$$

3.3 The numerical results and discussion

Numerical calculations for the differential cross sections in the Wallace approximation are carried out by using the three-dimensional integral expressions for the Wallace correction

terms in which the functions $C_n^{(0)}$ and $C_n^{(1)}$ are obtained analytically. The computer programs for these expressions are checked numerically by resorting to the corresponding four-dimensional integral expressions. The Gaussian Legendre and Chebyshev quadratures are adopted in the numerical evaluations. The convergence of numerical integrals is tested properly by increasing the number of quadrature points stepwise. The scattering processes investigated are listed below:

$$e^{\pm} + \mathrm{H(1s)} \longrightarrow e^{\pm} + \mathrm{H(1s)}, \tag{3.70}$$

$$e^{\pm} + \mathrm{H(1s)} \longrightarrow e^{\pm} + \mathrm{H(2s)}, \tag{3.71}$$

$$e^{\pm} + \mathrm{H(1s)} \longrightarrow e^{\pm} + \mathrm{H(2p)}, \tag{3.72}$$

$$e^{\pm} + \mathrm{H(1s)} \longrightarrow e^{\pm} + \mathrm{H(3s)}, \tag{3.73}$$

$$e^{\pm} + \mathrm{H(1s)} \longrightarrow e^{\pm} + \mathrm{H(3p)}, \tag{3.74}$$

and

$$e^{\pm} + \mathrm{H(2s)} \longrightarrow e^{\pm} + \mathrm{H(2s)}, \tag{3.75}$$

$$e^{\pm} + \mathrm{H(2s)} \longrightarrow e^{\pm} + \mathrm{H(2p)}, \tag{3.76}$$

$$e^{\pm} + \mathrm{H(2s)} \longrightarrow e^{\pm} + \mathrm{H(3s)}, \tag{3.77}$$

$$e^{\pm} + \mathrm{H(2s)} \longrightarrow e^{\pm} + \mathrm{H(3p)}. \tag{3.78}$$

The incident energies of projectiles(electron and positron) are 50 eV, 100 eV, 200 eV, 300 eV, and 400 eV. Our results for the differential cross sections in the Wallace and Glauber approximations for both electron and positron scattering are summarized from tables 3.1 to 3.27.

From figures 3.1 to 3.8, we show our Wallace and Glauber electron and positron 2s-2s, 2s-2p, 2s-3s and 2s-3p results at 50 eV, 200 eV and 400 eV. Through comparison some general features can been seen. At small angles, for both electron and positron impacts, the Glauber results are in close accord with the Wallace ones. For s-s processes, the difference(on log scale) between the Glauber and Wallace approximations becomes small at large angles as the incident energy increases. For s-p transitions, however, the situation is completely different. The difference between the Glauber and Wallace results is very striking and becomes larger in the large angular region. Furthermore, this difference seems to be enhanced at higher energies. This means that the effect due to the straight line approximation which is inherent in the Glauber approximation is quite significant in the large momentum transfer region for s-p excitations. Therefore, inelastic scattering processes involving states which are not spherically symmetric are much more complicated than those with only symmetric states. Similar behaviors can also be observed for electron and positron scattering off 1s state of hydrogen, see figures 3.9-3.12.

In figures 3.13-3.24, we show the Wallace electron and positron scattering results, together with the Glauber approximation which makes no difference for cross sections between electron and positron impacts, at 50 eV, 200 eV and 400 eV respectively. It is seen that for s-s processes the difference among the Wallace electron, Wallace positron and Glauber results, which is pronounced at lower energies, tends to be smaller throughout the entire angular region at higher energies. In other words, the Wallace correction terms are not essential, under these circumstances. Now let us consider s-p excitations. The Wallace electron, Wallace positron and Glauber results are very close to each other at small angles; this may be explained by the fact that for a transition which changes target parity, there is a

pole at $q = 0$ in the first Born term (see for example p7 of ref. [34]), and the exact scattering amplitude also has a pole at $q = 0$ which is identical with that in the first Born term. Thus for scattering at small q, the pole term dominates the scattering amplitude, masking the difference among the Wallace electron, Wallace positron and Glauber scattering amplitudes. At lower energies, as angle increases, the Wallace electron and positron results first depart and then begin to converge with each other in the intermediate and large angular regions where the interaction between the projectile and the target nucleus dominates the scattering dynamics, thus making the sign of the projectile less important. As energy increases, this phenomenon becomes less pronounced and the difference between the Wallace electron and positron results is almost negligibly small at 400 eV in the whole angular region as seen in s-s cases; this can be understood by noting that the sign of projectile charge is contained only in the parameter $\eta = -Q/k_0$ which goes to zero as k_0 goes to be infinity, thus making the Wallace electron and positron scattering amplitudes identical at any scattering angle. In addition, in contrast with the s-s processes mentioned above, the Glauber amplitude, however, departs monotonically from the Wallace ones and never returns back.

Let us discuss some relative behaviors of scattering from both 1s ground state and 2s metastable state of hydrogen, in the Wallace approximation. The results are shown in figures 3.25 to 3.36. The energies we used are also 50 eV, 200 eV and 400 eV. For s-s processes, the differential cross sections for the scattering from the 2s state are much larger than those from the corresponding 1s state(except for 1s-1s process), in both electron and positron impacts. In addition, the difference between the electron and positron inelastic scattering from the 1s state is much more striking than those from the 2s state at 50 eV; and as energy increases this phenomenon soon becomes less noticeable and at 400 eV the curves for electron and

positron scattering coincide with each other. In figures 3.25-3.27, we also show the results for 1s-1s electron and positron scattering. The differences between 1s-1s and 2s-2s results are larger at small angles than those at large angles. As the energy increases, both 1s-1s and 2s-2s results for electron and positron scattering approach each other at intermediate and large angles. This is because for elastic scattering, at large momentum transfer, the scattering dynamics is dominated by the interaction between projectile and nucleus, that is, the static potential. In the case of transitions to the 2p state the differential cross sections for 2s-2p are also rather larger than those for 1s-2p in the small and large angular regions. The difference between the electron and positron scattering from the 1s state is also more striking than those from the 2s state even at 400 eV. As for the transitions to the 3p state, at very small angles, the curves for 2s-3p stay higher in comparison with curves for 1s-3p. On the other hand, at large angles all these curves tend to converge with one another as energy becomes higher.

θ(deg)	50 eV	100 eV	200 eV	300 eV	400 eV
1	1.43 + 03	7.00 + 02	3.81 + 02	2.91 + 02	2.50 + 02
5	2.84 + 02	1.56 + 02	9.28 + 01	6.57 + 01	4.88 + 01
10	7.90 + 01	3.99 + 01	1.62 + 01	8.15 + 00	4.72 + 00
15	2.58 + 01	1.11 + 01	3.51 + 00	1.61 + 00	9.05 − 01
20	1.01 + 01	3.94 + 00	1.13 + 00	5.09 − 01	2.89 − 01
30	2.65 + 00	8.62 − 01	2.28 − 01	1.04 − 01	5.96 − 02
40	9.70 − 01	2.79 − 01	7.43 − 02	3.43 − 02	1.97 − 02
60	2.01 − 01	5.75 − 02	1.61 − 02	7.49 − 03	4.32 − 03
80	6.68 − 02	2.02 − 02	5.82 − 03	2.73 − 03	1.58 − 03
100	3.11 − 02	9.77 − 03	2.86 − 03	1.34 − 03	7.78 − 04
120	1.83 − 02	5.87 − 03	1.73 − 03	8.18 − 04	4.74 − 04
140	1.29 − 02	4.19 − 03	1.24 − 03	5.88 − 04	3.41 − 04
160	1.06 − 02	3.45 − 03	1.03 − 03	4.86 − 04	2.82 − 04
180	9.96 − 03	3.24 − 03	9.64 − 04	4.57 − 04	2.65 − 04

Table 3.1: Differential cross sections in atomic units for electron-hydrogen 2s-2s process in the Wallace approximation. Three significant figures are given. Powers of ten are located after third significant figure.

θ(deg)	50 eV	100 eV	200 eV	300 eV	400 eV
1	1.37 + 03	6.65 + 02	3.62 + 02	2.78 + 02	2.40 + 02
5	2.43 + 02	1.35 + 02	8.47 + 01	6.18 + 01	4.67 + 01
10	6.05 + 01	3.37 + 01	1.50 + 01	7.79 + 00	4.58 + 00
15	1.86 + 01	9.43 + 00	3.28 + 00	1.54 + 00	8.79 − 01
20	6.94 + 00	3.34 + 00	1.06 + 00	4.88 − 01	2.80 − 01
30	1.74 + 00	7.37 − 01	2.14 − 01	9.94 − 02	5.76 − 02
40	6.48 − 01	2.42 − 01	6.95 − 02	3.27 − 02	1.90 − 02
60	1.45 − 01	5.06 − 02	1.50 − 02	7.14 − 03	4.16 − 03
80	5.02 − 02	1.78 − 02	5.42 − 03	2.60 − 03	1.52 − 03
100	2.39 − 02	8.60 − 03	2.66 − 03	1.28 − 03	7.49 − 04
120	1.43 − 02	5.17 − 03	1.61 − 03	7.78 − 04	4.57 − 04
140	1.02 − 02	3.69 − 03	1.16 − 03	5.59 − 04	3.28 − 04
160	8.39 − 03	3.04 − 03	9.55 − 04	4.62 − 04	2.72 − 04
180	7.89 − 03	2.86 − 03	8.97 − 04	4.35 − 04	2.55 − 04

Table 3.2: Differential cross sections in atomic units for positron-hydrogen 2s-2s process in the Wallace approximation.

θ(deg)	50 eV	100 eV	200 eV	300 eV	400 eV
1	3.12 + 04	1.54 + 04	7.56 + 03	4.94 + 03	3.62 + 03
5	7.61 + 02	3.00 + 02	9.09 + 01	3.67 + 01	1.67 + 01
10	5.53 + 01	1.10 + 01	9.97 − 01	2.06 − 01	8.89 − 02
15	4.21 + 00	6.08 − 01	1.30 − 01	4.49 − 02	1.78 − 02
20	7.47 − 01	2.38 − 01	3.87 − 02	9.53 − 03	3.20 − 03
30	2.21 − 01	4.01 − 02	4.50 − 03	1.16 − 03	4.43 − 04
40	5.95 − 02	1.19 − 02	1.62 − 03	4.73 − 04	1.97 − 04
60	2.56 − 02	4.73 − 03	6.60 − 04	2.00 − 04	8.54 − 05
80	1.76 − 02	2.84 − 03	3.92 − 04	1.20 − 04	5.13 − 05
100	1.26 − 02	1.97 − 03	2.74 − 04	8.39 − 05	3.60 − 05
120	9.66 − 03	1.52 − 03	2.13 − 04	6.54 − 05	2.81 − 05
140	8.01 − 03	1.28 − 03	1.80 − 04	5.54 − 05	2.38 − 05
160	7.16 − 03	1.15 − 03	1.63 − 04	5.04 − 05	2.17 − 05
180	6.90 − 03	1.11 − 03	1.58 − 04	4.88 − 05	2.10 − 05

Table 3.3: Differential cross sections in atomic units for electron-hydrogen 2s-2p process in the Wallace approximation.

θ(deg)	50 eV	100 eV	200 eV	300 eV	400 eV
1	3.13 + 04	1.55 + 04	7.58 + 03	4.95 + 03	3.63 + 03
5	8.07 + 02	3.22 + 02	9.91 + 01	4.04 + 01	1.86 + 01
10	7.43 + 01	1.65 + 01	1.76 + 00	3.54 − 01	1.20 − 01
15	9.96 + 00	1.56 + 00	1.90 − 01	4.98 − 02	1.70 − 02
20	2.53 + 00	4.85 − 01	5.20 − 02	1.03 − 02	2.97 − 03
30	7.22 − 01	9.45 − 02	6.51 − 03	1.31 − 03	4.50 − 04
40	2.67 − 01	2.70 − 02	2.11 − 03	5.25 − 04	2.08 − 04
60	6.17 − 02	6.75 − 03	7.37 − 04	2.13 − 04	8.91 − 05
80	2.59 − 02	3.34 − 03	4.16 − 04	1.24 − 04	5.27 − 05
100	1.50 − 02	2.16 − 03	2.84 − 04	8.60 − 05	3.67 − 05
120	1.04 − 02	1.60 − 03	2.18 − 04	6.66 − 05	2.85 − 05
140	8.22 − 03	1.32 − 03	1.83 − 04	5.62 − 05	2.41 − 05
160	7.17 − 03	1.18 − 03	1.66 − 04	5.10 − 05	2.19 − 05
180	6.86 − 03	1.14 − 03	1.61 − 04	4.94 − 05	2.12 − 05

Table 3.4: Differential cross sections in atomic units for positron-hydrogen 2s-2p process in the Wallace approximation.

θ(deg)	50 eV	100 eV	200 eV	300 eV	400 eV
0	3.77 + 02	3.35 + 02	2.71 + 02	2.36 + 02	2.14 + 02
5	3.78 + 01	2.16 + 01	8.47 + 00	3.39 + 00	1.42 + 00
10	2.60 + 00	1.06 + 00	4.00 − 01	1.64 − 01	6.88 − 02
15	1.07 + 00	5.74 − 01	9.27 − 02	2.17 − 02	7.76 − 03
20	9.00 − 01	2.04 − 01	2.03 − 02	5.35 − 03	2.32 − 03
30	2.27 − 01	2.94 − 02	3.69 − 03	1.23 − 03	5.69 − 04
40	6.86 − 02	8.95 − 03	1.35 − 03	4.50 − 04	2.02 − 04
60	1.30 − 02	2.03 − 03	3.21 − 04	1.04 − 04	4.56 − 05
80	4.29 − 03	7.48 − 04	1.18 − 04	3.80 − 05	1.67 − 05
100	2.00 − 03	3.67 − 04	5.82 − 05	1.87 − 05	8.20 − 06
120	1.19 − 03	2.22 − 04	3.53 − 05	1.14 − 05	4.99 − 06
140	8.39 − 04	1.59 − 04	2.53 − 05	8.15 − 06	3.58 − 06
160	6.89 − 04	1.31 − 04	2.09 − 05	6.73 − 06	2.96 − 06
180	6.46 − 04	1.23 − 04	1.96 − 05	6.32 − 06	2.78 − 06

Table 3.5: Differential cross sections in atomic units for electron-hydrogen 2s-3s process in the Wallace approximation.

θ(deg)	50 eV	100 eV	200 eV	300 eV	400 eV
0	3.65 + 02	3.27 + 02	2.66 + 02	2.33 + 02	2.11 + 02
5	3.41 + 01	2.07 + 01	8.53 + 00	3.49 + 00	1.47 + 00
10	2.46 + 00	1.01 + 00	3.74 − 01	1.59 − 01	6.84 − 02
15	6.18 − 01	4.89 − 01	9.21 − 02	2.22 − 02	7.96 − 03
20	5.90 − 01	1.91 − 01	2.08 − 02	5.44 − 03	2.33 − 03
30	1.79 − 01	2.91 − 02	3.64 − 03	1.21 − 03	5.59 − 04
40	5.64 − 02	8.72 − 03	1.30 − 03	4.39 − 04	1.99 − 04
60	1.18 − 02	1.94 − 03	3.11 − 04	1.02 − 04	4.54 − 05
80	4.15 − 03	7.16 − 04	1.16 − 04	3.78 − 05	1.67 − 05
100	2.00 − 03	3.54 − 04	5.75 − 05	1.87 − 05	8.28 − 06
120	1.20 − 03	2.16 − 04	3.51 − 05	1.14 − 05	5.05 − 06
140	8.62 − 04	1.55 − 04	2.53 − 05	8.23 − 06	3.64 − 06
160	7.13 − 04	1.29 − 04	2.09 − 05	6.81 − 06	3.01 − 06
180	6.70 − 04	1.21 − 04	1.96 − 05	6.40 − 06	2.83 − 06

Table 3.6: Differential cross sections in atomic units for positron-hydrogen 2s-3s process in the Wallace approximation.

θ(deg)	50 eV	100 eV	200 eV	300 eV	400 eV
0	8.33 + 03	1.80 + 04	3.73 + 04	5.64 + 04	7.55 + 04
5	8.99 + 01	1.83 + 01	9.08 − 01	9.95 − 01	1.29 + 00
10	2.07 + 00	2.17 + 00	4.95 − 01	7.89 − 02	1.13 − 02
15	2.21 + 00	3.44 − 01	1.06 − 02	2.34 − 03	1.03 − 03
20	4.73 − 01	3.40 − 02	3.38 − 03	6.59 − 04	1.61 − 04
30	5.95 − 02	8.15 − 03	4.09 − 04	6.19 − 05	1.89 − 05
40	2.73 − 02	2.15 − 03	1.20 − 04	2.74 − 05	1.08 − 05
60	6.07 − 03	4.79 − 04	4.53 − 05	1.28 − 05	5.36 − 06
80	2.56 − 03	2.42 − 04	2.70 − 05	7.85 − 06	3.29 − 06
100	1.50 − 03	1.60 − 04	1.89 − 05	5.54 − 06	2.32 − 06
120	1.05 − 03	1.21 − 04	1.47 − 05	4.33 − 06	1.82 − 06
140	8.37 − 04	1.01 − 04	1.24 − 05	3.67 − 06	1.54 − 06
160	7.33 − 04	9.08 − 05	1.13 − 05	3.33 − 06	1.40 − 06
180	7.02 − 04	8.78 − 05	1.09 − 05	3.23 − 06	1.36 − 06

Table 3.7: Differential cross sections in atomic units for electron-hydrogen 2s-3p process in the Wallace approximation.

θ(deg)	50 eV	100 eV	200 eV	300 eV	400 eV
0	8.37 + 03	1.81 + 04	3.73 + 04	5.64 + 04	7.55 + 04
5	1.05 + 02	2.28 + 01	1.27 + 00	8.80 − 01	1.17 + 00
10	2.51 + 00	2.09 + 00	5.05 − 01	7.93 − 02	9.61 − 03
15	2.70 + 00	4.61 − 01	6.88 − 03	4.71 − 04	6.33 − 04
20	9.55 − 01	3.98 − 02	2.99 − 04	2.72 − 04	1.40 − 04
30	8.04 − 02	7.73 − 04	6.27 − 05	4.53 − 05	2.35 − 05
40	1.75 − 02	1.99 − 04	6.80 − 05	2.76 − 05	1.25 − 05
60	3.82 − 03	2.68 − 04	4.28 − 05	1.34 − 05	5.67 − 06
80	2.01 − 03	2.01 − 04	2.69 − 05	8.05 − 06	3.39 − 06
100	1.36 − 03	1.49 − 04	1.90 − 05	5.63 − 06	2.37 − 06
120	1.04 − 03	1.18 − 04	1.48 − 05	4.39 − 06	1.84 − 06
140	8.58 − 04	1.00 − 04	1.26 − 05	3.71 − 06	1.56 − 06
160	7.68 − 04	9.09 − 05	1.14 − 05	3.37 − 06	1.42 − 06
180	7.40 − 04	8.80 − 05	1.10 − 05	3.27 − 06	1.37 − 06

Table 3.8: Differential cross sections in atomic units for positron-hydrogen 2s-3p process in the Wallace approximation.

θ(deg)	50 eV	100 eV	200 eV	300 eV	400 eV
0	1.71 + 00	2.01 + 00	1.90 + 00	1.77 + 00	1.67 + 00
5	1.25 + 00	1.09 + 00	7.84 − 01	6.39 − 01	5.43 − 01
10	6.76 − 01	4.80 − 01	2.79 − 01	1.76 − 01	1.15 − 01
15	3.38 − 01	1.99 − 01	7.98 − 02	3.62 − 02	1.82 − 02
20	1.62 − 01	7.59 − 02	2.13 − 02	7.82 − 03	3.51 − 03
30	3.48 − 02	1.24 − 02	3.07 − 03	1.18 − 03	5.69 − 04
40	1.12 − 02	4.76 − 03	1.22 − 03	4.49 − 04	2.08 − 04
60	6.08 − 03	1.86 − 03	3.40 − 04	1.11 − 04	4.82 − 05
80	3.63 − 03	8.18 − 04	1.29 − 04	4.05 − 05	1.74 − 05
100	2.14 − 03	4.23 − 04	6.35 − 05	1.97 − 05	8.48 − 06
120	1.39 − 03	2.59 − 04	3.83 − 05	1.19 − 05	5.12 − 06
140	1.02 − 03	1.85 − 04	2.72 − 05	8.47 − 06	3.66 − 06
160	8.50 − 04	1.52 − 04	2.24 − 05	6.97 − 06	3.01 − 06
180	8.00 − 04	1.43 − 04	2.10 − 05	6.54 − 06	2.83 − 06

Table 3.9: Differential cross sections in atomic units for electron-hydrogen 1s-2s process in the Wallace approximation.

θ(deg)	50 eV	100 eV	200 eV	300 eV	400 eV
0	1.42 + 00	1.80 + 00	1.78 + 00	1.68 + 00	1.61 + 00
5	9.95 − 01	9.21 − 01	7.02 − 01	5.91 − 01	5.13 − 01
10	4.94 − 01	3.92 − 01	2.55 − 01	1.69 − 01	1.13 − 01
15	2.31 − 01	1.67 − 01	7.79 − 02	3.74 − 02	1.92 − 02
20	1.07 − 01	6.78 − 02	2.25 − 02	8.61 − 03	3.89 − 03
30	2.24 − 02	1.17 − 02	3.08 − 03	1.18 − 03	5.65 − 04
40	4.81 − 03	3.29 − 03	1.03 − 03	4.07 − 04	1.95 − 04
60	1.06 − 03	9.92 − 04	2.75 − 04	9.95 − 05	4.54 − 05
80	8.04 − 04	4.57 − 04	1.08 − 04	3.73 − 05	1.68 − 05
100	6.02 − 04	2.51 − 04	5.43 − 05	1.85 − 05	8.28 − 06
120	4.63 − 04	1.62 − 04	3.34 − 05	1.13 − 05	5.05 − 06
140	3.80 − 04	1.20 − 04	2.41 − 05	8.15 − 06	3.63 − 06
160	3.37 − 04	1.01 − 04	2.00 − 05	6.75 − 06	3.01 − 06
180	3.24 − 04	9.51 − 05	1.88 − 05	6.34 − 06	2.83 − 06

Table 3.10: Differential cross sections in atomic units for positron-hydrogen 1s-2s process in the Wallace approximation.

θ(deg)	50 eV	100 eV	200 eV	300 eV	400 eV
0	3.62 + 01	9.50 + 01	2.12 + 02	3.29 + 02	4.45 + 02
5	2.02 + 01	2.13 + 01	1.24 + 01	7.64 + 00	5.13 + 00
10	6.88 + 00	3.92 + 00	1.34 + 00	5.75 − 01	2.83 − 01
15	2.22 + 00	8.27 − 01	1.69 − 01	4.95 − 02	1.79 − 02
20	7.06 − 01	1.76 − 01	2.18 − 02	4.72 − 03	1.44 − 03
30	6.09 − 02	7.18 − 03	7.35 − 04	2.39 − 04	1.11 − 04
40	3.20 − 03	9.00 − 04	2.92 − 04	1.13 − 04	5.32 − 05
60	1.58 − 03	7.39 − 04	1.56 − 04	5.32 − 05	2.39 − 05
80	2.07 − 03	5.73 − 04	1.01 − 04	3.32 − 05	1.47 − 05
100	1.96 − 03	4.51 − 04	7.40 − 05	2.38 − 05	1.05 − 05
120	1.77 − 03	3.72 − 04	5.90 − 05	1.89 − 05	8.26 − 06
140	1.61 − 03	3.23 − 04	5.05 − 05	1.61 − 05	7.04 − 06
160	1.51 − 03	2.98 − 04	4.62 − 05	1.47 − 05	6.42 − 06
180	1.48 − 03	2.89 − 04	4.48 − 05	1.43 − 05	6.23 − 06

Table 3.11: Differential cross sections in atomic units for electron-hydrogen 1s-2p process in the Wallace approximation.

θ(deg)	50 eV	100 eV	200 eV	300 eV	400 eV
0	3.77 + 01	9.61 + 01	2.13 + 02	3.29 + 02	4.45 + 02
5	2.16 + 01	2.22 + 01	1.28 + 01	7.94 + 00	5.34 + 00
10	7.99 + 00	4.53 + 00	1.57 + 00	6.86 − 01	3.42 − 01
15	3.00 + 00	1.17 + 00	2.58 − 01	8.08 − 02	3.12 − 02
20	1.21 + 00	3.46 − 01	5.32 − 02	1.36 − 02	4.71 − 03
30	2.46 − 01	4.84 − 02	5.64 − 03	1.37 − 03	4.84 − 04
40	7.21 − 02	1.32 − 02	1.53 − 03	3.82 − 04	1.40 − 04
60	1.63 − 02	3.00 − 03	3.58 − 04	9.59 − 05	3.76 − 05
80	6.98 − 03	1.28 − 03	1.63 − 04	4.64 − 05	1.90 − 05
100	3.96 − 03	7.46 − 04	1.00 − 04	2.96 − 05	1.24 − 05
120	2.67 − 03	5.21 − 04	7.32 − 05	2.20 − 05	9.33 − 06
140	2.06 − 03	4.14 − 04	5.98 − 05	1.82 − 05	7.77 − 06
160	1.77 − 03	3.64 − 04	5.33 − 05	1.64 − 05	7.00 − 06
180	1.69 − 03	3.49 − 04	5.14 − 05	1.58 − 05	6.77 − 06

Table 3.12: Differential cross sections in atomic units for positron-hydrogen 1s-2p process in the Wallace approximation.

θ(deg)	50 eV	100 eV	200 eV	300 eV	400 eV
0	2.41 – 01	2.83 – 01	2.65 – 01	2.46 – 01	2.31 – 01
5	1.93 – 01	1.78 – 01	1.33 – 01	1.11 – 01	9.84 – 02
10	1.20 – 01	9.22 – 02	5.92 – 02	4.07 – 02	2.83 – 02
15	6.84 – 02	4.46 – 02	2.04 – 02	9.90 – 03	5.12 – 03
20	3.67 – 02	1.93 – 02	5.92 – 03	2.19 – 03	9.69 – 04
30	9.25 – 03	3.32 – 03	7.71 – 04	2.88 – 04	1.37 – 04
40	2.72 – 03	1.11 – 03	2.88 – 04	1.07 – 04	4.95 – 05
60	1.33 – 03	4.38 – 04	8.15 – 05	2.64 – 05	1.15 – 05
80	8.59 – 04	1.98 – 04	3.11 – 05	9.67 – 06	4.15 – 06
100	5.27 – 04	1.03 – 04	1.53 – 05	4.71 – 06	2.02 – 06
120	3.48 – 04	6.34 – 05	9.20 – 06	2.83 – 06	1.22 – 06
140	2.58 – 04	4.54 – 05	6.55 – 06	2.02 – 06	8.68 – 07
160	2.15 – 04	3.73 – 05	5.38 – 06	1.66 – 06	7.15 – 07
180	2.03 – 04	3.50 – 05	5.05 – 06	1.56 – 06	6.71 – 07

Table 3.13: Differential cross sections in atomic units for electron-hydrogen 1s-3s process in the Wallace approximation.

θ(deg)	50 eV	100 eV	200 eV	300 eV	400 eV
0	1.93 – 01	2.49 – 01	2.46 – 01	2.32 – 01	2.21 – 01
5	1.49 – 01	1.49 – 01	1.17 – 01	1.02 – 01	9.19 – 02
10	8.60 – 02	7.35 – 02	5.30 – 02	3.84 – 02	2.76 – 02
15	4.53 – 02	3.60 – 02	1.95 – 02	1.01 – 02	5.37 – 03
20	2.32 – 02	1.66 – 02	6.17 – 03	2.41 – 03	1.08 – 03
30	5.80 – 03	3.21 – 03	8.08 – 04	2.96 – 04	1.39 – 04
40	1.36 – 03	8.36 – 04	2.49 – 04	9.76 – 05	4.66 – 05
60	1.96 – 04	2.28 – 04	6.51 – 05	2.36 – 05	1.08 – 05
80	1.52 – 04	1.06 – 04	2.56 – 05	8.87 – 06	3.98 – 06
100	1.24 – 04	5.88 – 05	1.29 – 05	4.41 – 06	1.97 – 06
120	9.95 – 05	3.80 – 05	7.96 – 06	2.69 – 06	1.20 – 06
140	8.38 – 05	2.83 – 05	5.75 – 06	1.94 – 06	8.62 – 07
160	7.54 – 05	2.38 – 05	4.76 – 06	1.60 – 06	7.13 – 07
180	7.27 – 05	2.25 – 05	4.48 – 06	1.51 – 06	6.70 – 07

Table 3.14: Differential cross sections in atomic units for positron-hydrogen 1s-3s process in the Wallace approximation.

θ(deg)	50 eV	100 eV	200 eV	300 eV	400 eV
0	4.13 + 00	1.09 + 01	2.43 + 01	3.76 + 01	5.09 + 01
5	2.75 + 00	3.43 + 00	2.27 + 00	1.51 + 00	1.07 + 00
10	1.19 + 00	8.19 − 01	3.31 − 01	1.58 − 01	8.31 − 02
15	4.73 − 01	2.15 − 01	5.22 − 02	1.65 − 02	6.23 − 03
20	1.80 − 01	5.44 − 02	7.72 − 03	1.72 − 03	5.22 − 04
30	2.15 − 02	2.84 − 03	2.43 − 04	6.81 − 05	2.97 − 05
40	1.67 − 03	2.57 − 04	7.30 − 05	2.80 − 05	1.30 − 05
60	2.94 − 04	1.72 − 04	3.67 − 05	1.24 − 05	5.56 − 06
80	4.47 − 04	1.33 − 04	2.34 − 05	7.64 − 06	3.37 − 06
100	4.40 − 04	1.05 − 04	1.70 − 05	5.46 − 06	2.39 − 06
120	4.03 − 04	8.63 − 05	1.36 − 05	4.31 − 06	1.88 − 06
140	3.70 − 04	7.51 − 05	1.16 − 05	3.68 − 06	1.60 − 06
160	3.49 − 04	6.91 − 05	1.06 − 05	3.36 − 06	1.46 − 06
180	3.41 − 04	6.72 − 05	1.03 − 05	3.26 − 06	1.42 − 06

Table 3.15: Differential cross sections in atomic units for electron-hydrogen 1s-3p process in the Wallace approximation.

θ(deg)	50 eV	100 eV	200 eV	300 eV	400 eV
0	4.33 + 00	1.10 + 01	2.44 + 01	3.76 + 01	5.09 + 01
5	2.93 + 00	3.55 + 00	2.34 + 00	1.56 + 00	1.11 + 00
10	1.36 + 00	9.21 − 01	3.77 − 01	1.82 − 01	9.69 − 02
15	6.05 − 01	2.83 − 01	7.36 − 02	2.47 − 02	9.85 − 03
20	2.77 − 01	9.43 − 02	1.61 − 02	4.20 − 03	1.44 − 03
30	6.57 − 02	1.39 − 02	1.60 − 03	3.80 − 04	1.31 − 04
40	1.98 − 02	3.60 − 03	4.03 − 04	9.86 − 05	3.54 − 05
60	4.24 − 03	7.64 − 04	8.81 − 05	2.31 − 05	8.96 − 06
80	1.76 − 03	3.17 − 04	3.89 − 05	1.09 − 05	4.41 − 06
100	9.89 − 04	1.81 − 04	2.36 − 05	6.87 − 06	2.85 − 06
120	6.64 − 04	1.25 − 04	1.71 − 05	5.09 − 06	2.14 − 06
140	5.10 − 04	9.89 − 05	1.39 − 05	4.20 − 06	1.78 − 06
160	4.39 − 04	8.66 − 05	1.24 − 05	3.76 − 06	1.60 − 06
180	4.18 − 04	8.30 − 05	1.19 − 05	3.63 − 06	1.55 − 06

Table 3.16: Differential cross sections in atomic units for positron-hydrogen 1s-3p process in the Wallace approximation.

θ(deg)	50 eV	100 eV	200 eV	300 eV	400 eV
1	1.61 + 01	7.62 + 00	3.79 + 00	2.65 + 00	2.13 + 00
5	5.98 + 00	2.94 + 00	1.63 + 00	1.26 + 00	1.08 + 00
10	3.24 + 00	1.66 + 00	9.64 − 01	7.33 − 01	6.03 − 01
15	2.05 + 00	1.07 + 00	5.96 − 01	4.19 − 01	3.18 − 01
20	1.38 + 00	7.14 − 01	3.67 − 01	2.35 − 01	1.65 − 01
30	6.84 − 01	3.32 − 01	1.42 − 01	7.86 − 02	4.97 − 02
40	3.61 − 01	1.63 − 01	6.03 − 02	3.08 − 02	1.85 − 02
60	1.19 − 01	4.87 − 02	1.57 − 02	7.50 − 03	4.36 − 03
80	4.93 − 02	1.95 − 02	5.97 − 03	2.81 − 03	1.62 − 03
100	2.53 − 02	9.94 − 03	2.99 − 03	1.40 − 03	8.04 − 04
120	1.56 − 02	6.12 − 03	1.83 − 03	8.55 − 04	4.91 − 04
140	1.13 − 02	4.42 − 03	1.32 − 03	6.16 − 04	3.54 − 04
160	9.36 − 03	3.66 − 03	1.09 − 03	5.10 − 04	2.93 − 04
180	8.80 − 03	3.44 − 03	1.02 − 03	4.79 − 04	2.75 − 04

Table 3.17: Differential cross sections in atomic units for electron-hydrogen 1s-1s process in the Wallace approximation.

θ(deg)	50 eV	100 eV	200 eV	300 eV	400 eV
1	1.51 + 01	6.95 + 00	3.14 + 00	2.39 + 00	1.93 + 00
5	5.11 + 00	2.36 + 00	1.32 + 00	1.04 + 00	9.23 − 01
10	2.48 + 00	1.18 + 00	7.21 − 01	5.85 − 01	5.05 − 01
15	1.42 + 00	6.88 − 01	4.31 − 01	3.31 − 01	2.65 − 01
20	8.74 − 01	4.31 − 01	2.62 − 01	1.86 − 01	1.38 − 01
30	3.77 − 01	1.87 − 01	1.01 − 01	6.25 − 02	4.19 − 02
40	1.83 − 01	8.96 − 02	4.31 − 02	2.47 − 02	1.57 − 02
60	5.69 − 02	2.67 − 02	1.13 − 02	6.06 − 03	3.72 − 03
80	2.39 − 02	1.09 − 02	4.35 − 03	2.28 − 03	1.39 − 03
100	1.27 − 02	5.63 − 03	2.19 − 03	1.14 − 03	6.90 − 04
120	8.09 − 03	3.52 − 03	1.35 − 03	6.98 − 04	4.22 − 04
140	5.99 − 03	2.57 − 03	9.73 − 04	5.03 − 04	3.04 − 04
160	5.04 − 03	2.15 − 03	8.07 − 04	4.17 − 04	2.52 − 04
180	4.76 − 03	2.02 − 03	7.59 − 04	3.92 − 04	2.37 − 04

Table 3.18: Differential cross sections in atomic units for positron-hydrogen 1s-1s process in the Wallace approximation.

θ(deg)	50 eV	100 eV	200 eV	300 eV	400 eV
1	1.40 + 03	6.81 + 02	3.71 + 02	2.84 + 02	2.45 + 02
5	2.62 + 02	1.45 + 02	8.87 + 01	6.37 + 01	4.77 + 01
10	6.94 + 01	3.69 + 01	1.56 + 01	7.98 + 00	4.65 + 00
15	2.23 + 01	1.04 + 01	3.41 + 00	1.58 + 00	8.93 − 01
20	8.66 + 00	3.69 + 00	1.10 + 00	5.00 − 01	2.85 − 01
30	2.30 + 00	8.20 − 01	2.23 − 01	1.02 − 01	5.89 − 02
40	8.75 − 01	2.71 − 01	7.32 − 02	3.38 − 02	1.95 − 02
60	2.00 − 01	5.81 − 02	[illegible]1 − 02	7.46 − 03	4.30 − 03
80	7.19 − 02	2.11 − 02	5.90 − 03	2.74 − 03	1.58 − 03
100	3.51 − 02	1.04 − 02	2.93 − 03	1.36 − 03	7.83 − 04
120	2.13 − 02	6.37 − 03	1.79 − 03	8.34 − 04	4.80 − 04
140	1.53 − 02	4.60 − 03	1.30 − 03	6.02 − 04	3.46 − 04
160	1.27 − 02	3.81 − 03	1.07 − 03	4.99 − 04	2.87 − 04
180	1.19 − 02	3.59 − 03	1.01 − 03	4.69 − 04	2.70 − 04

Table 3.19: Differential cross sections in atomic units for electron or positron-hydrogen 2s-2s process in the Glauber approximation.

θ(deg)	50 eV	100 eV	200 eV	300 eV	400 eV
1	3.12 + 04	1.55 + 04	7.57 + 03	4.94 + 03	3.63 + 03
5	7.86 + 02	3.11 + 02	9.50 + 01	3.85 + 01	1.76 + 01
10	6.51 + 01	1.37 + 01	1.36 + 00	2.71 − 01	1.01 − 01
15	7.02 + 00	1.03 + 00	1.49 − 01	4.39 − 02	1.60 − 02
20	1.54 + 00	3.25 − 01	3.93 − 02	8.10 − 03	2.33 − 03
30	4.10 − 01	4.87 − 02	2.86 − 03	4.54 − 04	1.20 − 04
40	1.09 − 01	8.20 − 03	3.89 − 04	6.23 − 05	1.73 − 05
60	1.12 − 02	6.26 − 04	2.97 − 05	5.15 − 06	1.52 − 06
80	2.28 − 03	1.20 − 04	6.00 − 06	1.08 − 06	3.27 − 07
100	7.55 − 04	3.93 − 05	2.02 − 06	3.71 − 07	1.13 − 07
120	3.51 − 04	1.82 − 05	9.55 − 07	1.77 − 07	5.40 − 08
140	2.11 − 04	1.10 − 05	5.81 − 07	1.08 − 07	3.31 − 08
160	1.58 − 04	8.22 − 06	4.37 − 07	8.13 − 08	2.49 − 08
180	1.43 − 04	7.48 − 06	3.98 − 07	7.41 − 08	2.28 − 08

Table 3.20: Differential cross sections in atomic units for electron or positron-hydrogen 2s-2p process in the Glauber approximation.

θ(deg)	50 eV	100 eV	200 eV	300 eV	400 eV
0	3.71 + 02	3.31 + 02	2.68 + 02	2.34 + 02	2.13 + 02
5	3.61 + 01	2.12 + 01	8.51 + 00	3.44 + 00	1.45 + 00
10	2.56 + 00	1.04 + 00	3.88 − 01	1.62 − 01	6.87 − 02
15	8.54 − 01	5.37 − 01	9.28 − 02	2.20 − 02	7.88 − 03
20	7.68 − 01	2.01 − 01	2.07 − 02	5.42 − 03	2.33 − 03
30	2.18 − 01	3.02 − 02	3.72 − 03	1.23 − 03	5.67 − 04
40	6.91 − 02	9.24 − 03	1.36 − 03	4.51 − 04	2.02 − 04
60	1.45 − 02	2.14 − 03	3.28 − 04	1.05 − 04	4.62 − 05
80	5.18 − 03	8.16 − 04	1.23 − 04	3.91 − 05	1.71 − 05
100	2.55 − 03	4.13 − 04	6.18 − 05	1.95 − 05	8.47 − 06
120	1.56 − 03	2.55 − 04	3.80 − 05	1.19 − 05	5.19 − 06
140	1.12 − 03	1.85 − 04	2.74 − 05	8.62 − 06	3.74 − 06
160	9.32 − 04	1.54 − 04	2.28 − 05	7.15 − 06	3.10 − 06
180	8.77 − 04	1.45 − 04	2.14 − 05	6.72 − 06	2.92 − 06

Table 3.21: Differential cross sections in atomic units for electron or positron-hydrogen 2s-3s process in the Glauber approximation.

θ(deg)	50 eV	100 eV	200 eV	300 eV	400 eV
0	8.35 + 03	1.81 + 04	3.73 + 04	5.64 + 04	7.55 + 04
5	9.73 + 01	2.05 + 01	1.08 + 00	9.33 − 01	1.23 + 00
10	2.22 + 00	2.12 + 00	4.99 − 01	7.86 − 02	1.03 − 02
15	2.46 + 00	3.95 − 01	7.74 − 03	1.20 − 03	7.60 − 04
20	6.90 − 01	3.03 − 02	1.42 − 03	3.68 − 04	1.09 − 04
30	4.44 − 02	2.57 − 03	8.32 − 05	7.68 − 06	1.26 − 06
40	1.08 − 02	3.43 − 04	3.93 − 06	1.77 − 07	2.55 − 08
60	8.41 − 04	1.05 − 05	1.60 − 08	1.88 − 09	2.38 − 09
80	1.20 − 04	1.01 − 06	8.13 − 10	1.19 − 09	7.48 − 10
100	3.10 − 05	2.28 − 07	8.43 − 10	5.59 − 10	2.91 − 10
120	1.24 − 05	8.79 − 08	6.11 − 10	3.01 − 10	1.45 − 10
140	6.86 − 06	4.86 − 08	4.50 − 10	1.95 − 10	9.08 − 11
160	4.90 − 06	3.50 − 08	3.70 − 10	1.51 − 10	6.91 − 11
180	4.40 − 06	3.15 − 08	3.46 − 10	1.39 − 10	6.32 − 11

Table 3.22: Differential cross sections in atomic units for electron or positron-hydrogen 2s-3p process in the Glauber approximation.

ϑ(deg)	50 eV	100 eV	200 eV	300 eV	400 eV
0	1.56 + 00	1.90 + 00	1.84 + 00	1.73 + 00	1.64 + 00
5	1.12 + 00	1.00 + 00	7.43 − 01	6.15 − 01	5.28 − 01
10	5.87 − 01	4.38 − 01	2.67 − 01	1.72 − 01	1.14 − 01
15	2.90 − 01	1.85 − 01	7.96 − 02	3.70 − 02	1.88 − 02
20	1.41 − 01	7.43 − 02	2.23 − 02	8.30 − 03	3.73 − 03
30	3.32 − 02	1.31 − 02	3.18 − 03	1.20 − 03	5.72 − 04
40	1.03 − 02	4.51 − 03	1.17 − 03	4.37 − 04	2.04 − 04
60	4.31 − 03	1.62 − 03	3.24 − 04	1.08 − 04	4.76 − 05
80	2.72 − 03	7.46 − 04	1.27 − 04	4.04 − 05	1.75 − 05
100	1.75 − 03	4.05 − 04	6.39 − 05	2.00 − 05	8.64 − 06
120	1.22 − 03	2.57 − 04	3.93 − 05	1.22 − 05	5.27 − 06
140	9.43 − 04	1.89 − 04	2.84 − 05	8.81 − 06	3.79 − 06
160	8.08 − 04	1.58 − 04	2.35 − 05	7.29 − 06	3.13 − 06
180	7.68 − 04	1.49 − 04	2.21 − 05	6.85 − 06	2.95 − 06

Table 3.23: Differential cross sections in atomic units for electron or positron-hydrogen 1s-2s process in the Glauber approximation.

θ(deg)	50 eV	100 eV	200 eV	300 eV	400 eV
0	3.71 + 01	9.56 + 01	2.13 + 02	3.29 + 02	4.45 + 02
5	2.10 + 01	2.18 + 01	1.26 + 01	7.80 + 00	5.24 + 00
10	7.51 + 00	4.24 + 00	1.46 + 00	6.31 − 01	3.12 − 01
15	2.66 + 00	1.00 + 00	2.13 − 01	6.45 − 02	2.42 − 02
20	9.79 − 01	2.60 − 01	3.63 − 02	8.66 − 03	2.83 − 03
30	1.54 − 01	2.49 − 02	2.46 − 03	5.58 − 04	1.89 − 04
40	3.38 − 02	4.85 − 03	4.78 − 04	1.09 − 04	3.66 − 05
60	5.35 − 03	6.79 − 04	5.70 − 05	1.20 − 05	3.88 − 06
80	1.73 − 03	1.78 − 04	1.32 − 05	2.68 − 06	8.55 − 07
100	7.37 − 04	6.63 − 05	4.64 − 06	9.34 − 07	2.96 − 07
120	3.91 − 04	3.26 − 05	2.22 − 06	4.45 − 07	1.41 − 07
140	2.53 − 04	2.03 − 05	1.36 − 06	2.72 − 07	8.62 − 08
160	1.96 − 04	1.54 − 05	1.03 − 06	2.05 − 07	6.49 − 08
180	1.80 − 04	1.40 − 05	9.36 − 07	1.87 − 07	5.92 − 08

Table 3.24: Differential cross sections in atomic units for electron or positron-hydrogen 1s-2p process in the Glauber approximation.

θ(deg)	50 eV	100 eV	200 eV	300 eV	400 eV
0	2.16 – 01	2.65 – 01	2.55 – 01	2.39 – 01	2.26 – 01
5	1.71 – 01	1.63 – 01	1.25 – 01	1.07 – 01	9.51 – 02
10	1.03 – 01	8.31 – 02	5.63 – 02	3.96 – 02	2.80 – 02
15	5.76 – 02	4.08 – 02	2.01 – 02	1.00 – 02	5.27 – 03
20	3.12 – 02	1.85 – 02	6.15 – 03	2.33 – 03	1.03 – 03
30	8.62 – 03	3.54 – 03	8.17 – 04	2.97 – 04	1.39 – 04
40	2.64 – 03	1.10 – 03	2.80 – 04	1.04 – 04	4.86 – 05
60	9.39 – 04	3.80 – 04	7.73 – 05	2.57 – 05	1.13 – 05
80	6.21 – 04	1.78 – 04	3.03 – 05	9.63 – 06	4.16 – 06
100	4.15 – 04	9.76 – 05	1.53 – 05	4.77 – 06	2.05 – 06
120	2.95 – 04	6.24 – 05	9.41 – 06	2.91 – 06	1.25 – 06
140	2.30 – 04	4.59 – 05	6.79 – 06	2.10 – 06	8.99 – 07
160	1.98 – 04	3.84 – 05	5.63 – 06	1.73 – 06	7.44 – 07
180	1.88 – 04	3.62 – 05	5.30 – 06	1.63 – 06	6.99 – 07

Table 3.25: Differential cross sections in atomic units for electron or positron-hydrogen 1s-3s process in the Glauber approximation.

θ(deg)	50 eV	100 eV	200 eV	300 eV	400 eV
0	4.25 + 00	1.10 + 01	2.43 + 01	3.76 + 01	5.09 + 01
5	2.86 + 00	3.49 + 00	2.31 + 00	1.53 + 00	1.09 + 00
10	1.29 + 00	8.74 – 01	3.55 – 01	1.70 – 01	8.99 – 02
15	5.49 – 01	2.51 – 01	6.29 – 02	2.05 – 02	7.96 – 03
20	2.34 – 01	7.47 – 02	1.17 – 02	2.85 – 03	9.27 – 04
30	4.47 – 02	7.85 – 03	7.57 – 04	1.66 – 04	5.51 – 05
40	1.03 – 02	1.44 – 03	1.38 – 04	3.12 – 05	1.04 – 05
60	1.53 – 03	1.95 – 04	1.63 – 05	3.42 – 06	1.10 – 06
80	5.00 – 04	5.15 – 05	3.77 – 06	7.62 – 07	2.42 – 07
100	2.17 – 04	1.93 – 05	1.33 – 06	2.65 – 07	8.37 – 08
120	1.17 – 04	9.51 – 06	6.35 – 07	1.26 – 07	3.98 – 08
140	7.59 – 05	5.90 – 06	3.8° – 07	7.70 – 08	2.43 – 08
160	5.89 – 05	4.48 – 06	2.93 – 07	5.80 – 08	1.83 – 08
180	5.42 – 05	4.09 – 06	2.67 – 07	5.29 – 08	1.67 – 08

Table 3.26: Differential cross sections in atomic units for electron or positron-hydrogen 1s-3p process in the Glauber approximation.

θ(deg)	50 eV	100 eV	200 eV	300 eV	400 eV
1	1.49 + 01	7.09 + 00	3.55 + 00	2.50 + 00	2.02 + 00
5	5.12 + 00	2.54 + 00	1.45 + 00	1.14 + 00	9.97 − 01
10	2.58 + 00	1.35 + 00	8.29 − 01	6.55 − 01	5.52 − 01
15	1.54 + 00	8.35 − 01	5.07 − 01	3.74 − 01	2.91 − 01
20	9.91 − 01	5.46 − 01	3.11 − 01	2.10 − 01	1.51 − 01
30	4.66 − 01	2.52 − 01	1.21 − 01	7.08 − 02	4.59 − 02
40	2.44 − 01	1.25 − 01	5.22 − 02	2.80 − 02	1.72 − 02
60	8.49 − 02	3.90 − 02	1.39 − 02	6.90 − 03	4.09 − 03
80	3.81 − 02	1.63 − 02	5.39 − 03	2.61 − 03	1.53 − 03
100	2.10 − 02	8.57 − 03	2.74 − 03	1.31 − 03	7.66 − 04
120	1.36 − 02	5.41 − 03	1.70 − 03	8.09 − 04	4.71 − 04
140	1.02 − 02	3.97 − 03	1.23 − 03	5.86 − 04	3.40 − 04
160	8.60 − 03	3.32 − 03	1.03 − 03	4.86 − 04	2.82 − 04
180	8.14 − 03	3.13 − 03	9.65 − 04	4.58 − 04	2.66 − 04

Table 3.27: Differential cross sections in atomic units for electron or positron-hydrogen 1s-1s process in the Glauber approximation.

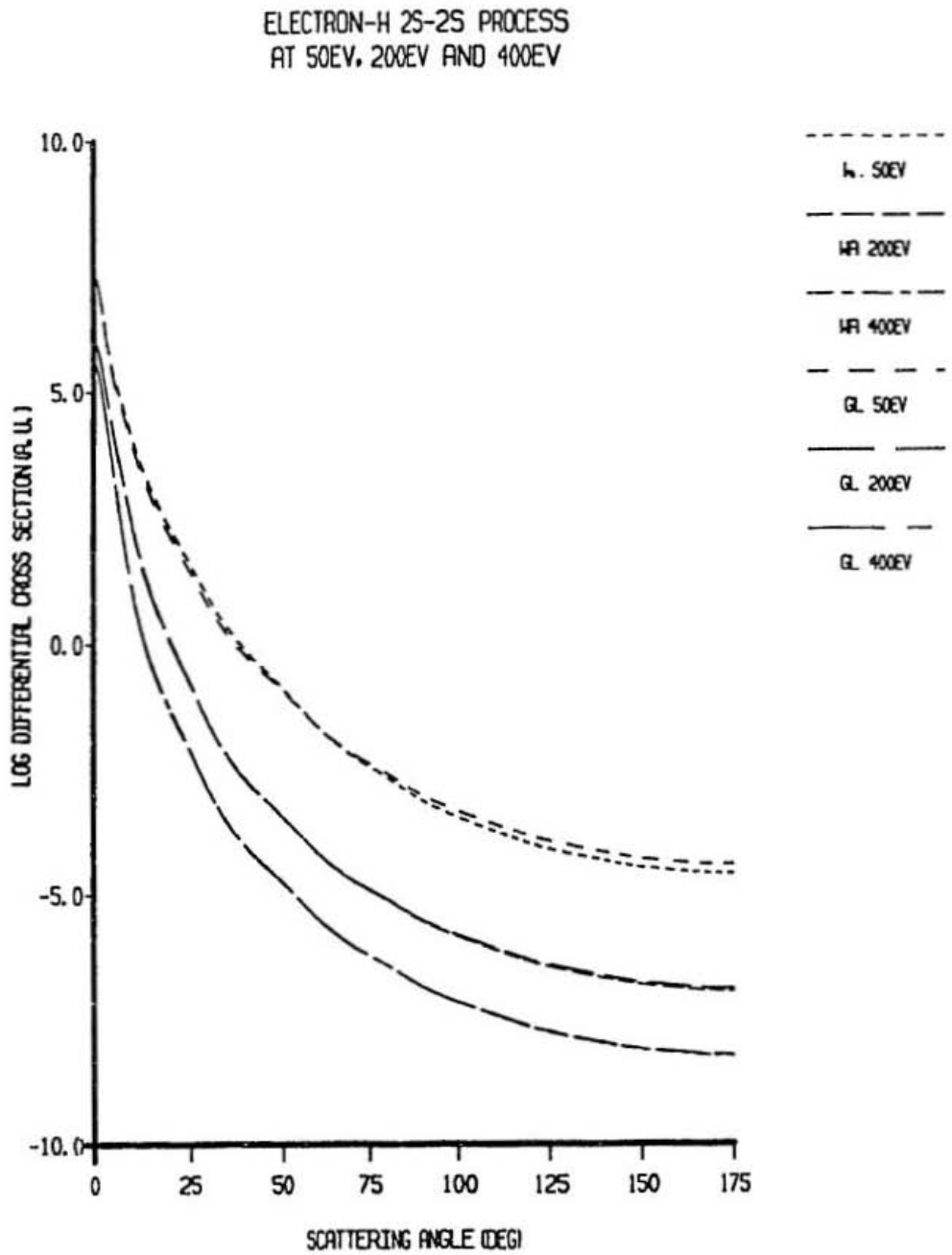

Figure 3.1: e^--H 2s-2s process at 50 eV, 200 eV, and 400 eV in the Wallace approximation(WA) and Glauber approximation(GL).

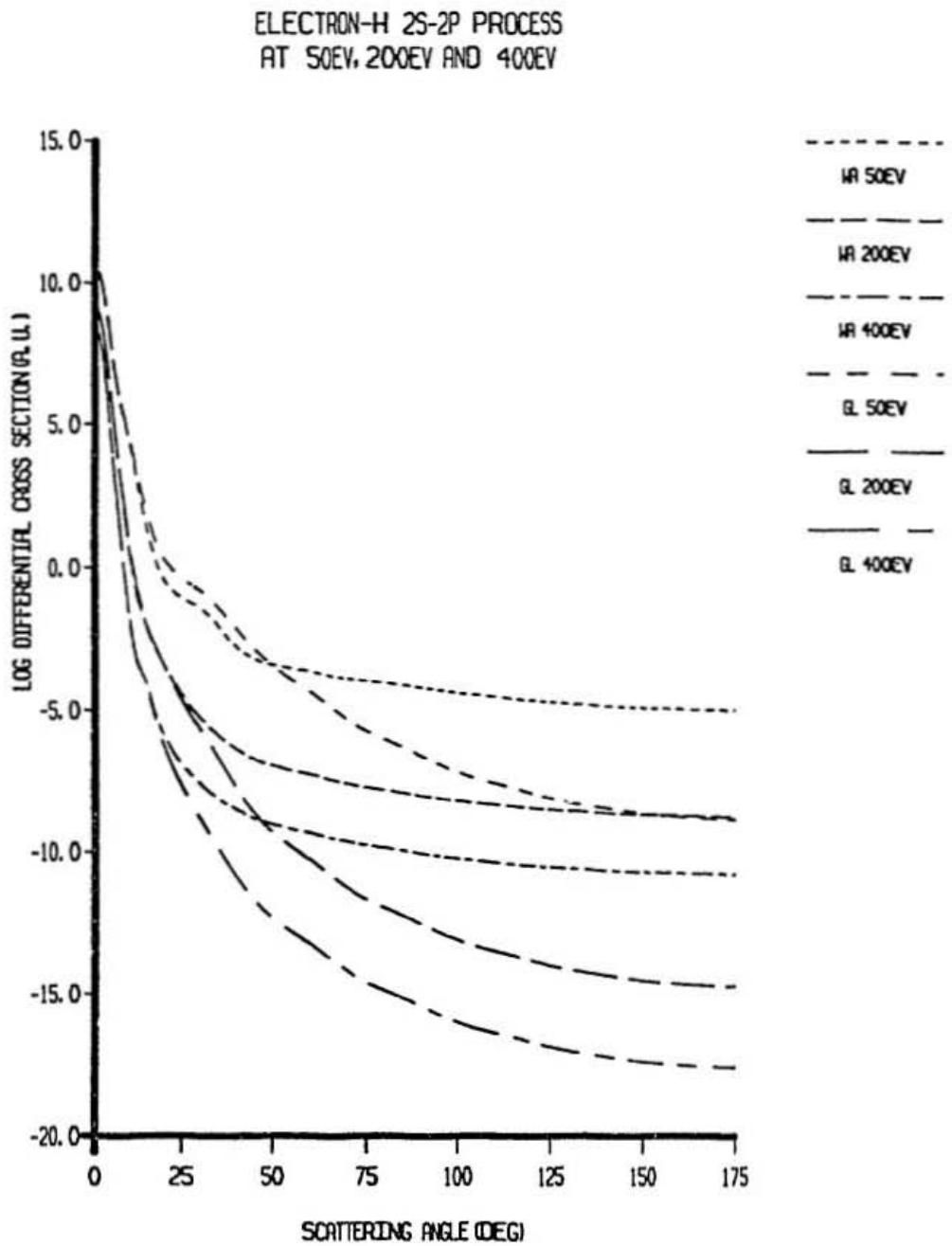

Figure 3.2: e^--H 2s-2p process at 50 eV, 200 eV, and 400 eV in the Wallace approximation(WA) and Glauber approximation(GL).

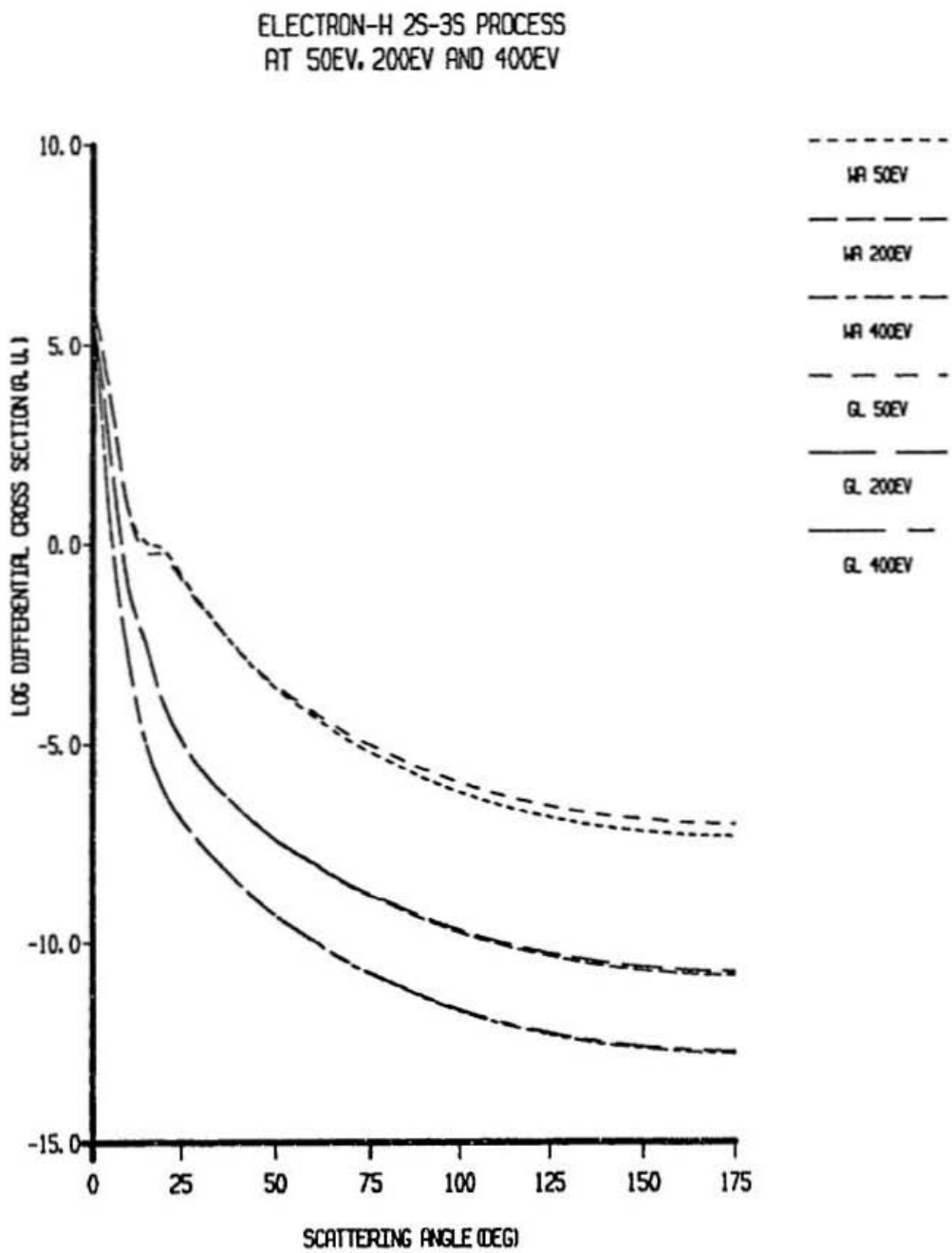

Figure 3.3: e^--H 2s-3s process at 50 eV, 200 eV, and 400 eV in the Wallace approximation(WA) and Glauber approximation(GL).

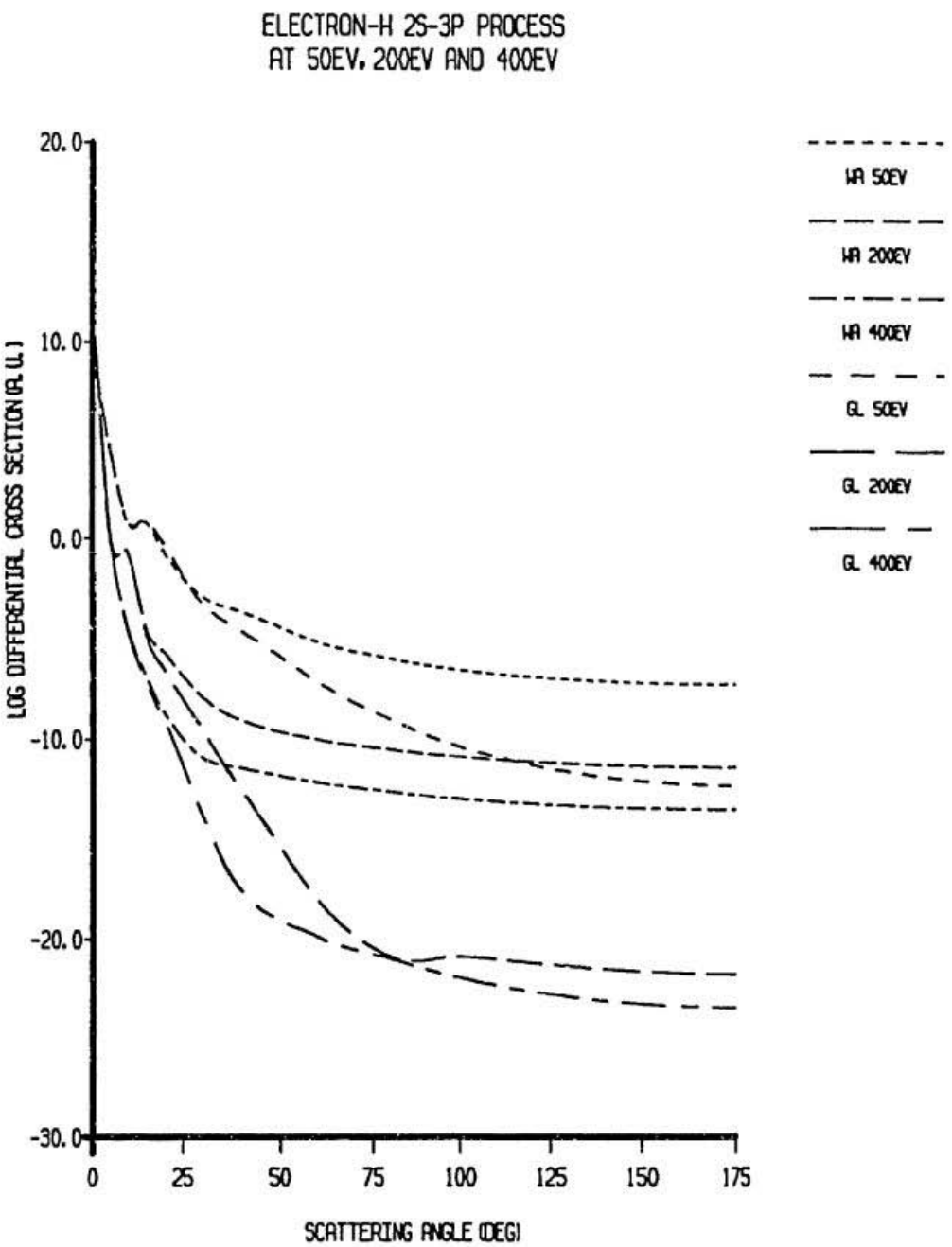

Figure 3.4: e^--H 2s-3p process at 50 eV, 200 eV, and 400 eV in the Wallace approximation(WA) and Glauber approximation(GL).

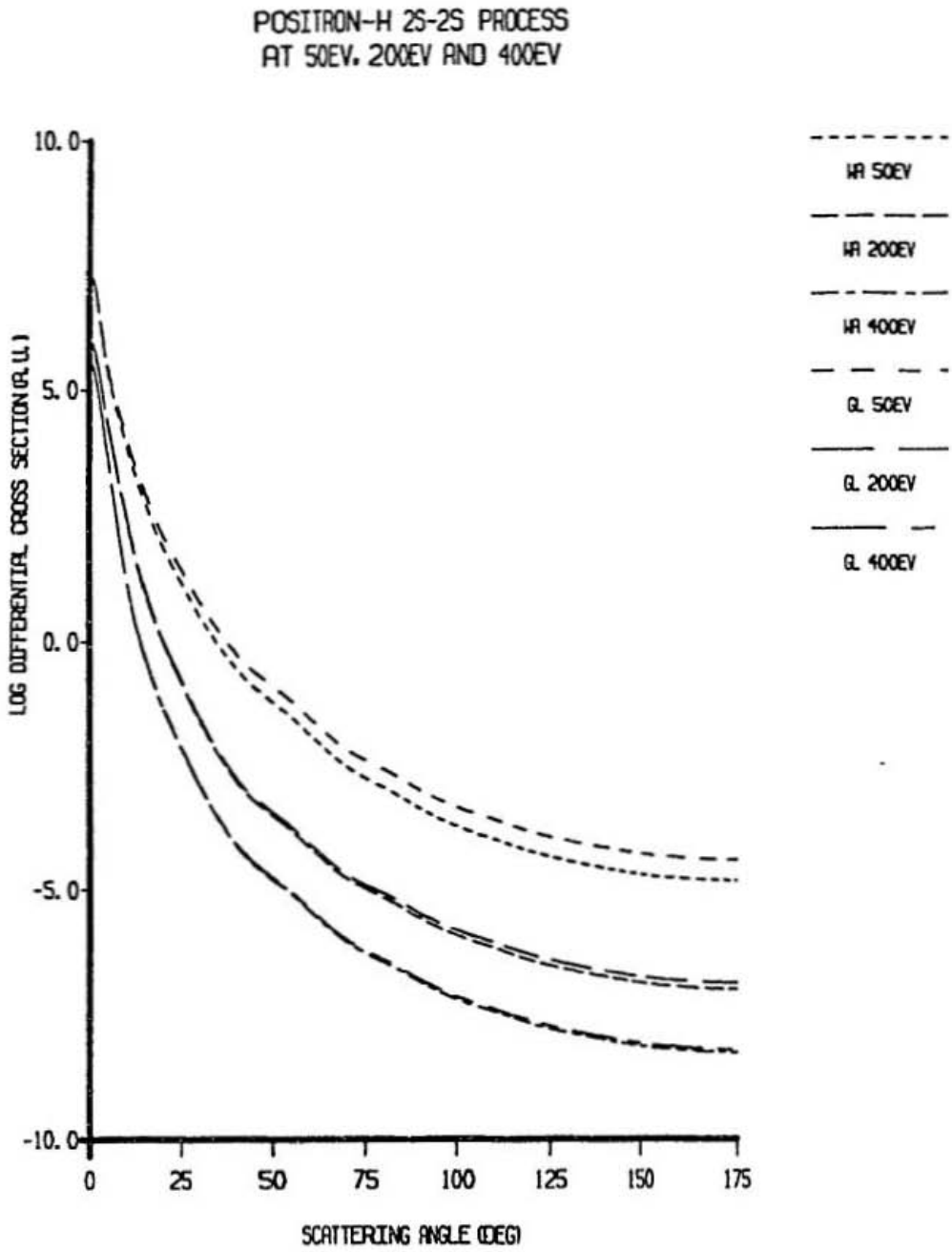

Figure 3.5: e^+-H 2s-2s process at 50 eV, 200 eV, and 400 eV in the Wallace approximation(WA) and Glauber approximation(GL).

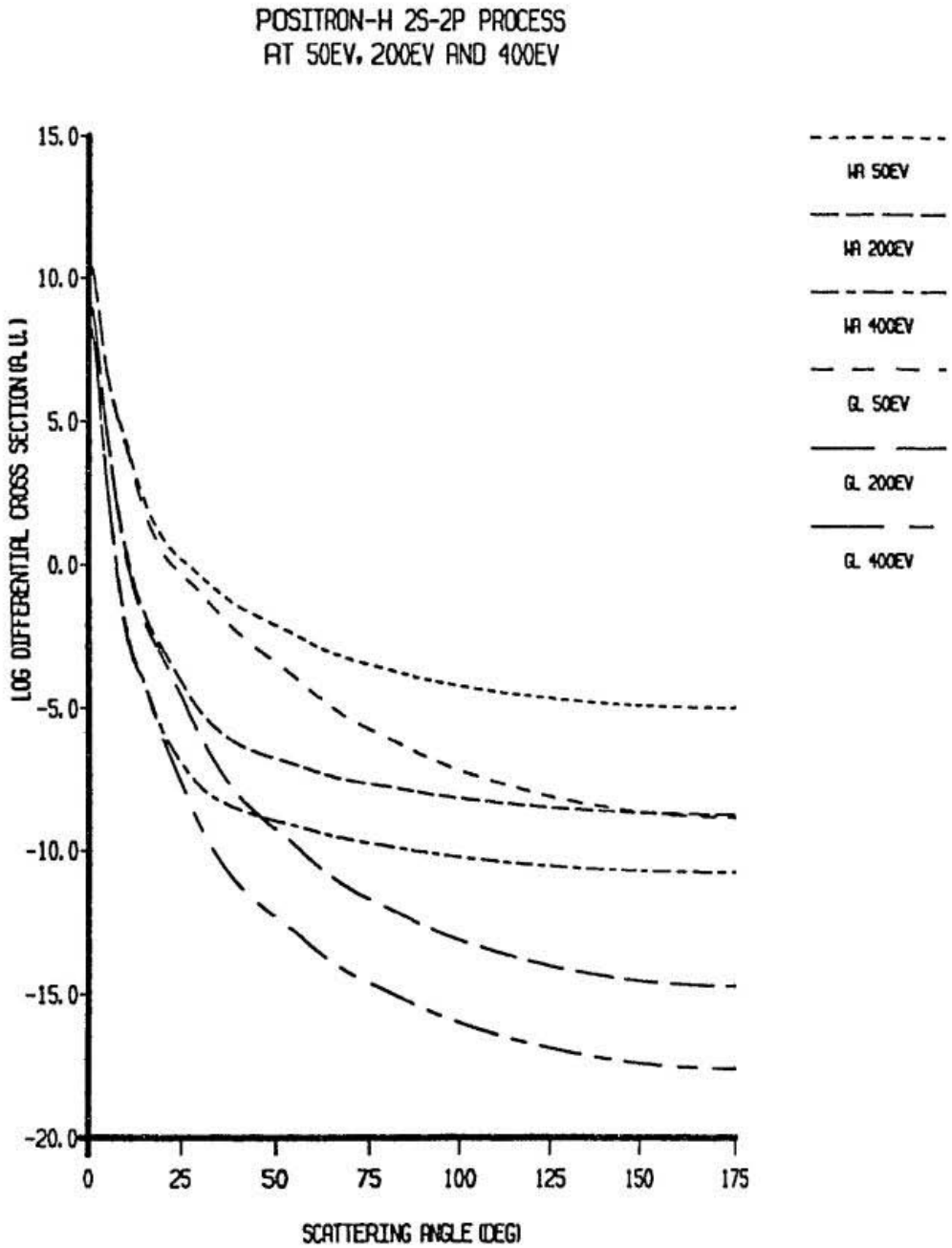

Figure 3.6: e^+-H 2s-2p process at 50 eV, 200 eV, and 400 eV in the Wallace approximation(WA) and Glauber approximation(GL).

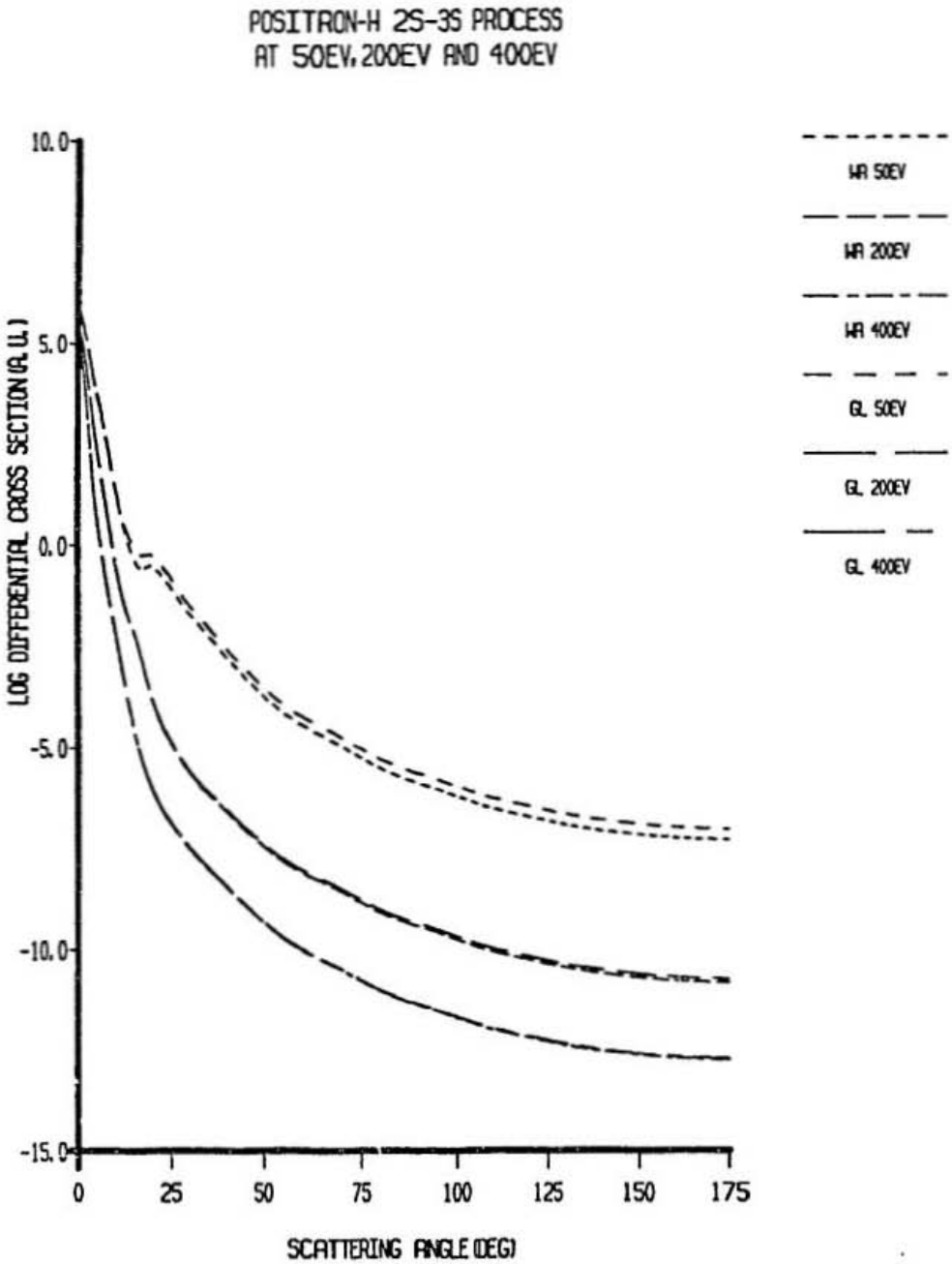

Figure 3.7: e^+-H 2s-3s process at 50 eV, 200 eV, and 400 eV in the Wallace approximation(WA) and Glauber approximation(GL).

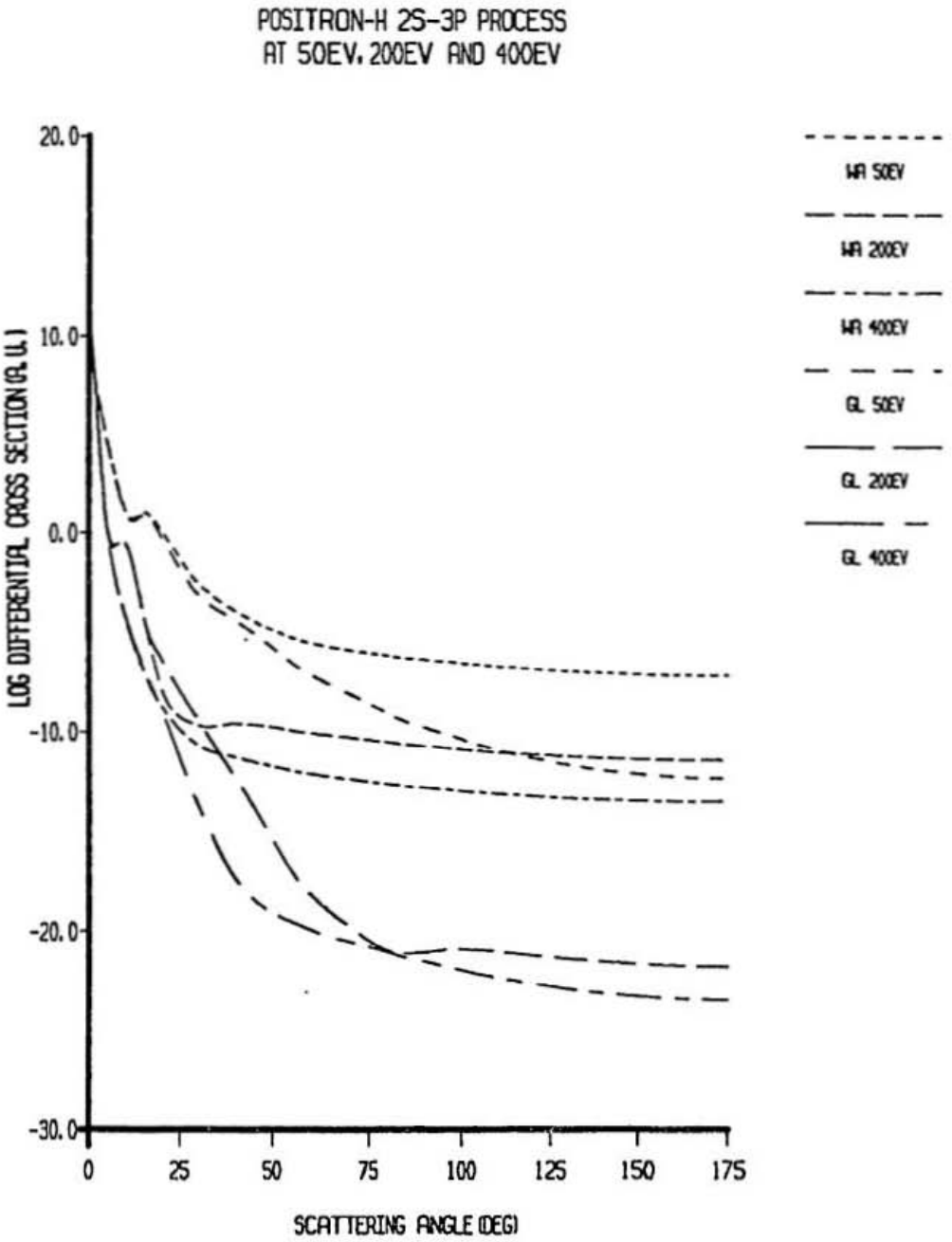

Figure 3.8: e^+-H 2s-3p process at 50 eV, 200 eV, and 400 eV in the Wallace approximation(WA) and Glauber approximation(GL).

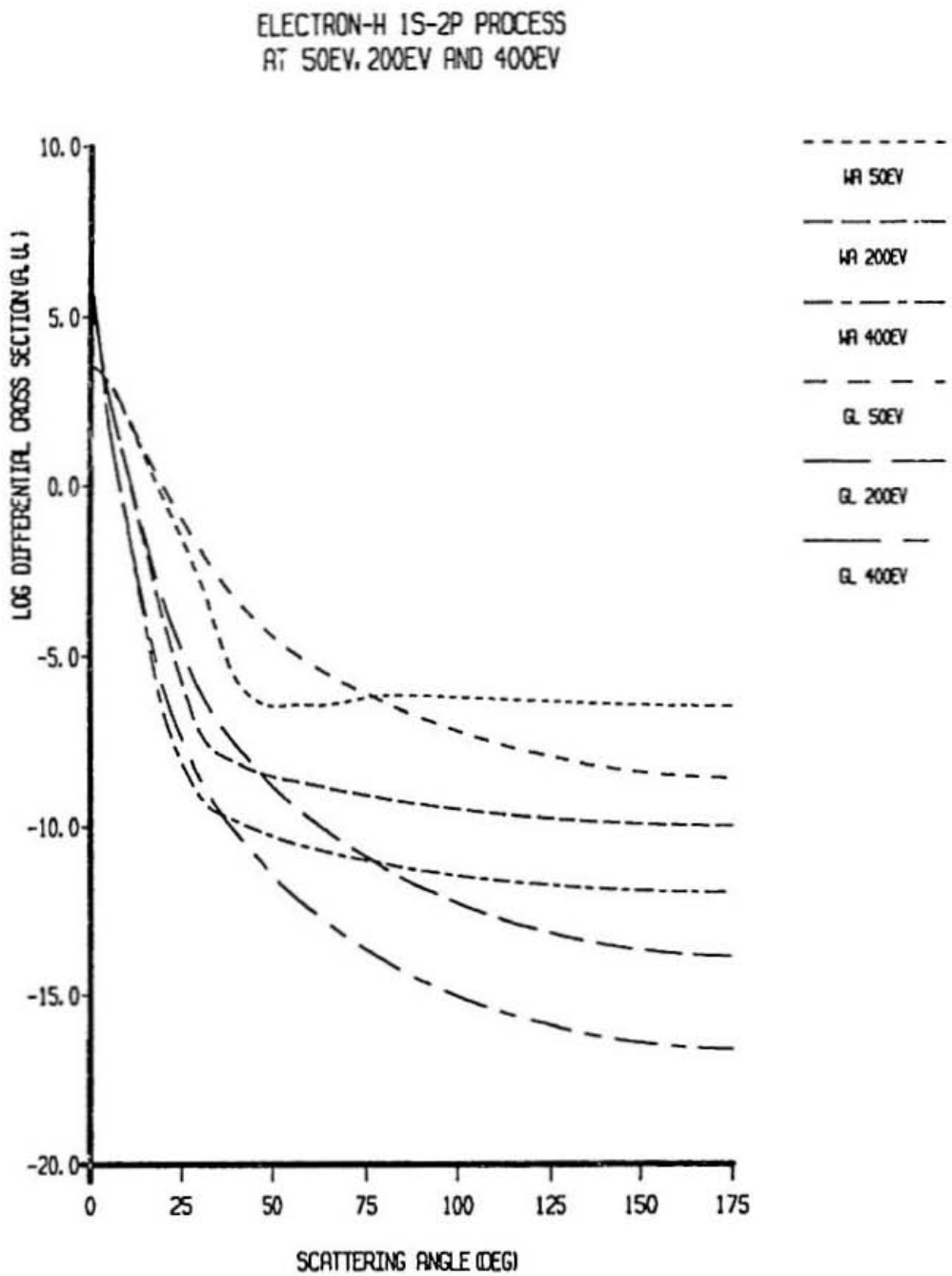

Figure 3.9: e^--H 1s-2p process at 50 eV, 200 eV, and 400 eV in the Wallace approximation(WA) and Glauber approximation(GL).

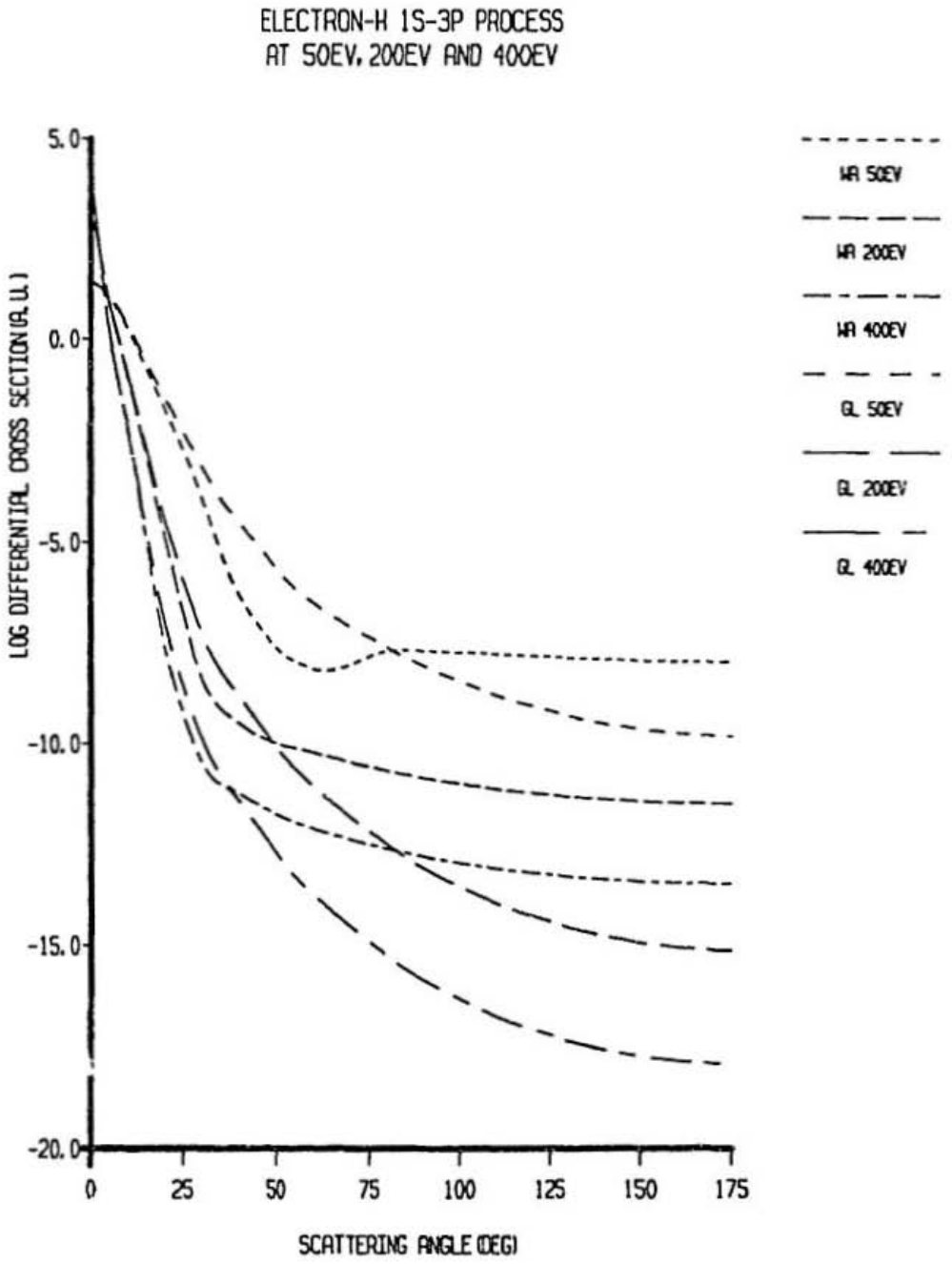

Figure 3.10: e^--H 1s-3p process at 50 eV, 200 eV, and 400 eV in the Wallace approximation(WA) and Glaube approximation(GL).

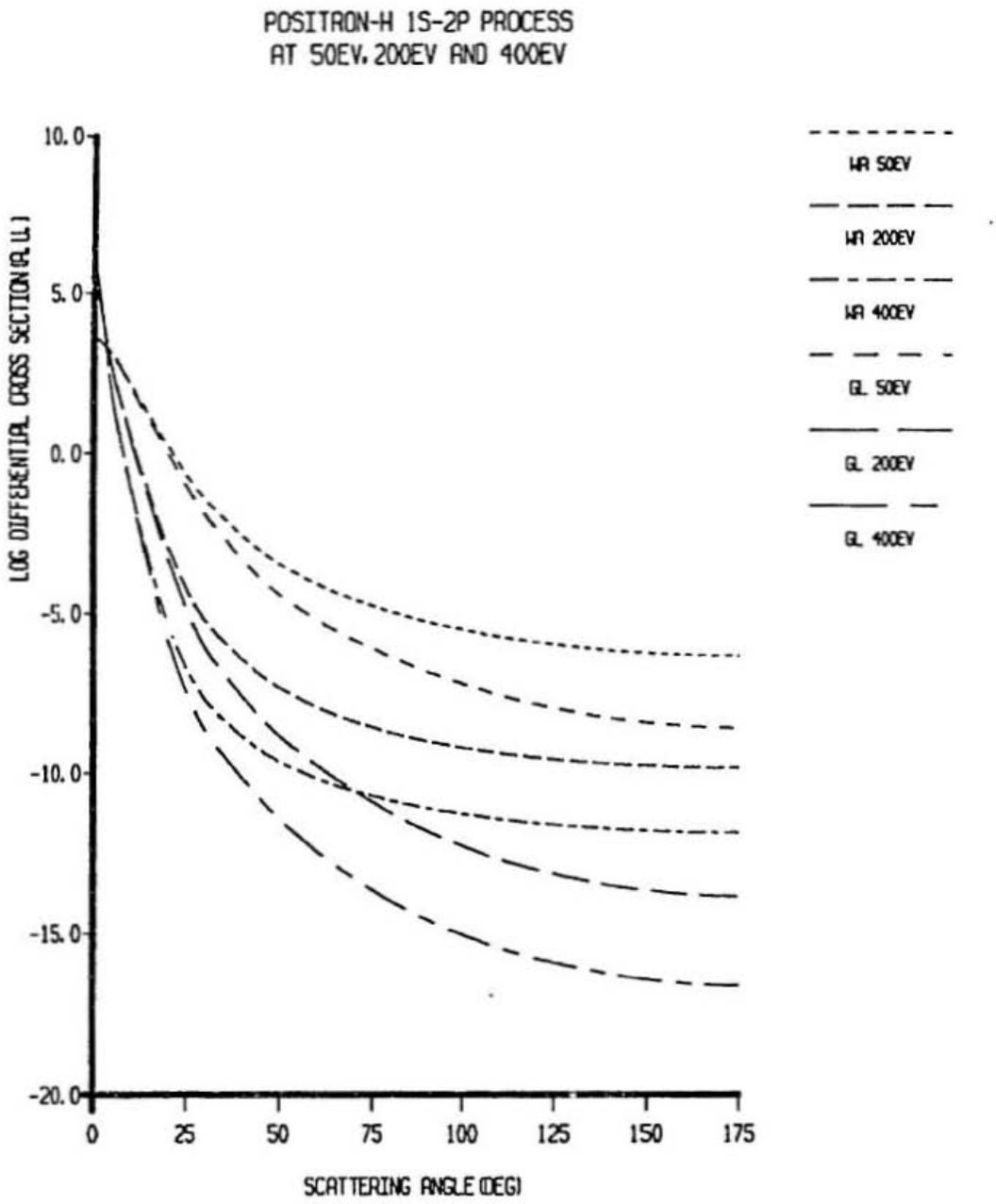

Figure 3.11: e^+-H 1s-2p process at 50 eV, 200 eV, and 400 eV in the Wallace approximation(WA) and Glauber approximation(GL).

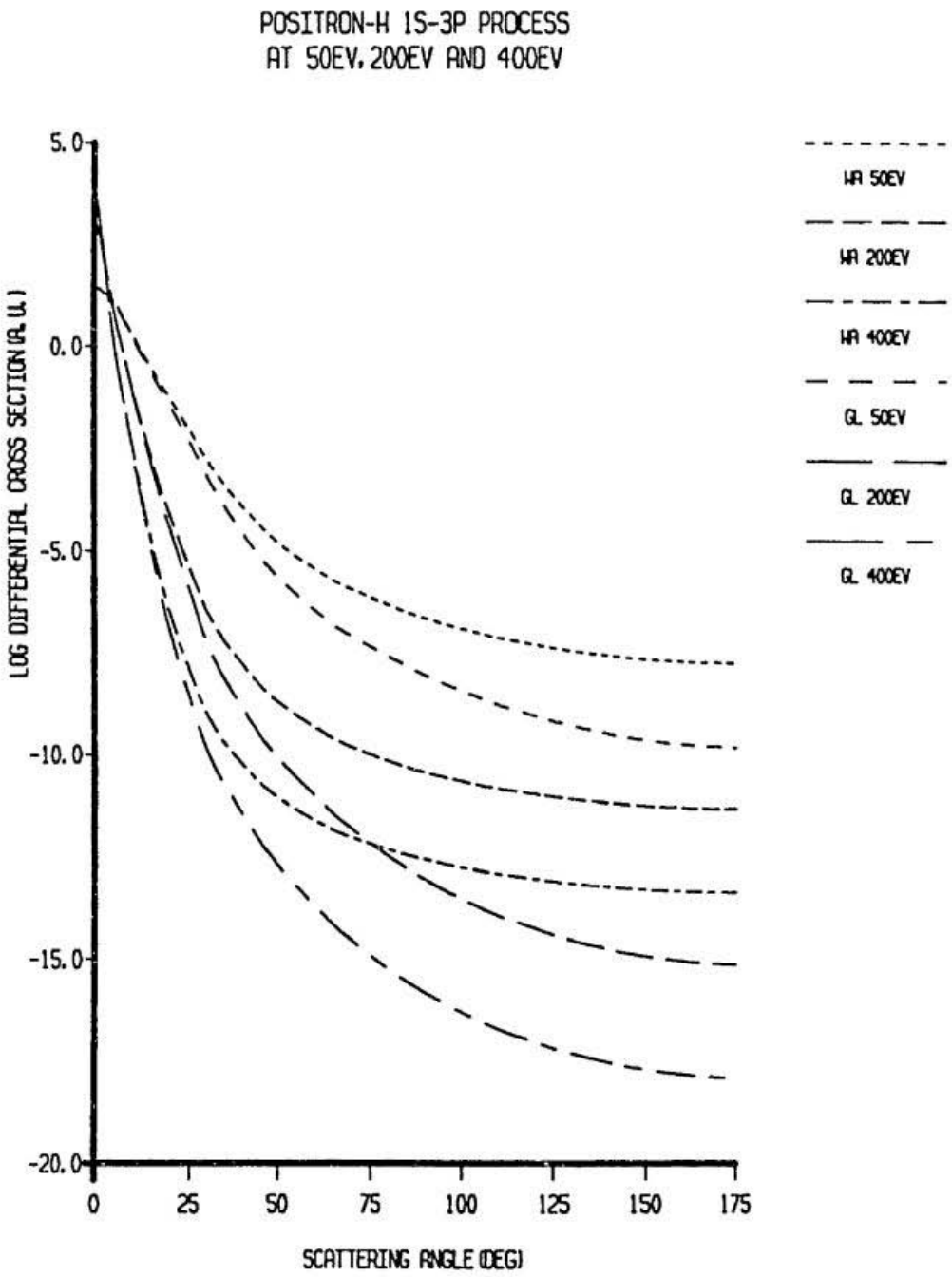

Figure 3.12: e^+-H 1s-3p process at 50 eV, 200 eV, and 400 eV in the Wallace approximation(WA) and Glauber approximation(GL).

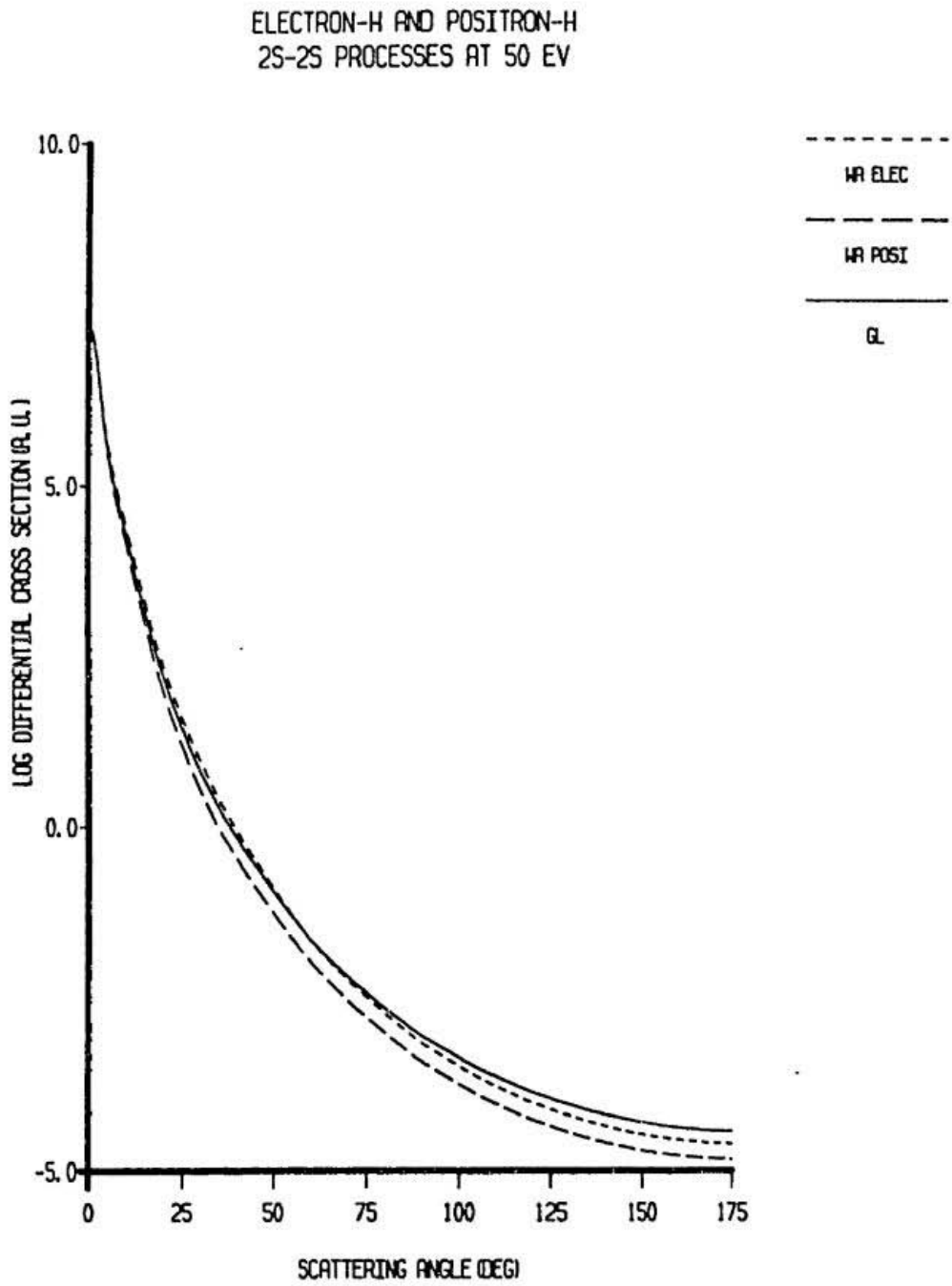

Figure 3.13: e^--H and e^+-H 2s-2s processes at 50 eV in the Wallace approximation(WA) and the Glauber approximation(GL).

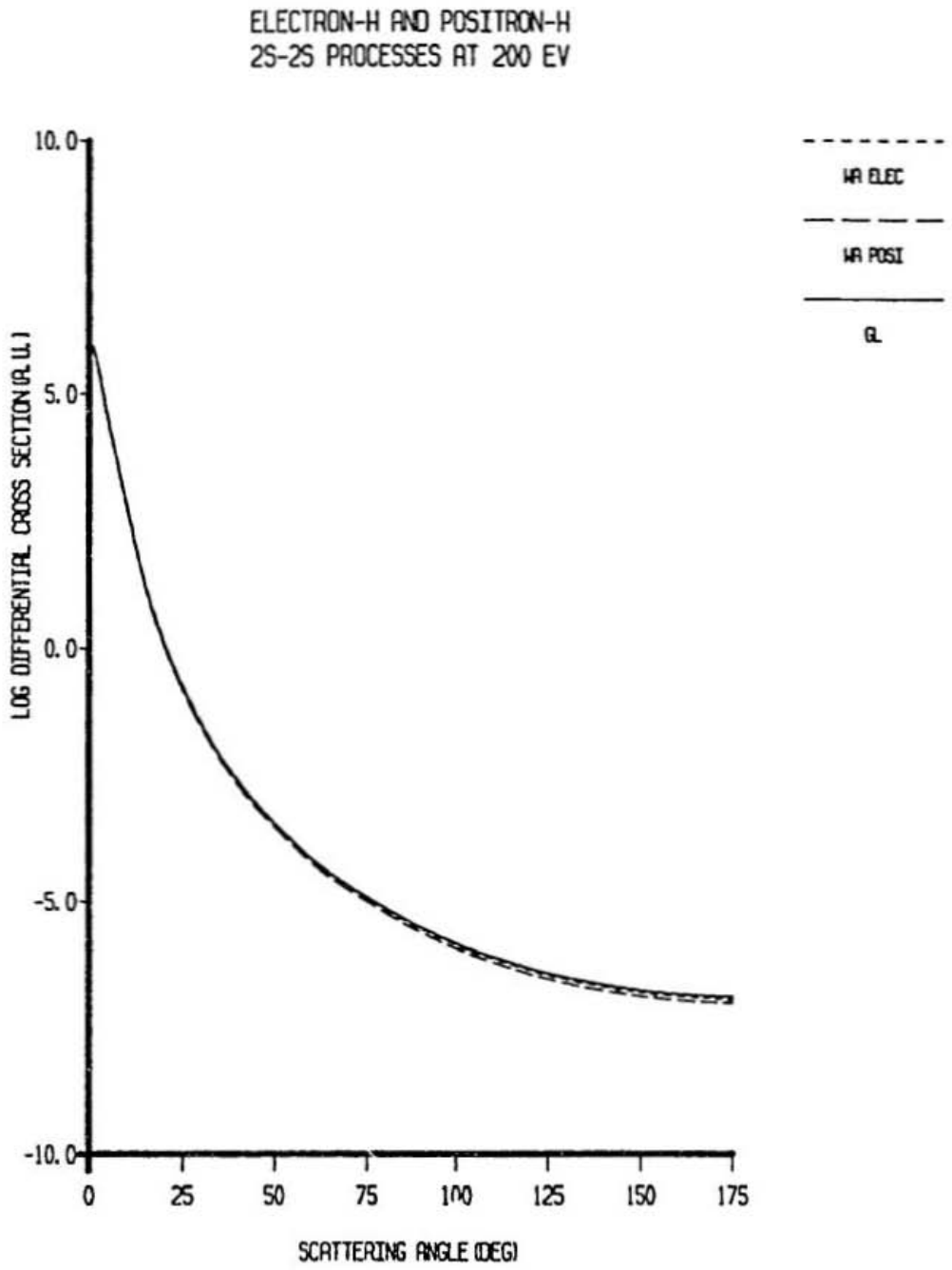

Figure 3.14: e^--H and e^+-H 2s-2s processes at 200 eV in the Wallace approximation(WA) and the Glauber approximation(GL).

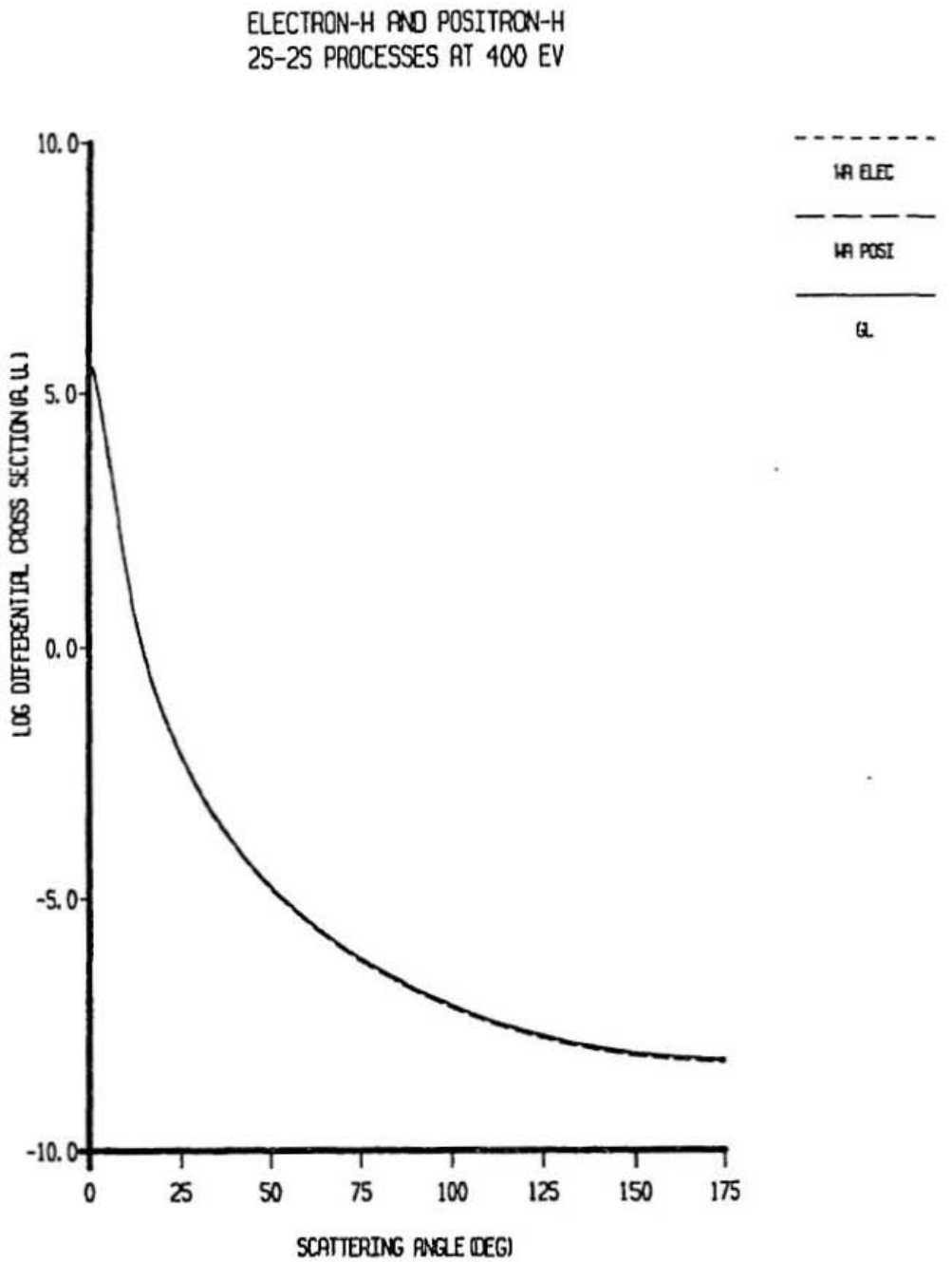

Figure 3.15: e^--H and e^+-H 2s-2s processes at 400 eV in the Wallace approximation(WA) and the Glauber approximation(GL).

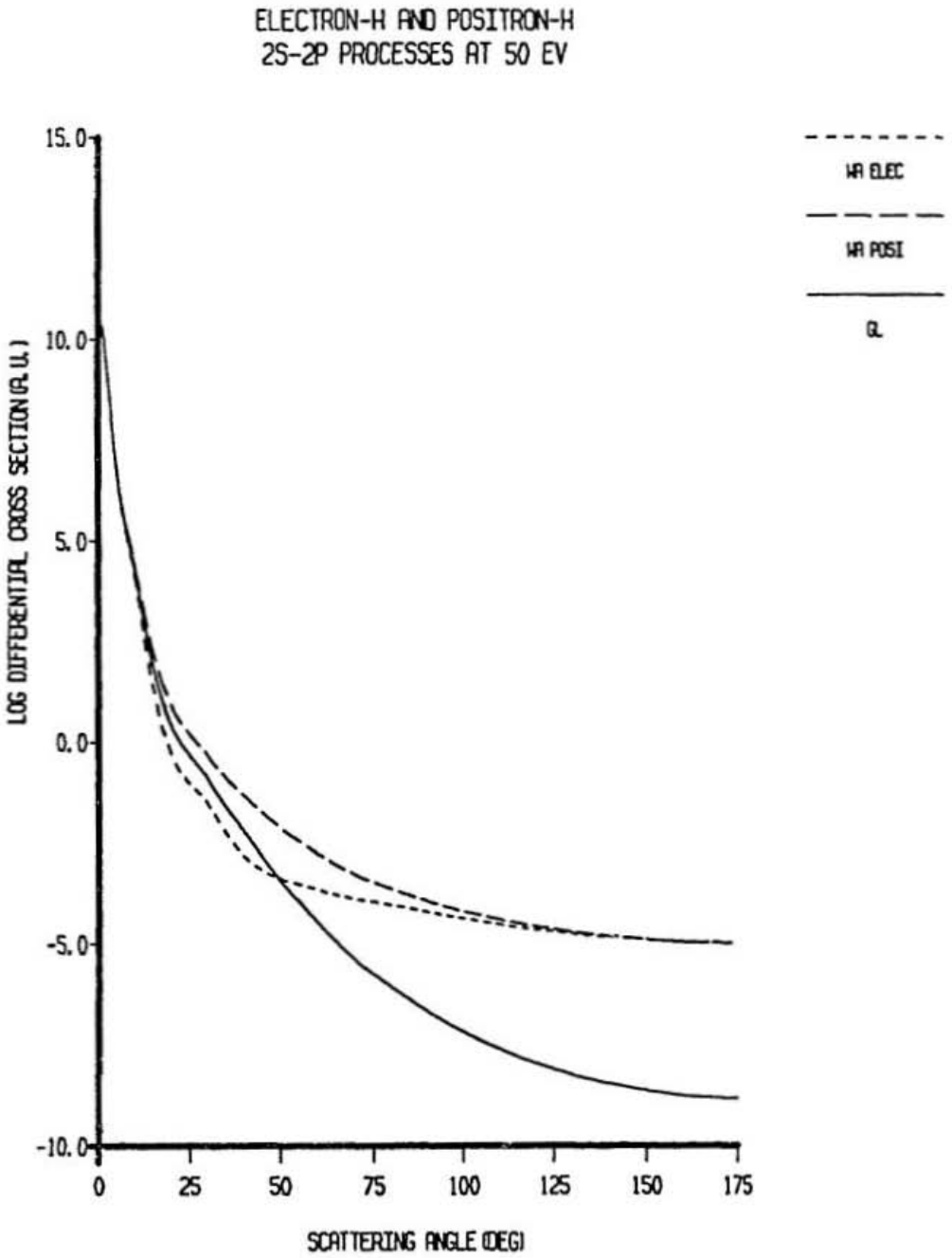

Figure 3.16: e^--H and e^+-H 2s-2p processes at 50 eV in the Wallace approximation(WA) and the Glauber approximation(GL).

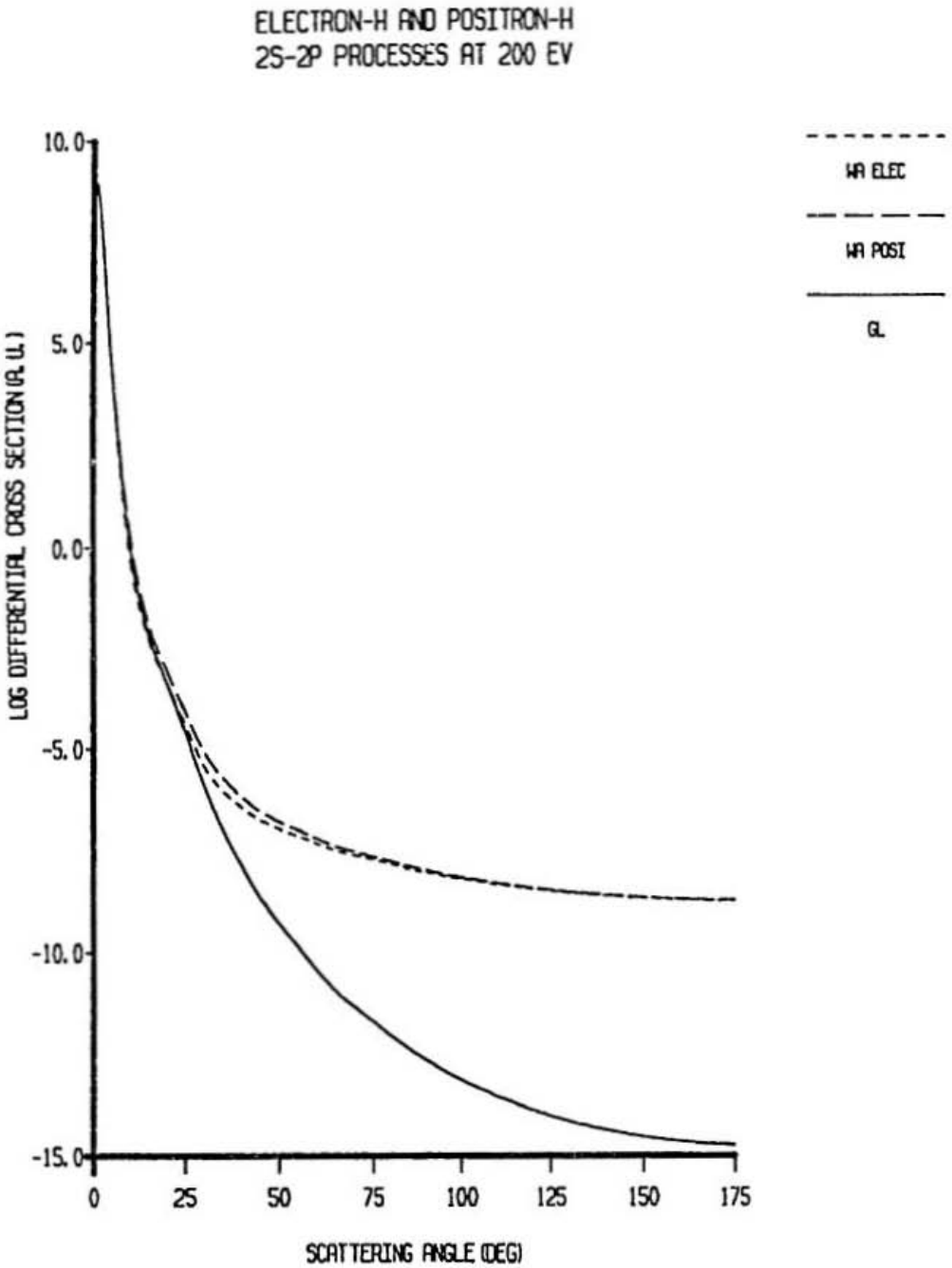

Figure 3.17: e^--H and e^+-H 2s-2p processes at 200 eV in the Wallace approximation(WA) and the Glauber approximation(GL).

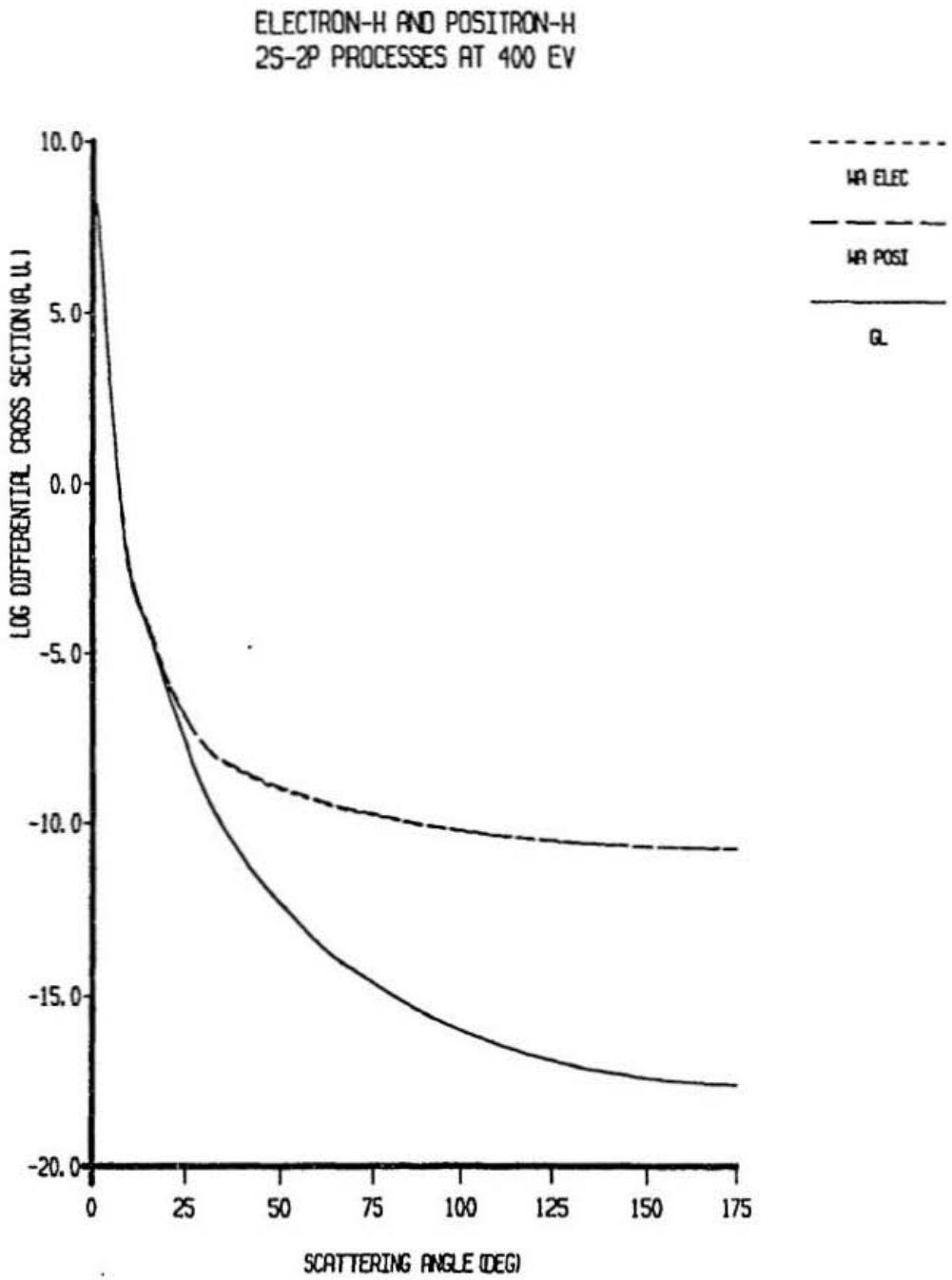

Figure 3.18: e^--H and e^+-H 2s-2p processes at 400 eV in the Wallace approximation(WA) and the Glauber approximation(GL).

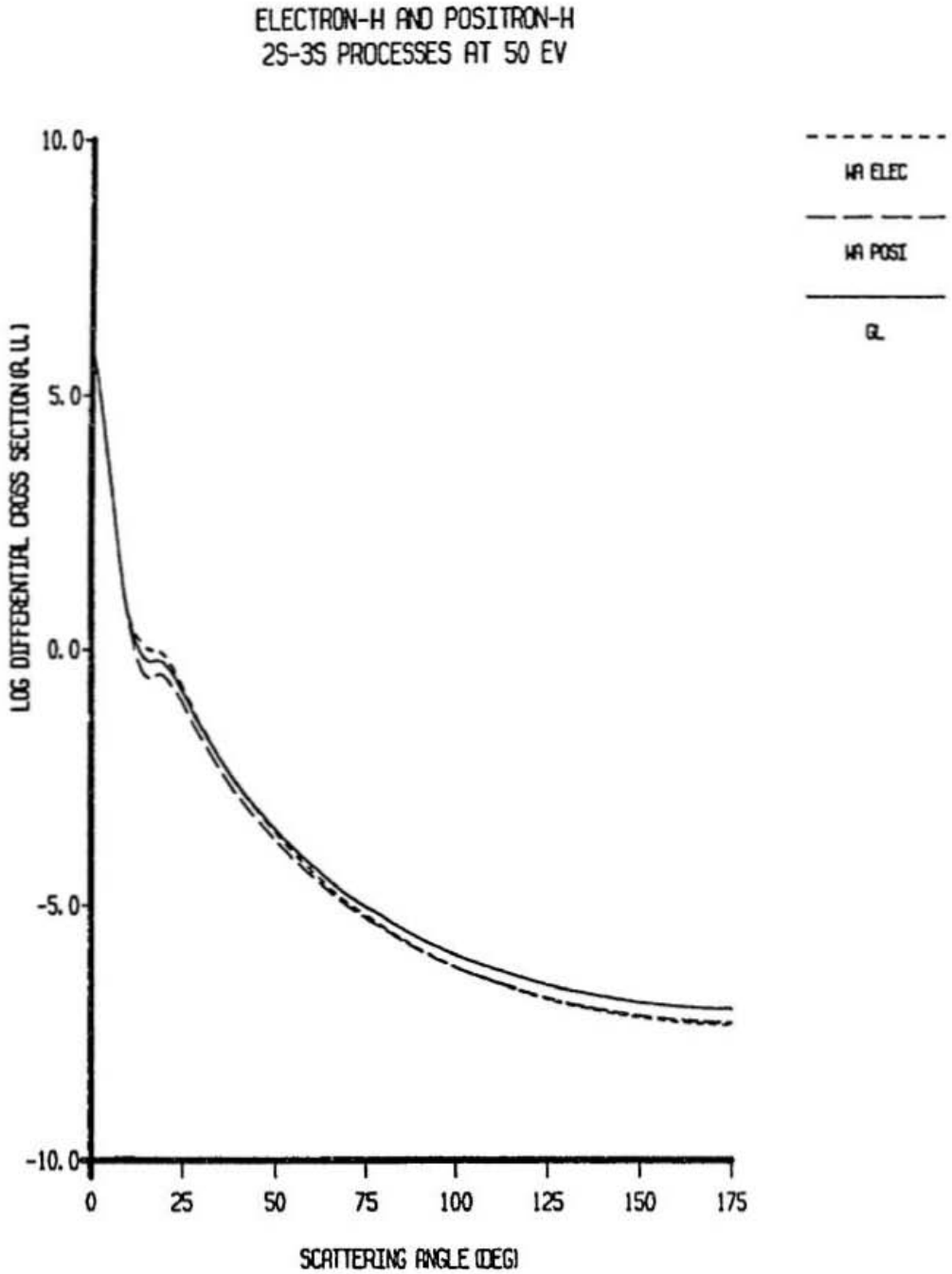

Figure 3.19: e^--H and e^+-H 2s-3s processes at 50 eV in the Wallace approximation(WA) and the Glauber approximation(GL).

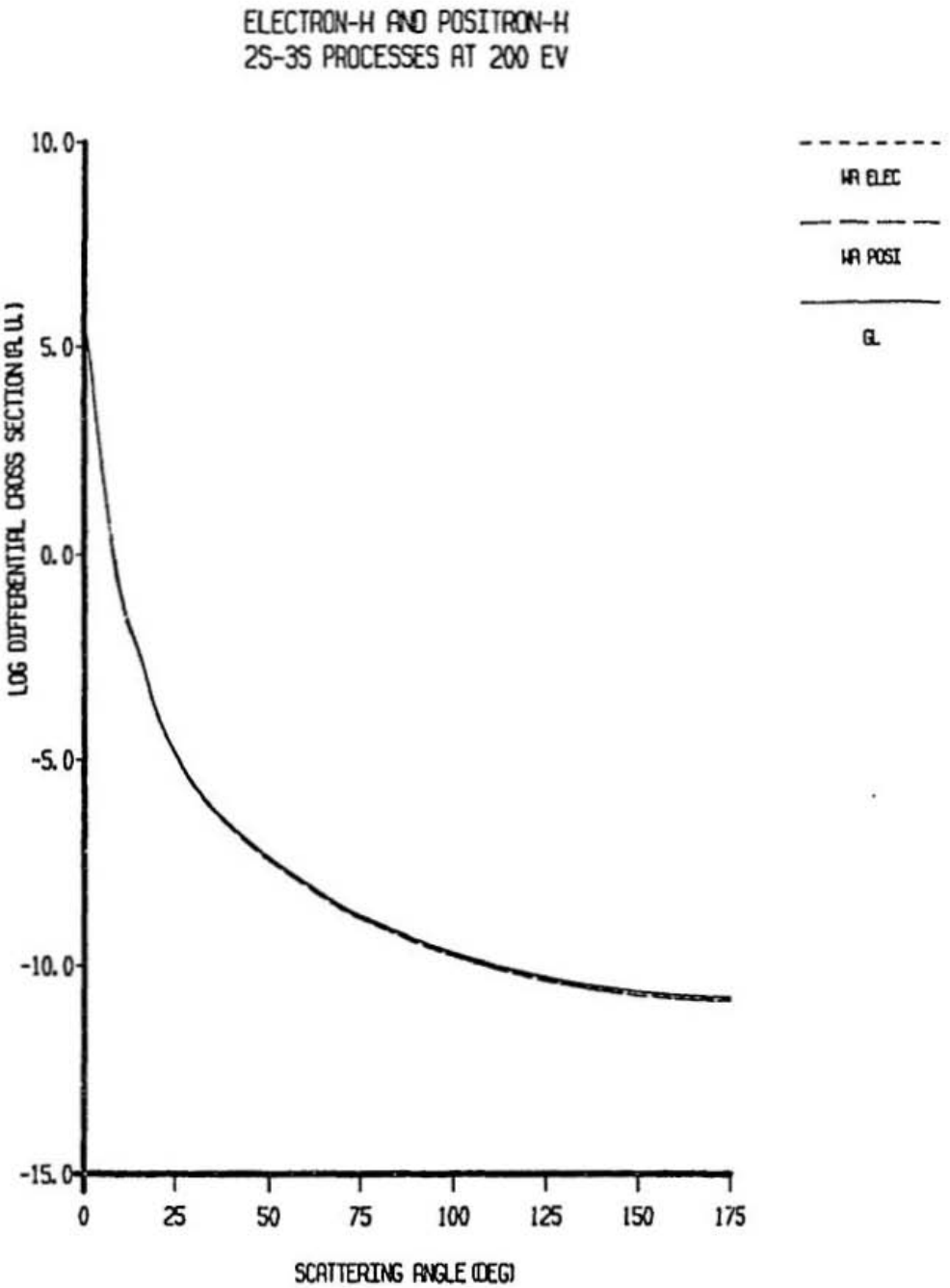

Figure 3.20: e^--H and e^+-H 2s-3s processes at 200 eV in the Wallace approximation(WA) and the Glauber approximation(GL).

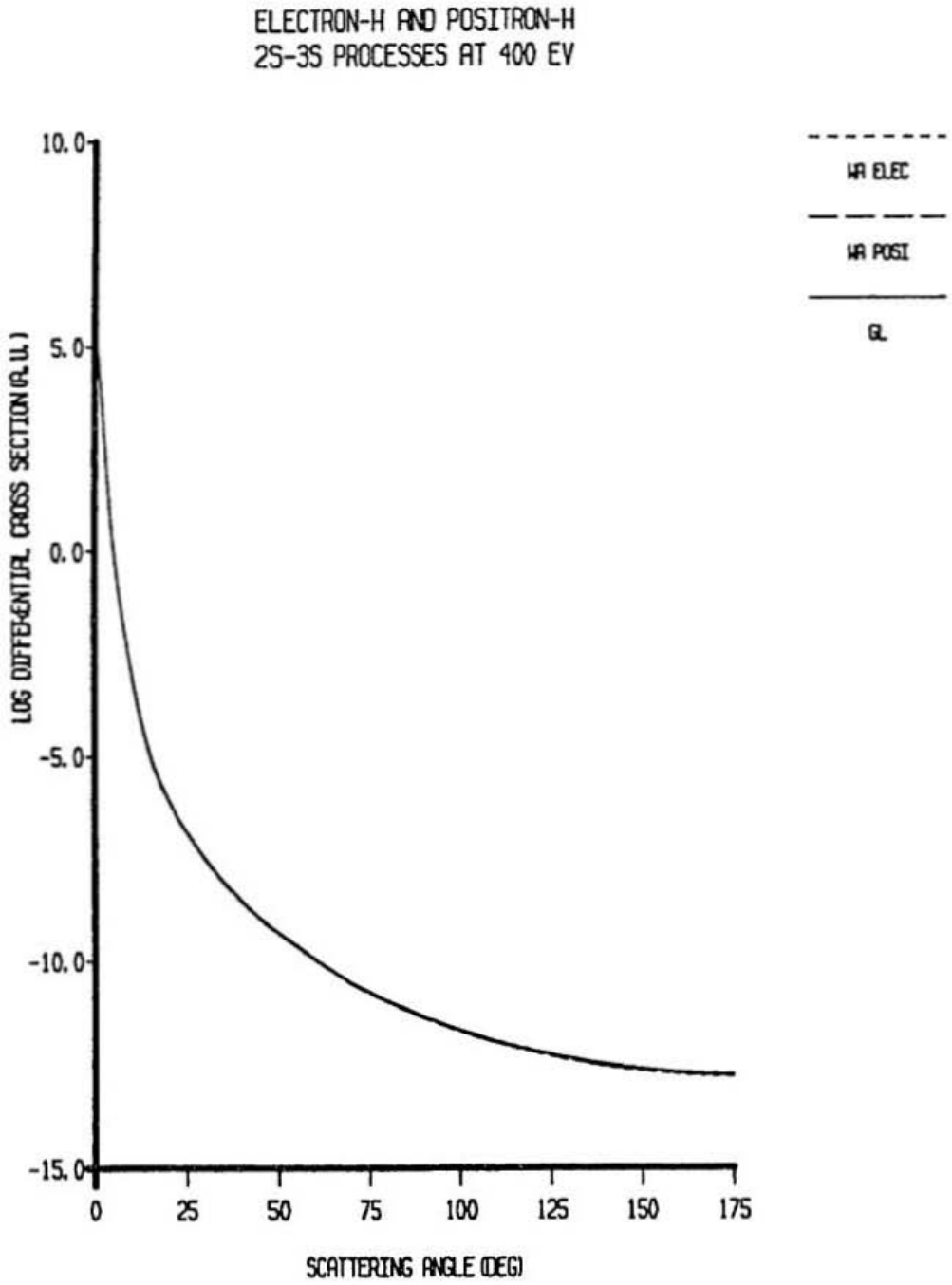

Figure 3.21: e^--H and e^+-H 2s-3s processes at 400 eV in the Wallace approximation(WA) and the Glauber approximation(GL).

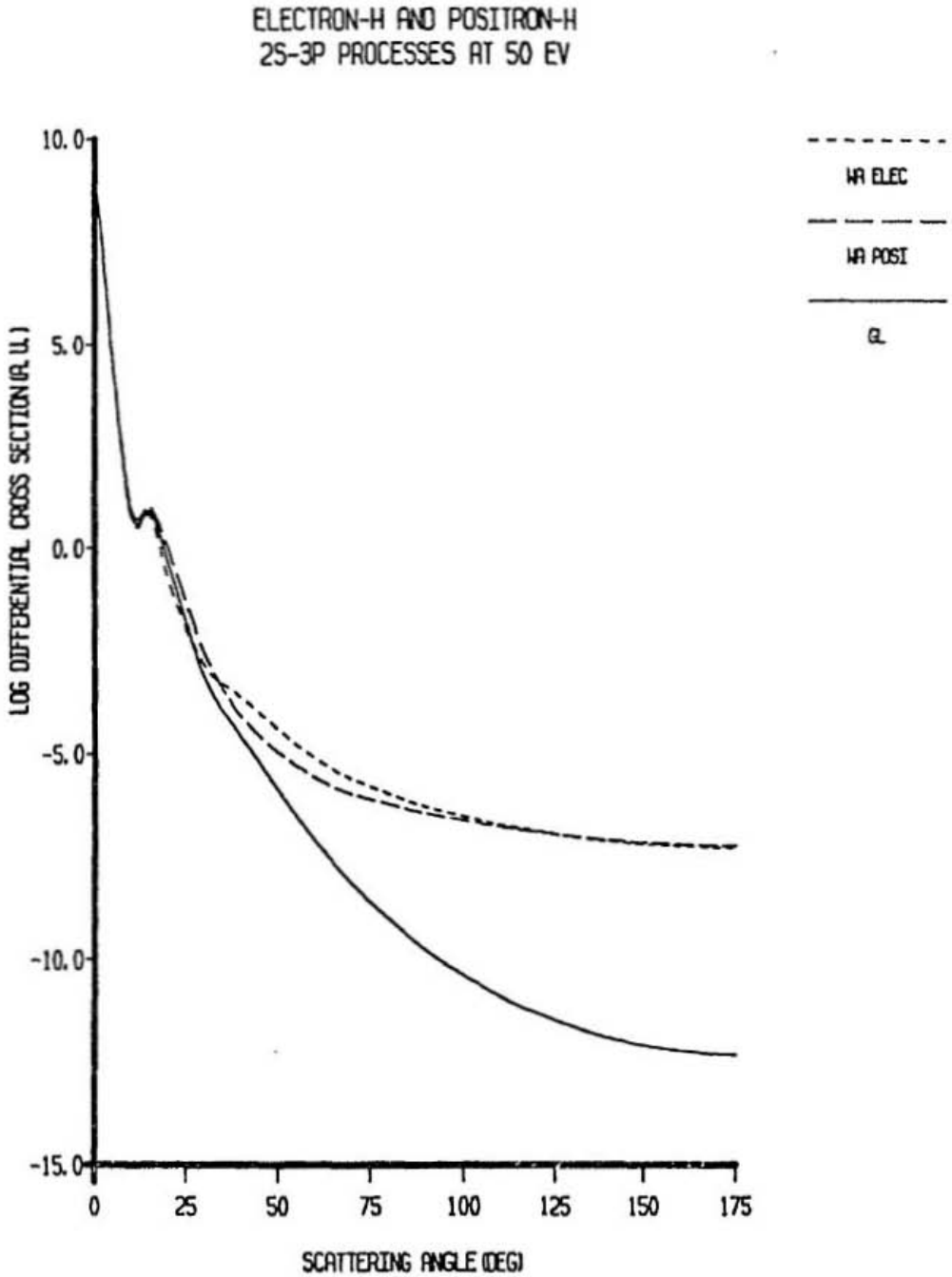

Figure 3.22: e^--H and e^+-H 2s-3p processes at 50 eV in the Wallace approximation(WA) and the Glauber approximation(GL).

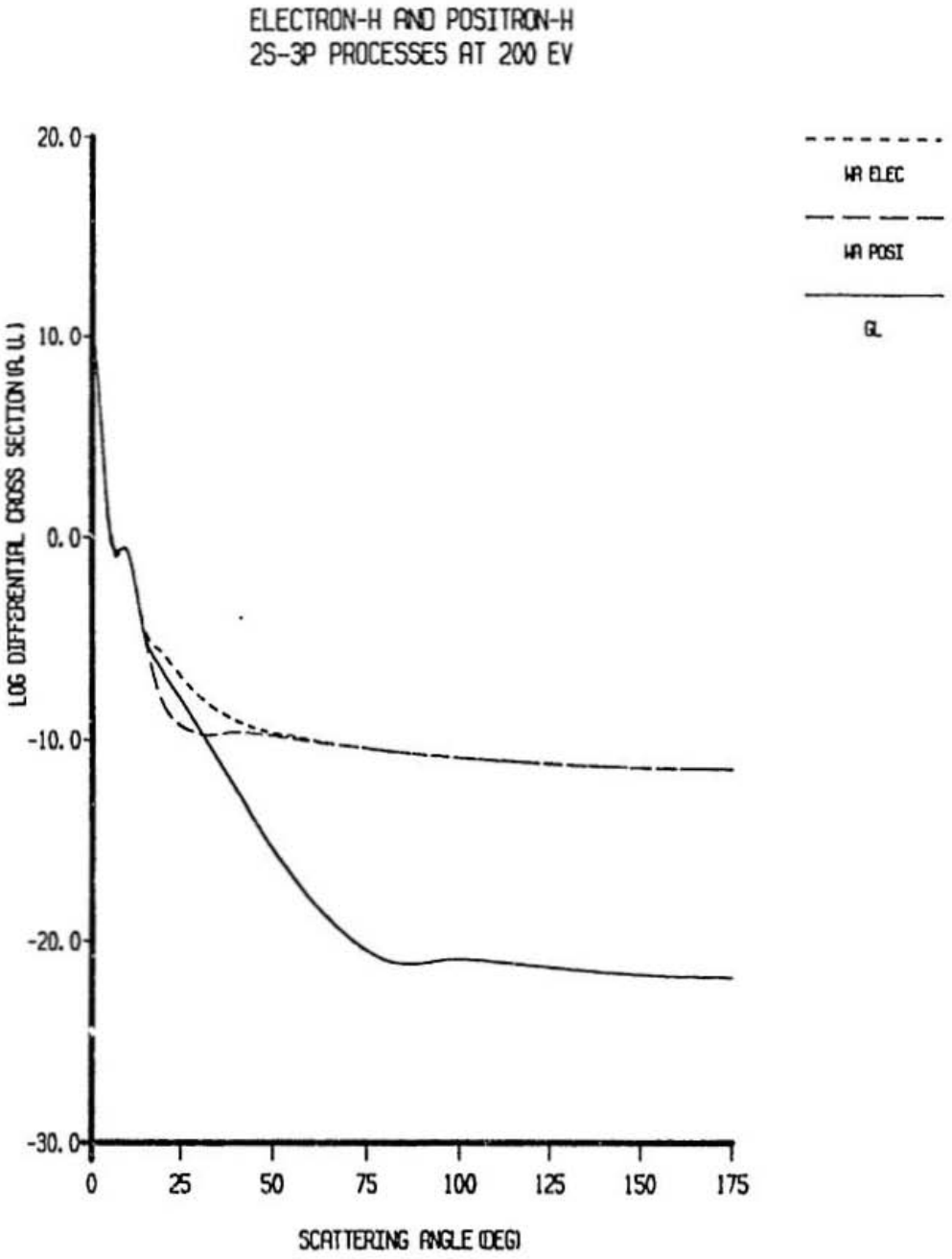

Figure 3.23: e^--H and e^+-H 2s-3p processes at 200 eV in the Wallace approximation(WA) and the Glauber approximation(GL).

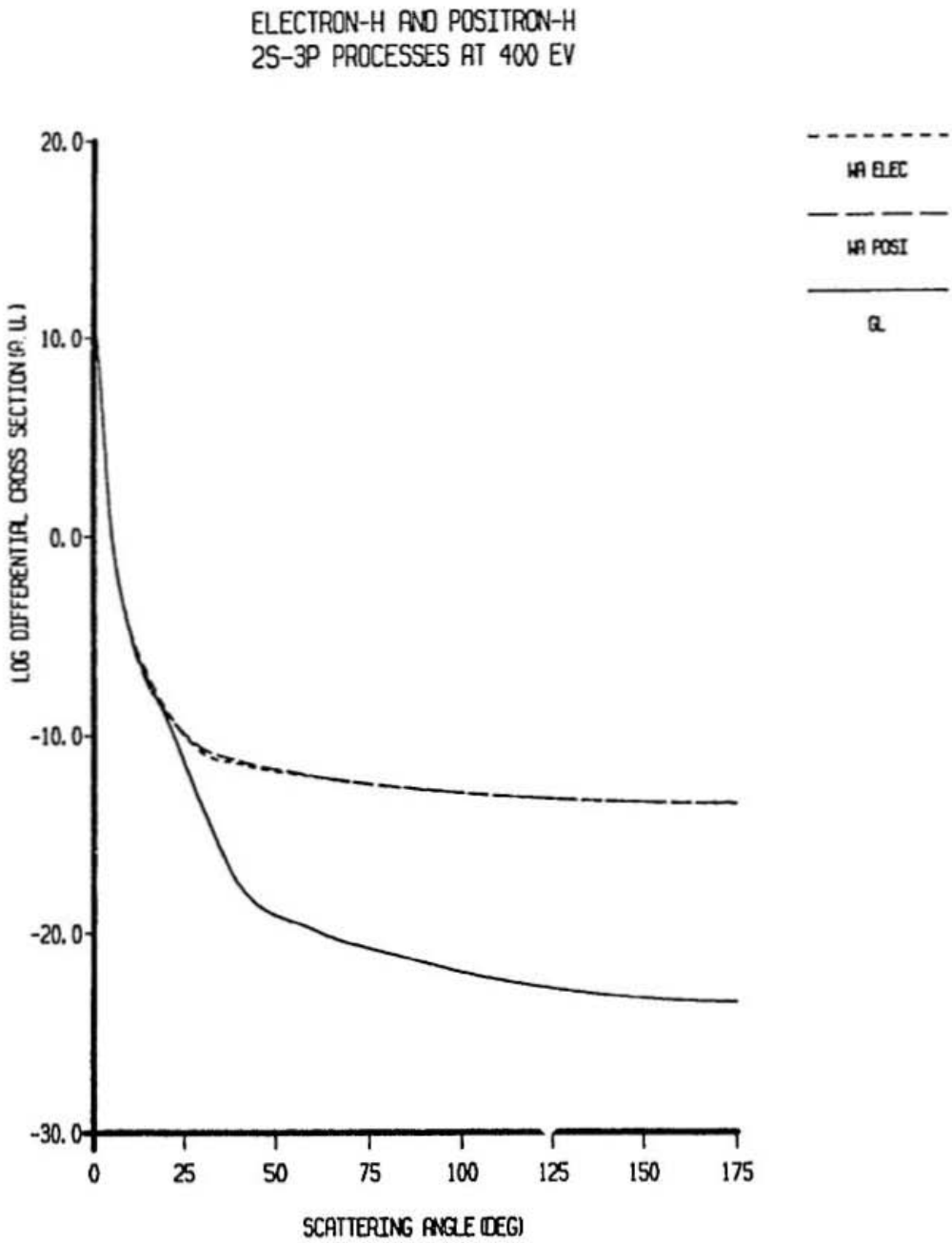

Figure 3.24: e^--H and e^+-H 2s-3p processes at 400 eV in the Wallace approximation(WA) and the Glauber approximation(GL).

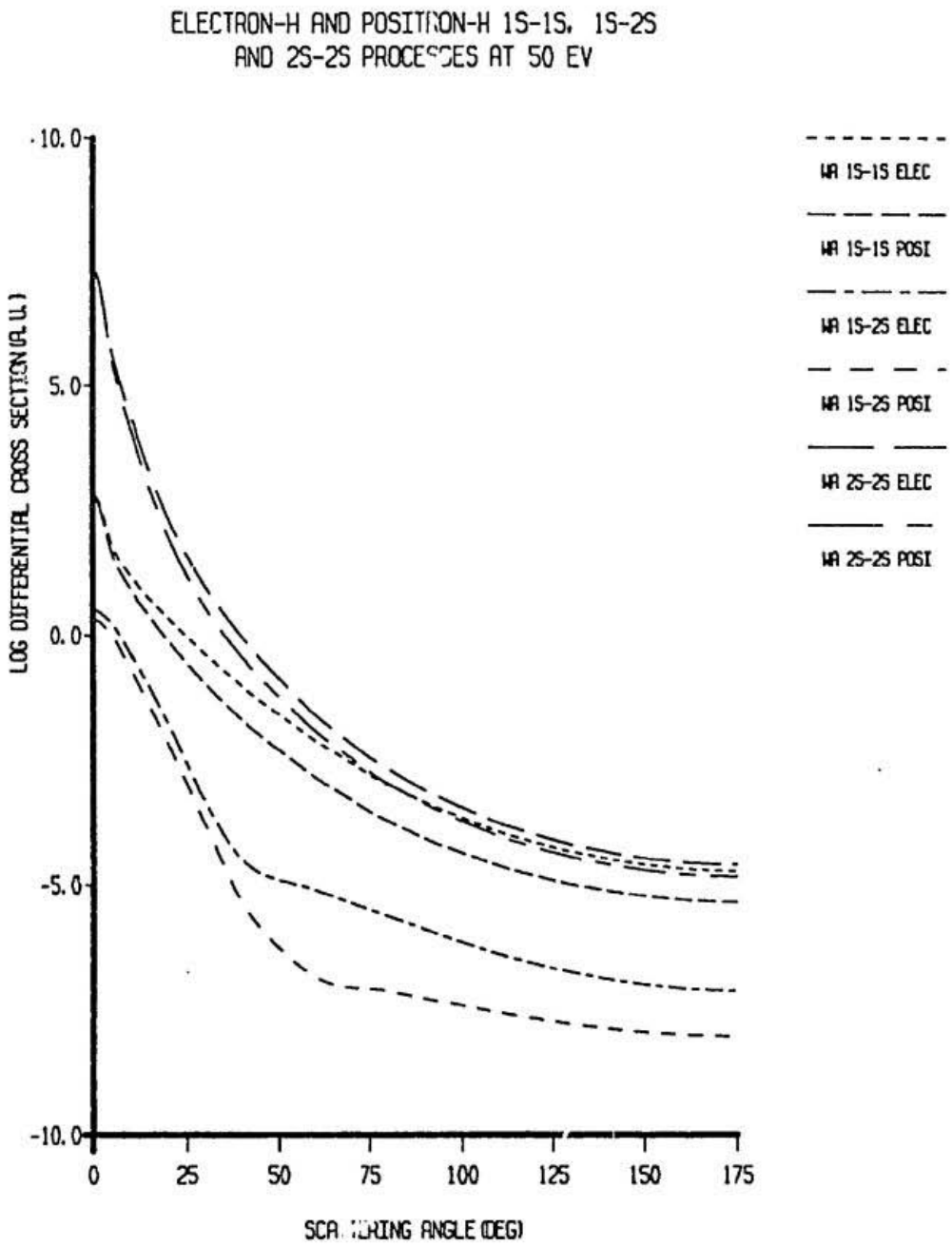

Figure 3.25: e^--H and e^+-H 1s-1s, 1s-2s, and 2s-2s processes at 50 eV in the Wallace approximation(WA).

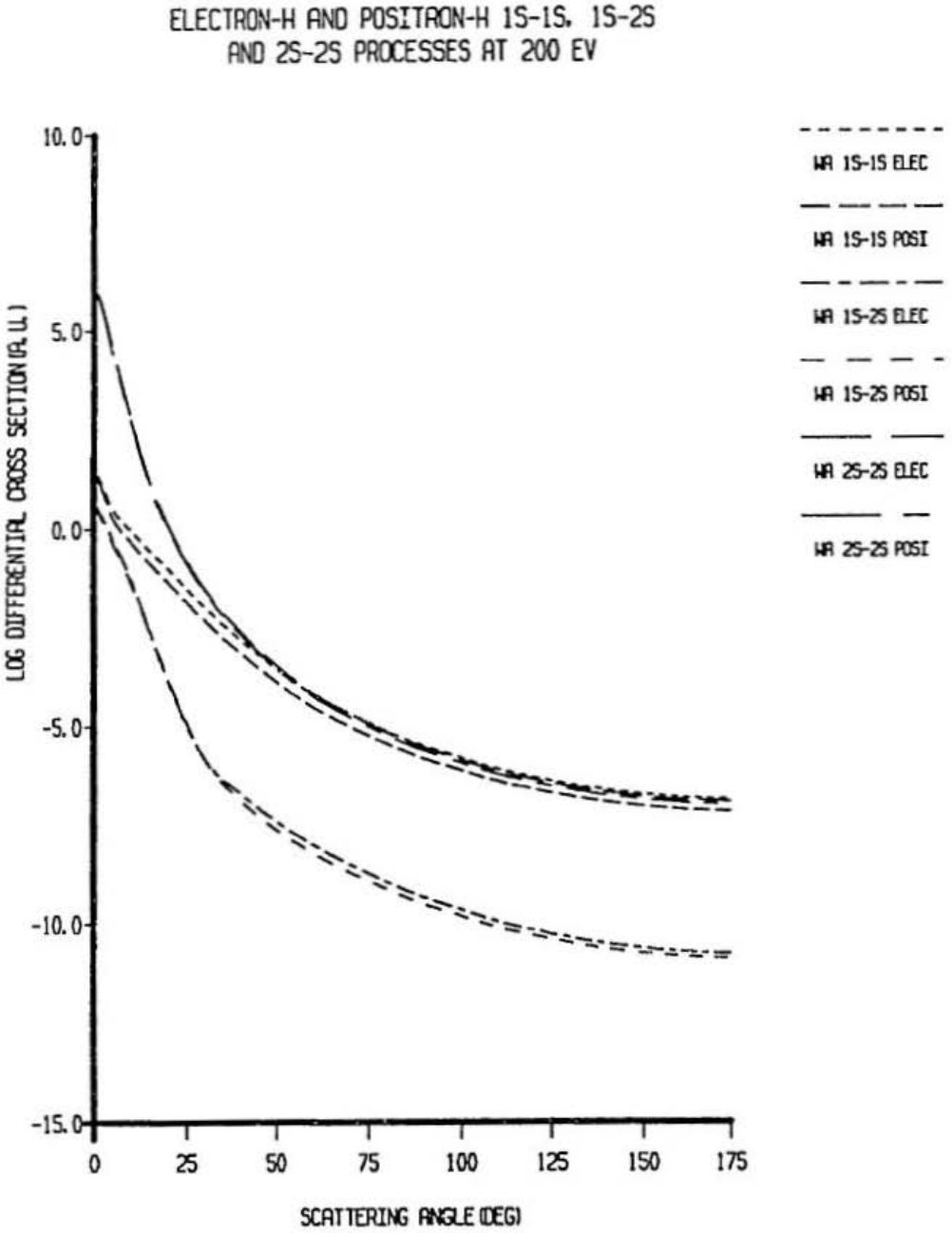

Figure 3.26: e^--H and e^+-H 1s-1s, 1s-2s, and 2s-2s processes at 200 eV in the Wallace approximation(WA).

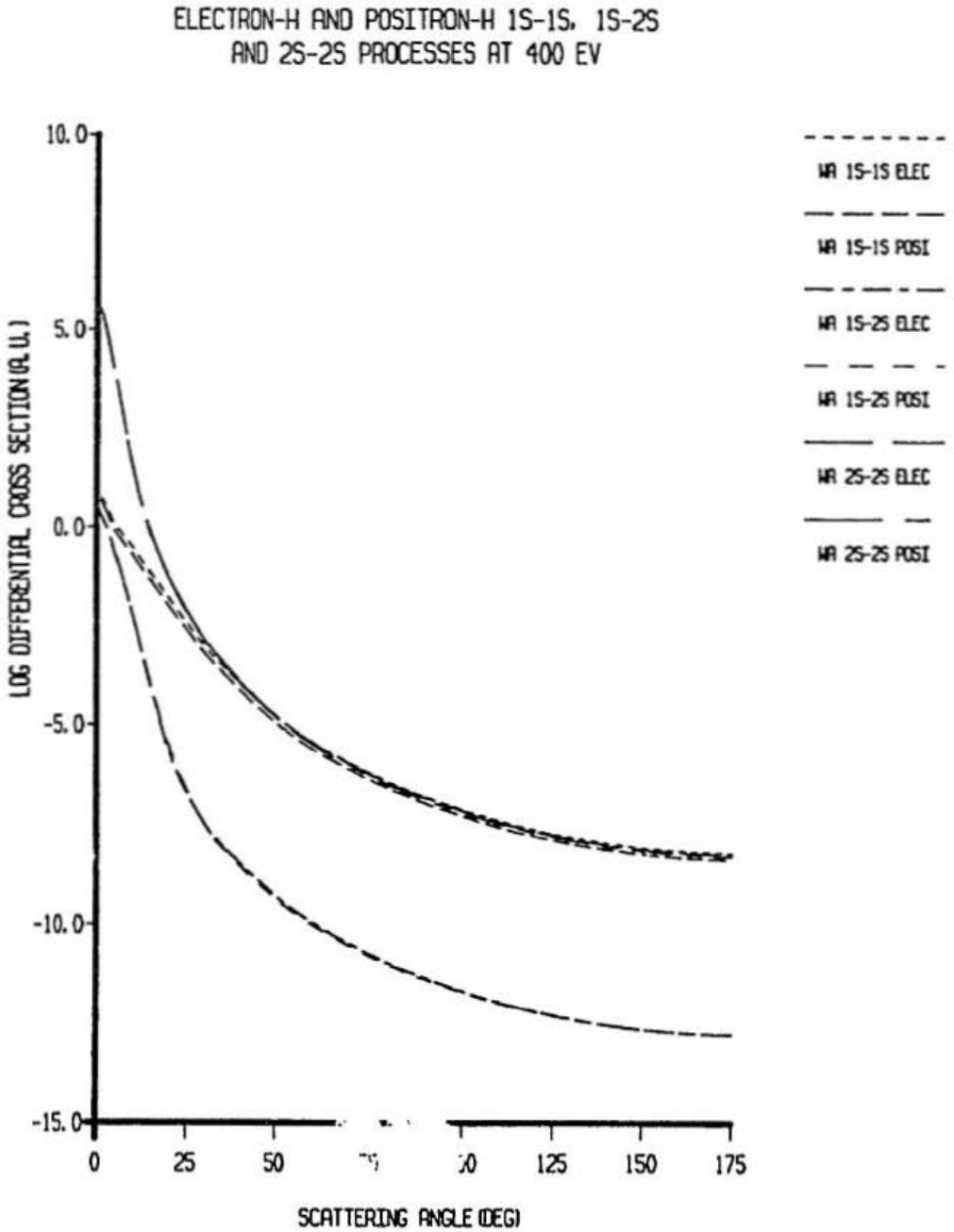

Figure 3.27: e^--H and e^+-H 1s-1s, 1s-2s, and 2s-2s processes at 400 eV in the Wallace approximation(WA).

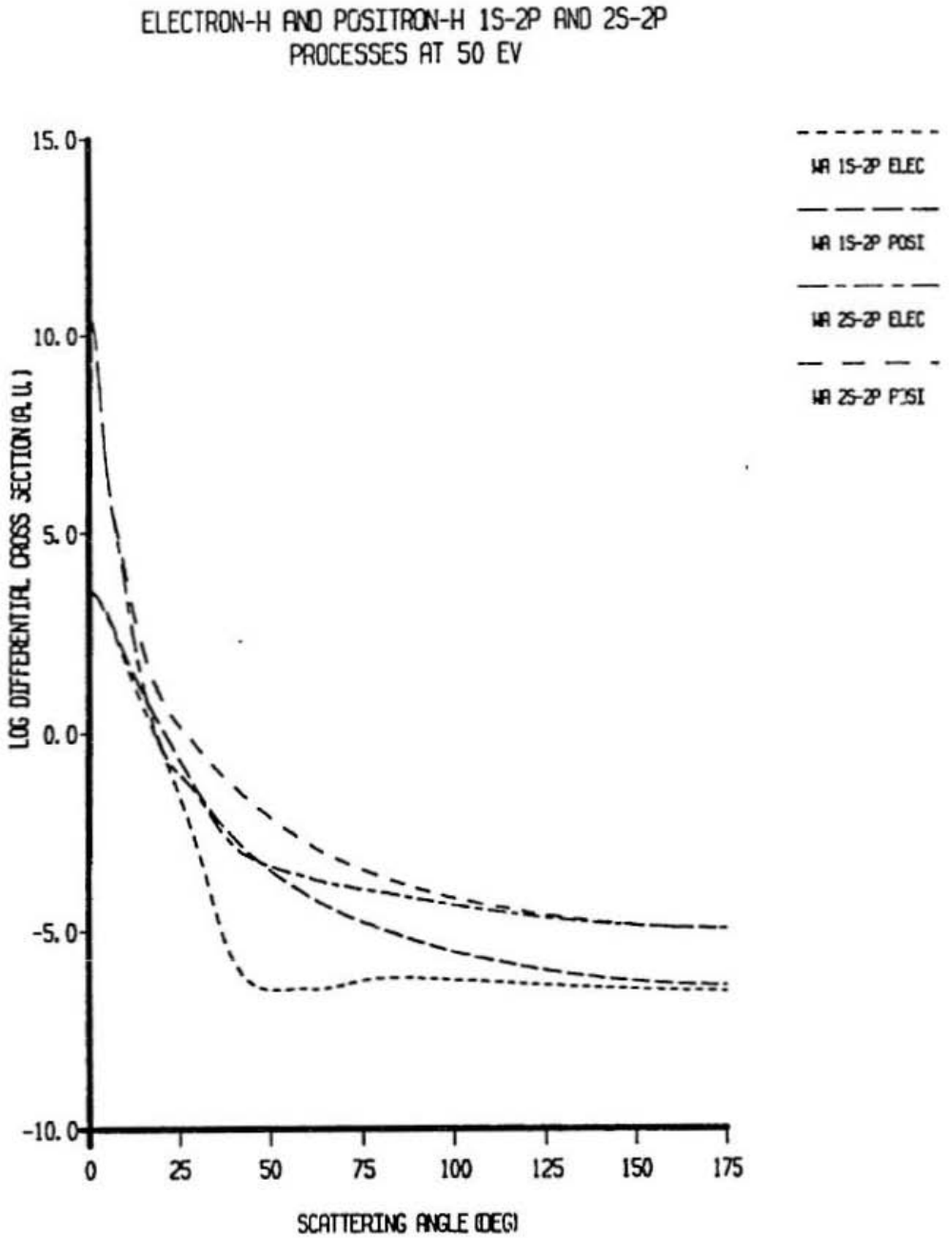

Figure 3.28: e^--H and e^+-H 1s-2p, and 2s-2p processes at 50 eV in the Wallace approximation(WA).

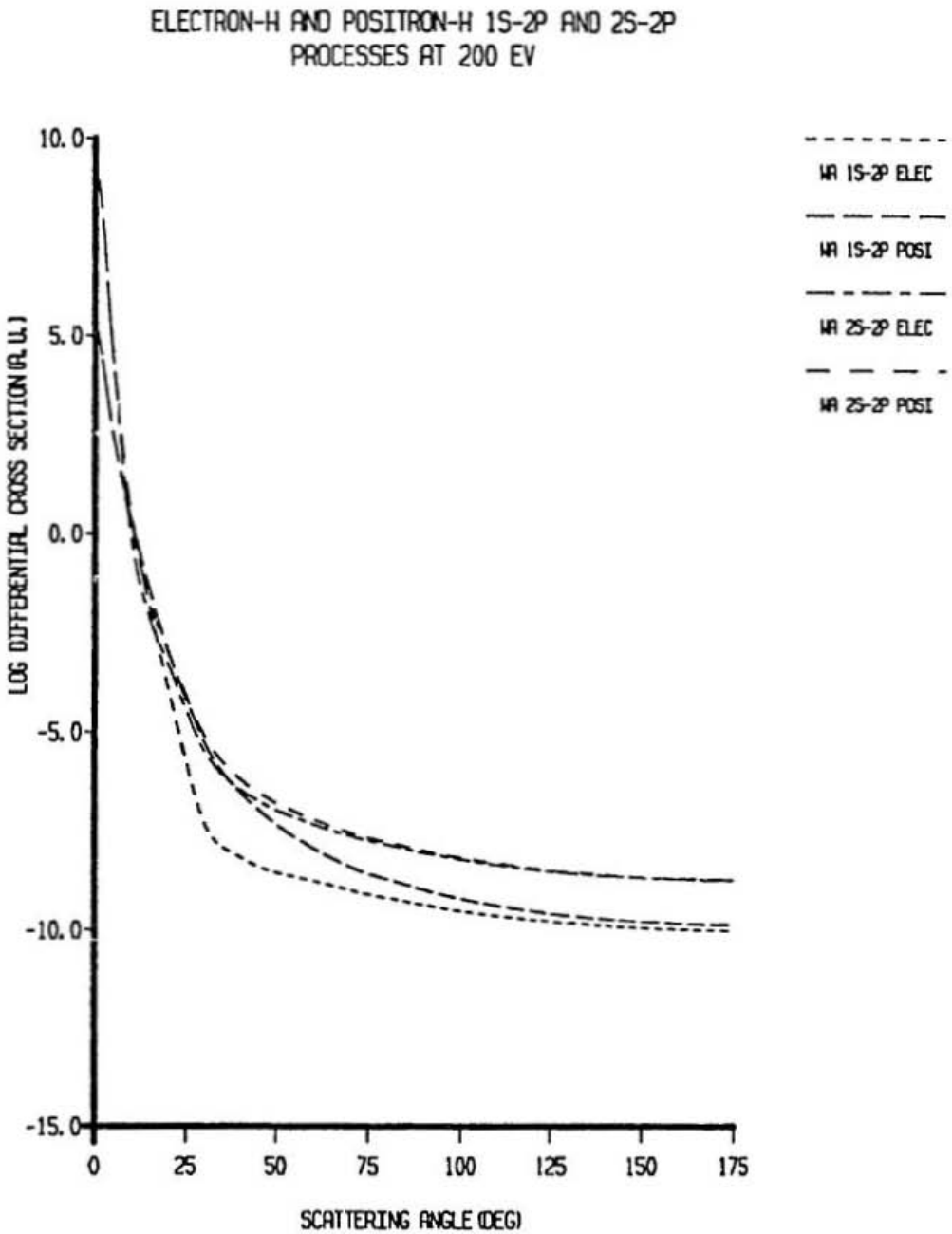

Figure 3.29: e^--H and e^+-H 1s-2p, and 2s-2p processes at 200 eV in the Wallace approximation(WA).

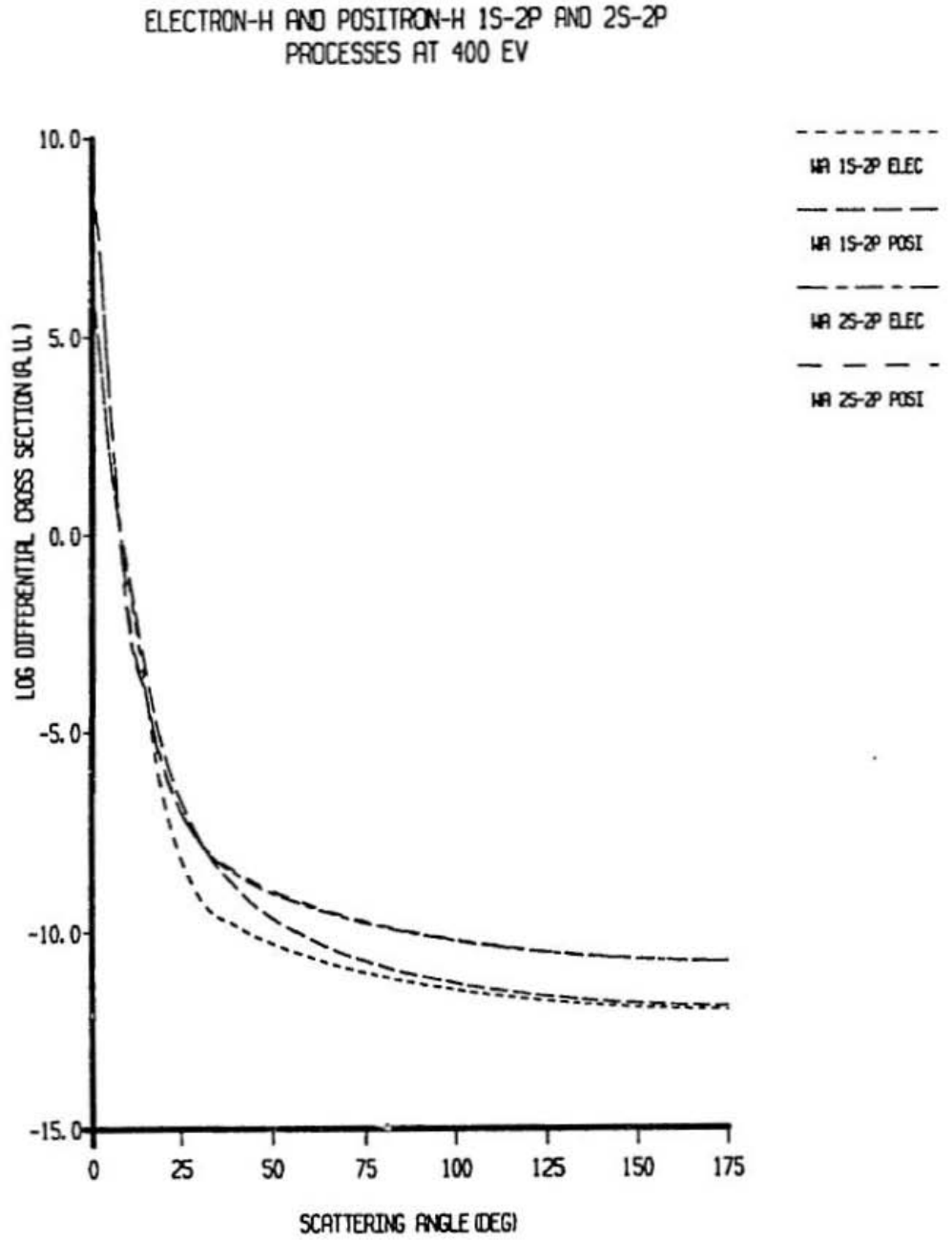

Figure 3.30: e^--H and e^+-H 1s-2p, and 2s-2p processes at 400 eV in the Wallace approximation(WA).

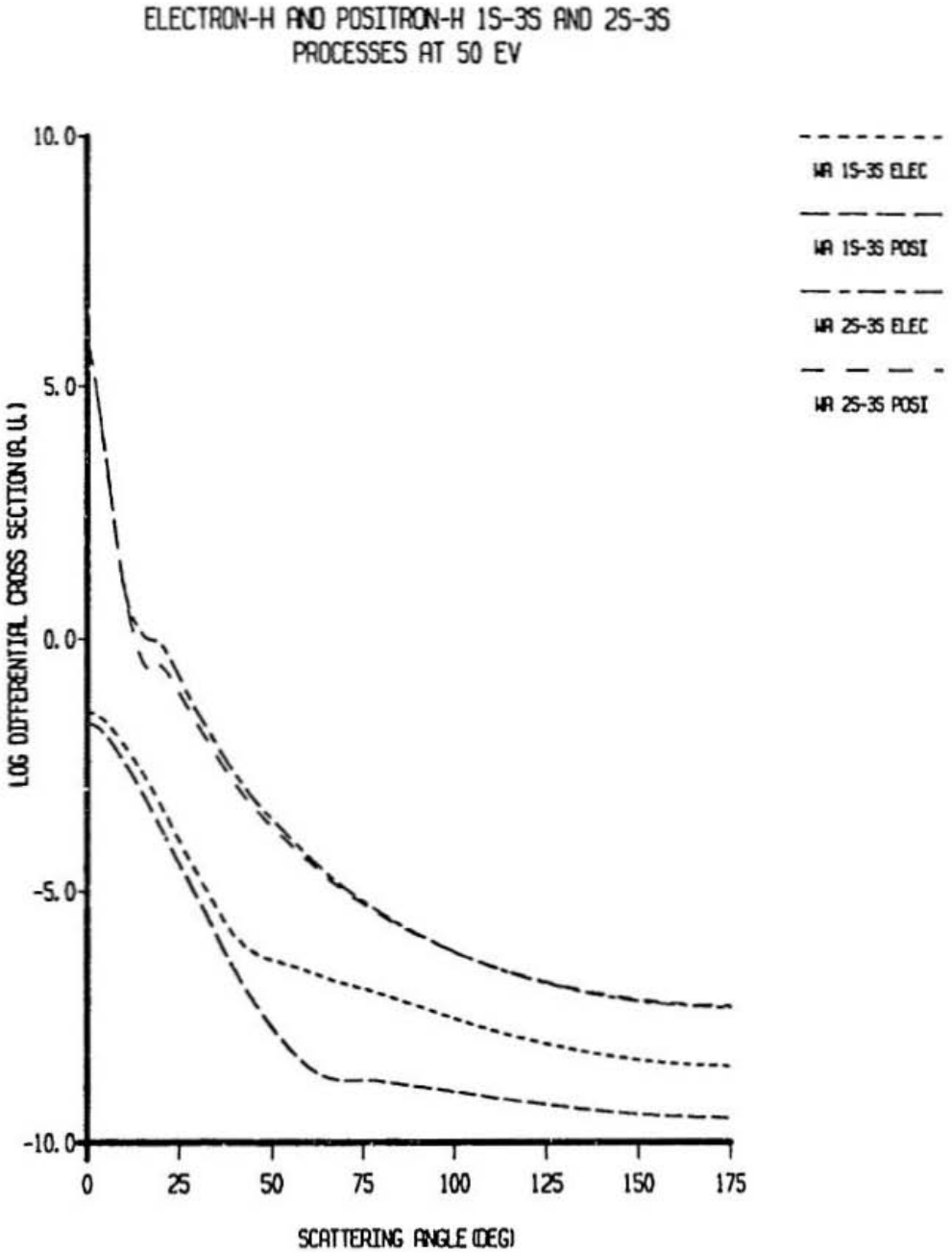

Figure 3.31: e^--H and e^+-H 1s-3s, and 2s-3s processes at 50 eV in the Wallace approximation(WA).

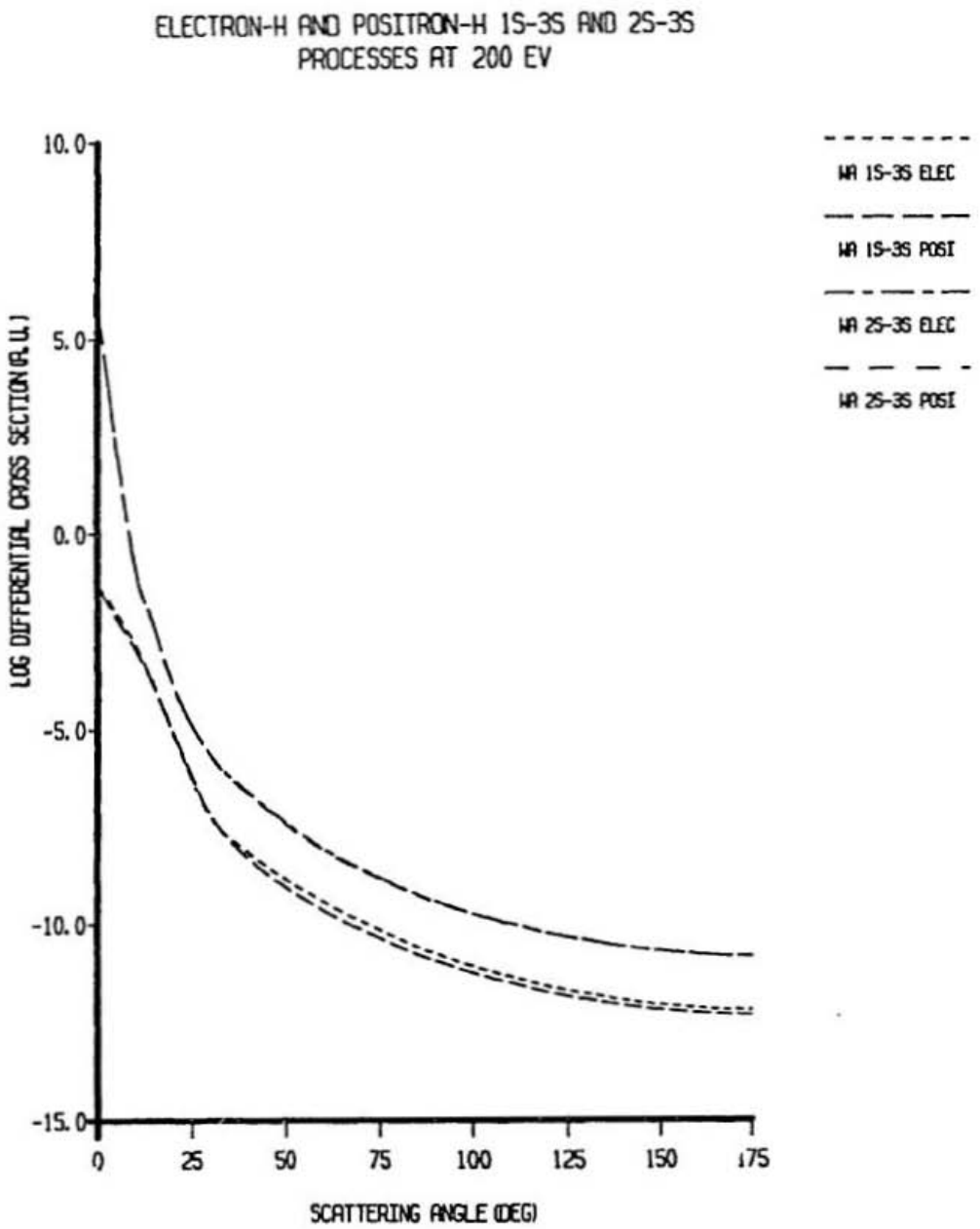

Figure 3.32: e^--H and e^+-H 1s-3s, and 2s-3s processes at 200 eV in the Wallace approximation(WA).

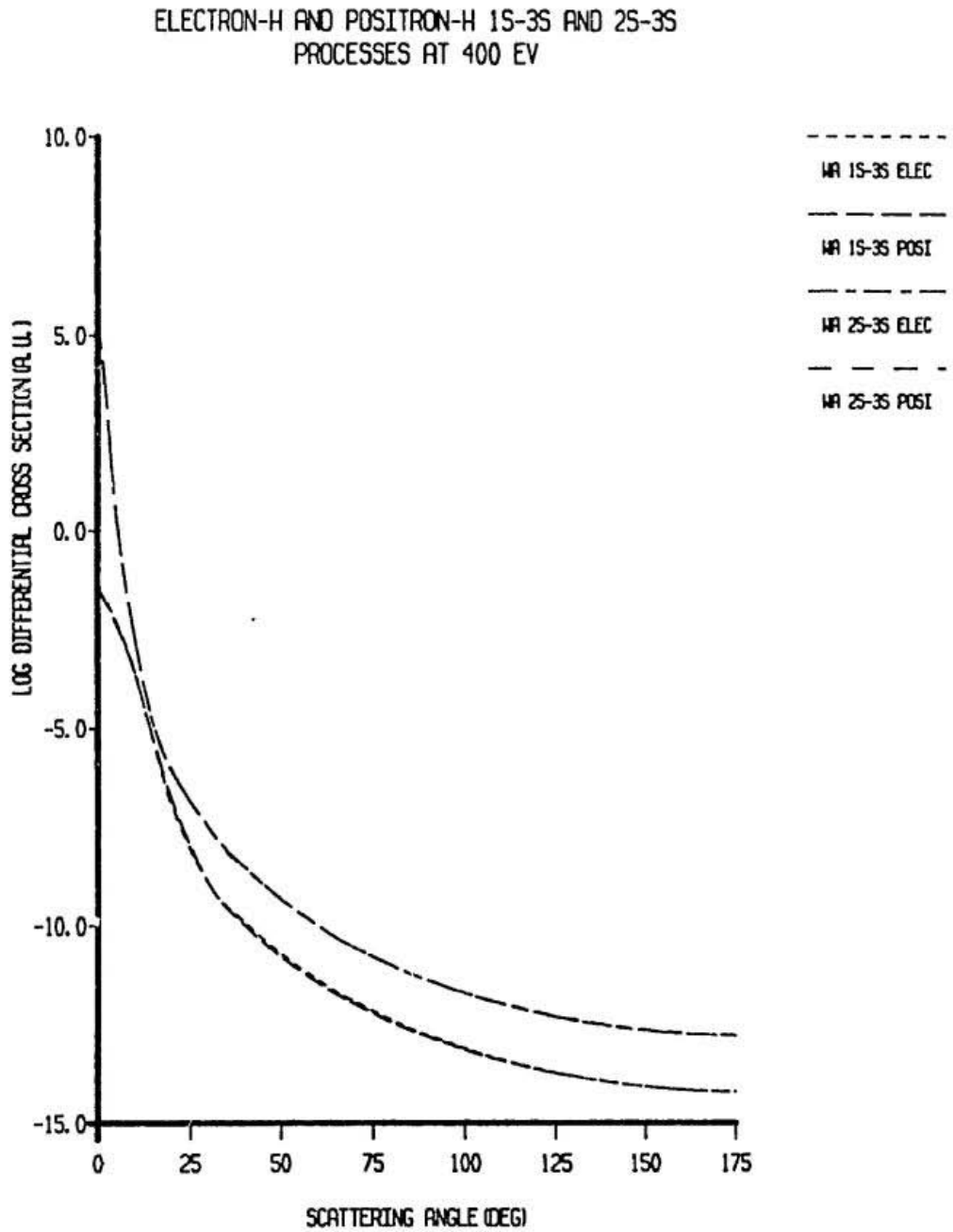

Figure 3.33: e^--H and e^+-H 1s-3s, and 2s-3s processes at 400 eV in the Wallace approximation(WA).

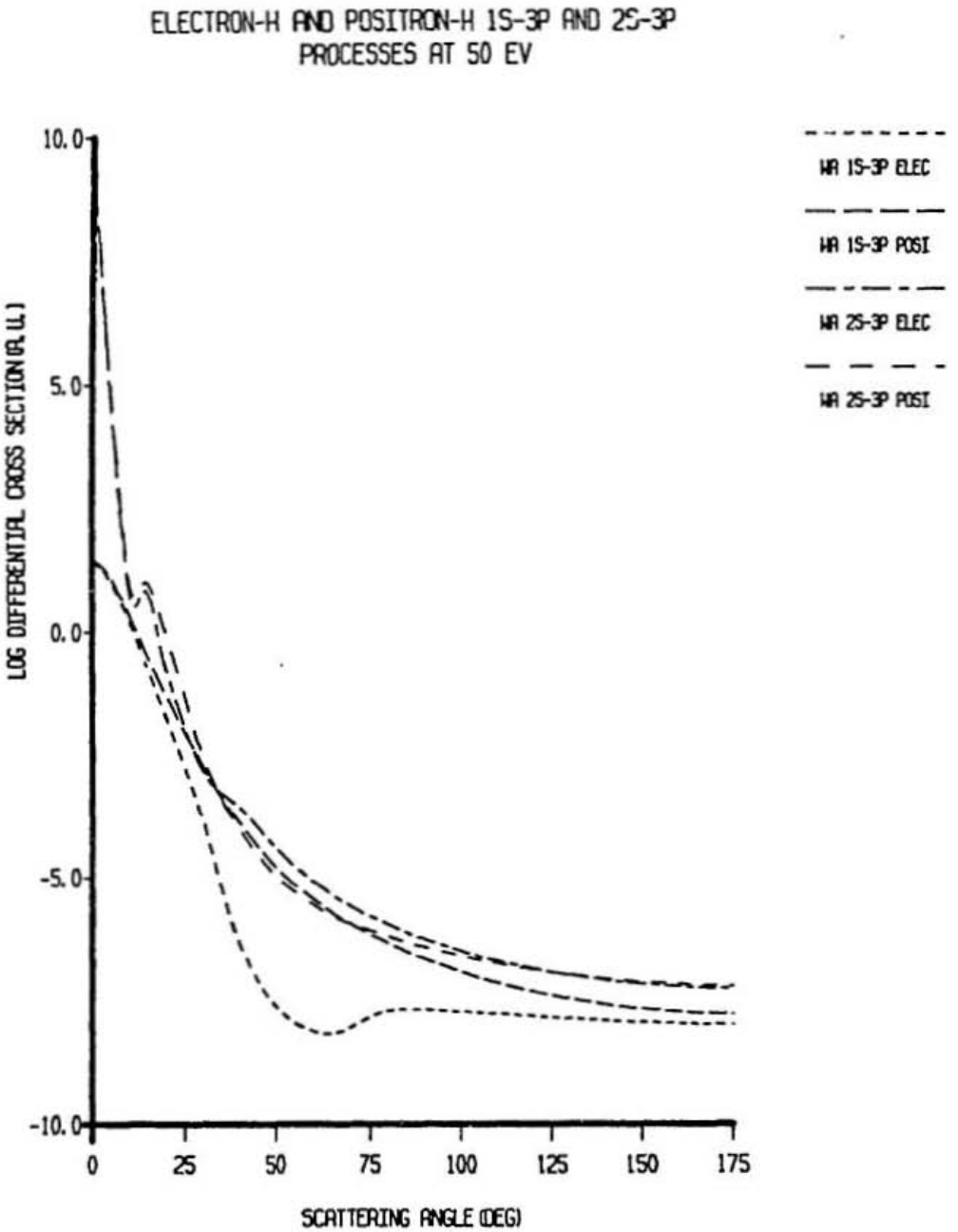

Figure 3.34: e^--H and e^+-H 1s-3p, and 2s-3p processes at 50 eV in the Wallace approximation(WA).

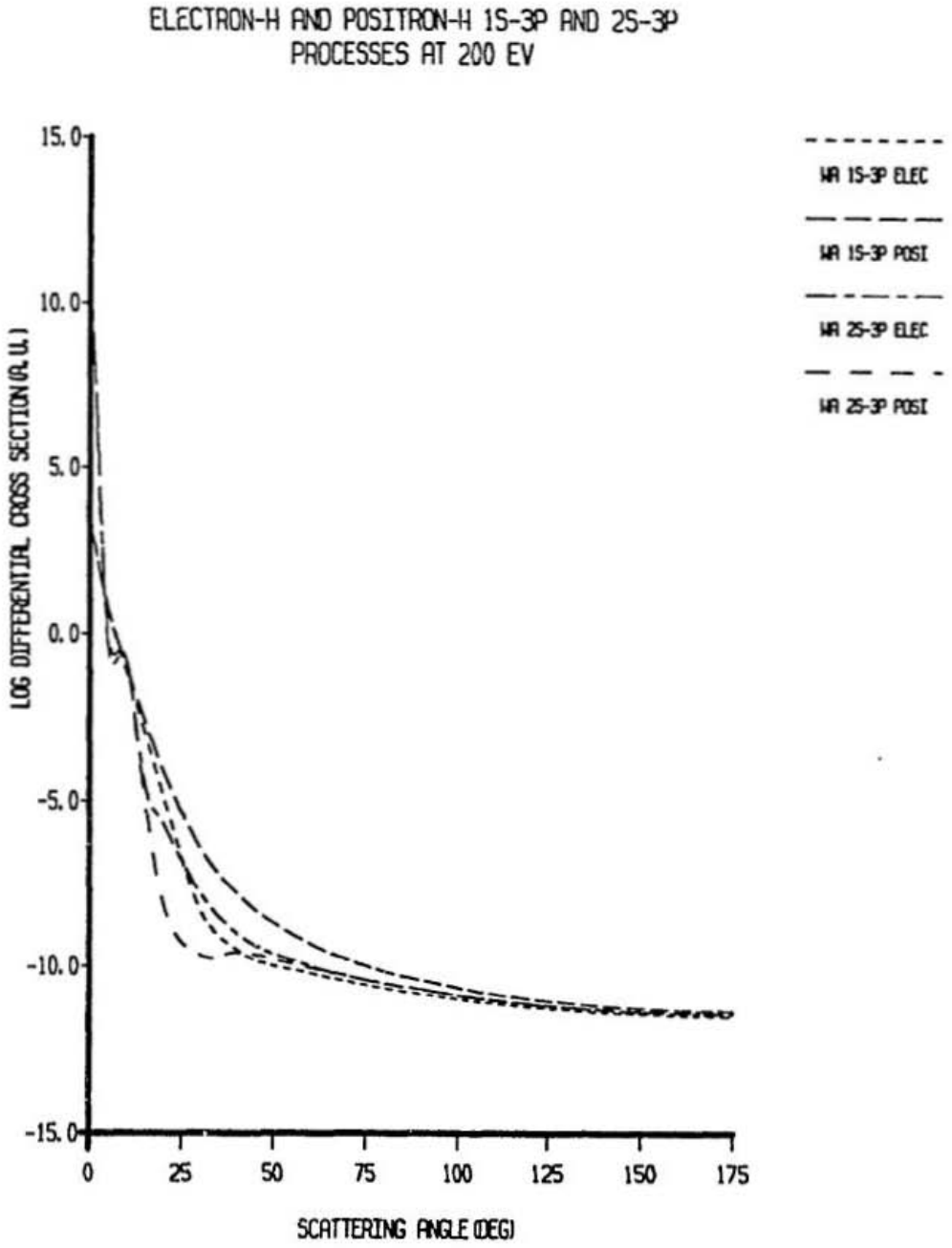

Figure 3.35: e^--H and e^+-H 1s-3p, and 2s-3p processes at 200 eV in the Wallace approximation(WA).

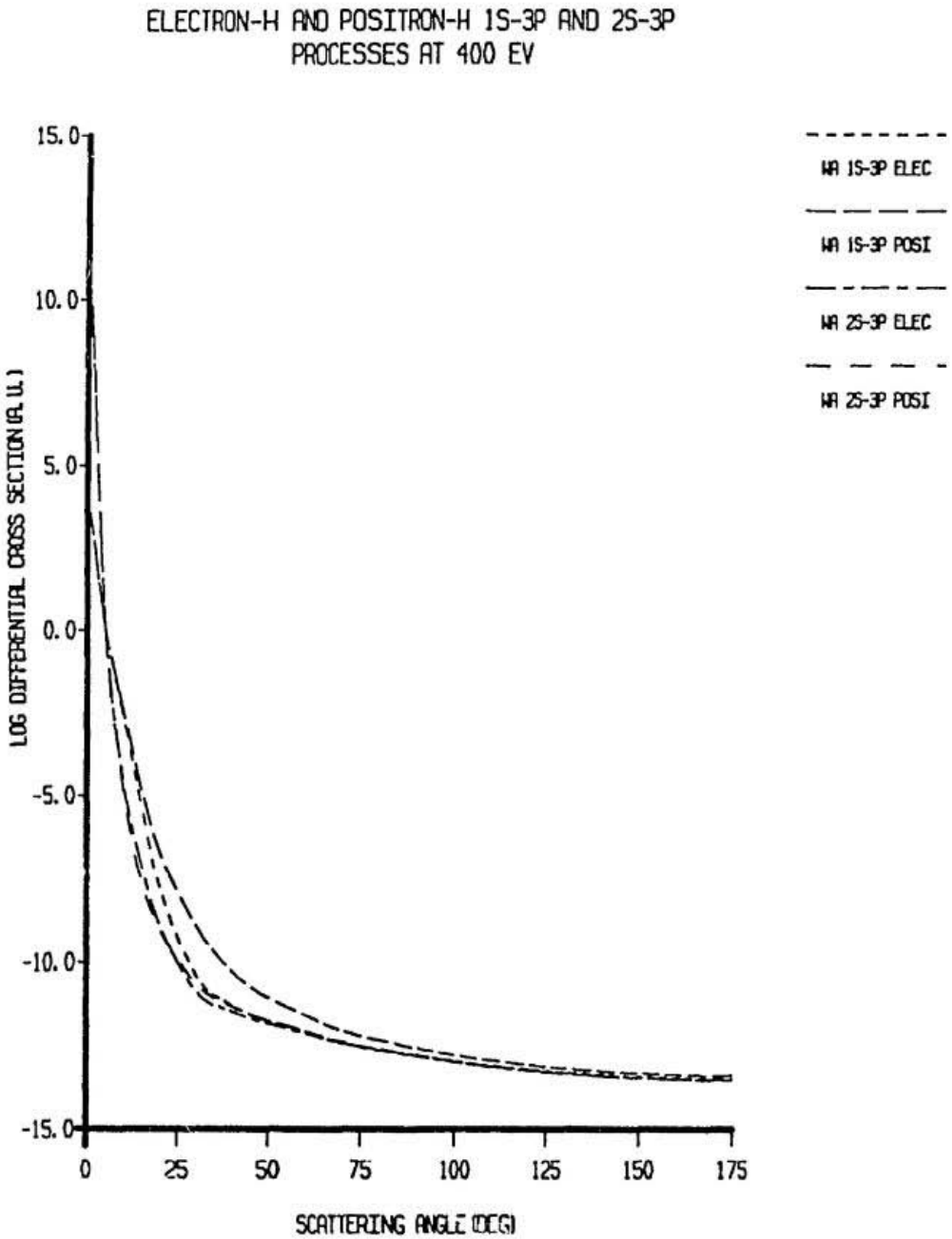

Figure 3.36: e^--H and e^+-H 1s-3p, and 2s-3p processes at 400 eV in the Wallace approximation(WA).

Chapter 4

Conclusions

In this thesis, the Glauber and Wallace approximations have been used to calculate the elastic and inelastic differential cross sections of electron and positron scattering from the metastable hydrogen H(2s) (2s-2s, 2s-2p, 2s-3s, and 2s-3p), as well as from the ground state hydrogen H(1s) (1s-1s,1s-2s, 1s-2p,1s-3s, and 1s-3p), at several intermediate incident energies (from 50 eV to 400 eV). Some general features have been obtained. 1) The Wallace approximation corrects the Glauber one; the corrections are very significant for s-p excitations at large scattering angles. 2) The Wallace approximation predicts different differential cross sections between electron and positron scattering; the difference becomes smaller as the energy becomes higher. 3) The difference between the electron and positron inelastic scattering from H(1s) is more striking than that of the corresponding scattering from H(2s). 4) At small angles, the differential cross sections for the scattering from H(2s) are much larger than those from the corresponding H(1s).

We hope our results will be confirmed experimentally in the near future; although the experimental differential cross sections for electron-H scattering are limited to the 1s-1s

elastic scattering and to the 1s-2s and 1s-2p excitation processes, and as for positron-H scattering there are no experimental results for the differential cross sections so far [45]. We should point out that the future of the application of the Wallace approximation to scattering by atomic targets beyond hydrogen lies on whether the Wallace amplitude can further be reduced to an integral form with the dimension lower than three or even to a closed form.

Appendix A

Some expressions in the Glauber amplitudes

The derivatives of the $\Pi_0(\lambda)$ and $\Pi_1(\lambda)$ defined by eq. (3.15) and eq. (3.16) can be obtained by using the formula [46]:

$$\frac{\partial}{\partial\gamma}F(x,y;z;\gamma)=\frac{xy}{z}F(x+1,y+1;z+1;\gamma). \tag{A.1}$$

We list the final expressions below.

$$\begin{aligned}\frac{\partial\Pi_0}{\partial\lambda} &= -2(1+i\eta)\lambda^{-3-2i\eta}F(1-i\eta,1-i\eta;1;-\frac{\lambda^2}{q^2})\\ &- 2(1-i\eta)^2q^{-2}\lambda^{-1-2i\eta}F(2-i\eta,2-i\eta;2;-\frac{\lambda^2}{q^2}),\end{aligned} \tag{A.2}$$

$$\begin{aligned}\frac{\partial^2\Pi_0}{\partial\lambda^2} &= 2(1+i\eta)(3+2i\eta)\lambda^{-4-2i\eta}F(1-i\eta,1-i\eta;1;-\frac{\lambda^2}{q^2})\\ &+ 2(1-i\eta)^2(3+4i\eta)q^{-2}\lambda^{-2-2i\eta}F(2-i\eta,2-i\eta;2;-\frac{\lambda^2}{q^2})\end{aligned}$$

$$+ \quad 2(1-i\eta)^2(2-i\eta)^2 q^{-4}\lambda^{-2i\eta}F(3-i\eta,3-i\eta;3;-\frac{\lambda^2}{q^2}), \qquad \text{(A.3)}$$

$$\begin{aligned}\frac{\partial^3\Pi_0}{\partial\lambda^3} &= -4(1+i\eta)(2+i\eta)(3+2i\eta)\lambda^{-5-2i\eta}F(1-i\eta,1-i\eta;1;-\frac{\lambda^2}{q^2})\\ &- 24(1+i\eta)^2(1-i\eta)^2 q^{-2}\lambda^{-3-2i\eta}F(2-i\eta,2-i\eta;2;-\frac{\lambda^2}{q^2})\\ &- 6(1-i\eta)^2(2-i\eta)^2(1+2i\eta)q^{-4}\lambda^{-1-2i\eta}F(3-i\eta,3-i\eta;3;-\frac{\lambda^2}{q^2})\\ &- \frac{4}{3}(1-i\eta)^2(2-i\eta)^2(3-i\eta)^2 q^{-6}\lambda^{1-2i\eta}F(4-i\eta,4-i\eta;4;-\frac{\lambda^2}{q^2}), \qquad \text{(A.4)}\end{aligned}$$

$$\begin{aligned}\frac{\partial^4\Pi_0}{\partial\lambda^4} &= 4(1+i\eta)(2+i\eta)(3+2i\eta)(5+2i\eta)\lambda^{-6-2i\eta}F(1-i\eta,1-i\eta;1;-\frac{\lambda^2}{q^2})\\ &+ 8(1+i\eta)(3+2i\eta)(1-i\eta)^2(5+4i\eta)q^{-2}\lambda^{-4-2i\eta}F(2-i\eta,2-i\eta;2;-\frac{\lambda^2}{q^2})\\ &+ 6(1-i\eta)^2(2-i\eta)^2(5-8\eta^2+12i\eta)q^{-4}\lambda^{-2-2i\eta}F(3-i\eta,3-i\eta;3;-\frac{\lambda^2}{q^2})\\ &+ \frac{8}{3}(1-i\eta)^2(2-i\eta)^2(3-i\eta)^2(1+4i\eta)q^{-6}\lambda^{-2i\eta}F(4-i\eta,4-i\eta;4;-\frac{\lambda^2}{q^2})\\ &+ \frac{2}{3}(1-i\eta)^2(2-i\eta)^2(3-i\eta)^2(4-i\eta)^2 q^{-8}\lambda^{2-2i\eta}F(5-i\eta,5-i\eta;5;-\frac{\lambda^2}{q^2}) \qquad \text{(A.5)}\end{aligned}$$

And

$$\begin{aligned}\frac{\partial\Pi_1}{\partial\lambda} &= 2(1+i\eta)\lambda^{-3-2i\eta}F(2-i\eta,1-i\eta;1;-\frac{\lambda^2}{q^2})\\ &+ 2(2-i\eta)(1-i\eta)q^{-2}\lambda^{-1-2i\eta}F(3-i\eta,2-i\eta;2;-\frac{\lambda^2}{q^2})\\ &- 2(1+i\eta)^2\lambda^{-3-2i\eta}F(2-i\eta,1-i\eta;2;-\frac{\lambda^2}{q^2})\\ &- (1+i\eta)(1-i\eta)(2-i\eta)q^{-2}\lambda^{-1-2i\eta}F(3-i\eta,2-i\eta;3;-\frac{\lambda^2}{q^2}), \qquad \text{(A.6)}\end{aligned}$$

$$\frac{\partial^2\Pi_1}{\partial\lambda^2} = -2(1+i\eta)(3+2i\eta)\lambda^{-4-2i\eta}F(2-i\eta,1-i\eta;1;-\frac{\lambda^2}{q^2})$$

$$
\begin{aligned}
&- 2(2-i\eta)(1-i\eta)(3+4i\eta)q^{-2}\lambda^{-2-2i\eta}F(3-i\eta,2-i\eta;2;-\frac{\lambda^2}{q^2}) \\
&- 2(2-i\eta)^2(1-i\eta)(3-i\eta)q^{-4}\lambda^{-2i\eta}F(4-i\eta,3-i\eta;3;-\frac{\lambda^2}{q^2}) \\
&+ 2(1+i\eta)^2(3+2i\eta)\lambda^{-4-2i\eta}F(2-i\eta,1-i\eta;2;-\frac{\lambda^2}{q^2}) \\
&+ (1+i\eta)(2-i\eta)(1-i\eta)(3+4i\eta)q^{-2}\lambda^{-2-2i\eta}F(3-i\eta,2-i\eta;3;-\frac{\lambda^2}{q^2}) \\
&+ \frac{2}{3}(1+i\eta)(1-i\eta)(2-i\eta)^2(3-i\eta)q^{-4}\lambda^{-2i\eta}F(4-i\eta,3-i\eta;4;-\frac{\lambda^2}{q^2}), \quad \text{(A.7)}
\end{aligned}
$$

$$
\begin{aligned}
\frac{\partial^3\Pi_1}{\partial\lambda^3} &= 4(1+i\eta)(2+i\eta)(3+2i\eta)\lambda^{-5-2i\eta}F(2-i\eta,1-i\eta;1;-\frac{\lambda^2}{q^2}) \\
&+ 24(1+i\eta)^2(2-i\eta)(1-i\eta)q^{-2}\lambda^{-3-2i\eta}F(3-i\eta,2-i\eta;2;-\frac{\lambda^2}{q^2}) \\
&+ 6(2-i\eta)^2(1-i\eta)(3-i\eta)(1+2i\eta)q^{-4}\lambda^{-1-2i\eta}F(4-i\eta,3-i\eta;3;-\frac{\lambda^2}{q^2}) \\
&+ \frac{4}{3}(2-i\eta)^2(1-i\eta)(3-i\eta)^2(4-i\eta)q^{-6}\lambda^{1-2i\eta}F(5-i\eta,4-i\eta;4;-\frac{\lambda^2}{q^2}) \\
&- 4(1+i\eta)^2(3+2i\eta)(2+i\eta)\lambda^{-5-2i\eta}F(2-i\eta,1-i\eta;2;-\frac{\lambda^2}{q^2}) \\
&- 12(1+i\eta)^3(2-i\eta)(1-i\eta)q^{-2}\lambda^{-3-2i\eta}F(3-i\eta,2-i\eta;3;-\frac{\lambda^2}{q^2}) \\
&- 2(1+i\eta)(2-i\eta)^2(1-i\eta)(3-i\eta)(1+2i\eta)q^{-4}\lambda^{-1-2i\eta}F(4-i\eta,3-i\eta;4;-\frac{\lambda^2}{q^2}) \\
&- \frac{1}{3}(1+i\eta)(1-i\eta)(2-i\eta)^2(3-i\eta)^2(4-i\eta)q^{-6}\lambda^{1-2i\eta}\times \\
&\quad F(5-i\eta,4-i\eta;5;-\frac{\lambda^2}{q^2}). \qquad \text{(A.8)}
\end{aligned}
$$

Appendix B

Derivations of the Wallace amplitudes for $e^{\pm}$-H scattering

If we use a cylindrical coordinate system in which the z direction is perpendicular to $\vec{q}$, the coordinates of the incident particle with respect to the atomic nucleus is $\vec{r}_0 = \vec{b}_0 + \vec{z}_0$, and the coordinate of the target electron is $\vec{r}_1 = \vec{b}_1 + \vec{z}_1$. The phase correction term χ_1 for the potential

$$V = Q(\frac{1}{r_0} - \frac{1}{|\vec{r}_0 - \vec{r}_1|}) \tag{B.1}$$

has been put into a closed form by Byron et al. [36] and subsequent., by Unnikrishnan et al. [38]:

$$\chi_1 = \frac{1}{b_0}(I_1 + \frac{\vec{b}_0 \cdot \vec{a}}{b_0 a^2} I_2), \tag{B.2}$$

where

$$\vec{a} = \frac{\vec{b}_1 - \vec{b}_0}{b_0}, \tag{B.3}$$

$$I_1 = 2gK(\nu), \tag{B.4}$$

$$I_2 = 2g^{-1}E(\nu), \tag{B.5}$$

$$g = \frac{2}{A+B}, \tag{B.6}$$

$$\nu = \frac{2}{A+B}\sqrt{AB}, \tag{B.7}$$

$$A = \sqrt{\gamma^2+(1+a)^2}, \tag{B.8}$$

$$B = \sqrt{\gamma^2+(1-a)^2}, \tag{B.9}$$

$$\gamma = z_1/b_0. \tag{B.10}$$

The functions $K(\nu)$ and $E(\nu)$ are the complete elliptic integrals of the first and second kind respectively:

$$K(\nu) = \int_0^{\pi/2} \frac{d\phi}{\sqrt{1-\nu^2\sin^2\phi}}, \tag{B.11}$$

$$E(\nu) = \int_0^{\pi/2} \sqrt{1-\nu^2\sin^2\phi}\,d\phi. \tag{B.12}$$

Let us derive $W(\vec{k}_f,\vec{k}_0)$ for 2s-2s case. The wavefunctions of hydrogen are

$$\Psi_0(r_1) = \Psi_f(r_1) = \frac{1}{2\sqrt{8\pi}}(2-r_1)\exp(-r_1/2). \tag{B.13}$$

The Glauber phase function χ_0 is

$$\chi_0(\vec{b}_0,\vec{b}_1) = -2Q\ln(\frac{|\vec{b}_1-\vec{b}_0|}{b_0}). \tag{B.14}$$

Substituting eq. (B.2), eq. (B.13) and eq. (B.14) into eq. (3.36), we obtain

$$W(\vec{k}_f,\vec{k}_0) = \frac{ik_0}{64\pi^2}\int(2-r_1)^2\exp(-r_1)(\frac{|\vec{b}_1-\vec{b}_0|}{b_0})^{2i\eta}\{1-\exp[\frac{i}{k_0^3b_0}(I_1+\frac{\vec{b}_0\cdot\vec{a}}{b_0a^2}I_2)]\}$$
$$\times\exp(i\vec{q}\cdot\vec{b}_0)d^2\vec{b}_0d^2\vec{b}_1dz_1, \tag{B.15}$$

where

$$\eta = -Q/k_0. \tag{B.16}$$

Since

$$\vec{b}_1 - \vec{b}_0 = b_0\vec{a}, \tag{B.17}$$

$$z_1 = b_0\gamma, \tag{B.18}$$

then

$$W(\vec{k}_f, \vec{k}_0) = \frac{ik_0}{64\pi^2}\int [2 - b_0(t + 2a\cos\phi_{ab})^{1/2}]^2 \exp[-b_0(t + 2a\cos\phi_{ab})^{1/2}]a^{2i\eta} \times$$
$$\{1 - \exp[\frac{i}{k_0^3 b_0}(I_1 + \frac{\cos\phi_{ab}}{a}I_2)]\}\exp[iqb_0\cos\phi_{bq}] \times$$
$$b_0^4 db_0 d\phi_{b_0} a da d\phi_a d\gamma, \tag{B.19}$$

where

$$t = 1 + a^2 + \gamma^2,$$
$$\phi_{ab} = \phi_a - \phi_{b_0},$$
$$\phi_{bq} = \phi_{b_0} - \phi_q. \tag{B.20}$$

By changing the variable:

$$\phi_{ab} = \phi,$$
$$d\phi_a = d\phi, \tag{B.21}$$

the integral over ϕ_{b_0} can be performed by using the formula (see p360 of ref. [46])

$$\int_0^\pi \exp(iqb_0\cos\phi)d\phi = \pi J_0(qb_0), \tag{B.22}$$

that is,

$$W(\vec{k}_f, \vec{k}_0) = \frac{ik_0}{8\pi}\int_0^\infty da a^{1+2i\eta}\int_0^\infty d\gamma\int_0^\pi d\phi\int_0^\infty db_0 \times$$
$$J_0(qb_0)\exp(-b_0\delta)(2 - b_0\delta)^2[1 - \exp(-M/b_0)]b_0^4, \tag{B.23}$$

where

$$\delta = (1 + a^2 + \gamma^2 + 2a\cos\phi)^{1/2}, \tag{B.24}$$

$$M = -\frac{i}{k_0^3}(I_1 + \frac{\cos\phi}{a} I_2). \tag{B.25}$$

By using the standard formulas [47], the integral of b_0 can be carried out and thus the $W(\vec{k}_f, \vec{k}_0)$ can be put into the following form [38]:

$$\begin{aligned} W(\vec{k}_f, \vec{k}_0) \;=\; & \frac{ik_0}{8\pi}\int_0^\infty da a^{1+2i\eta}\int_0^\infty d\gamma \int_0^\pi d\phi (4P_4 - 4\delta P_5 + \delta^2 P_6 + 8C_5^{(0)} \\ & + 8\delta C_6^{(0)} + 2\delta^2 C_7^{(0)}), \end{aligned} \tag{B.26}$$

where

$$P_i = \frac{\Gamma(i+1)}{\delta^{i+1}} F(\frac{i+1}{2}, \frac{i+2}{2}; 1; -\frac{q^2}{\delta^2}), \tag{B.27}$$

$$C_i^{(0)} = \frac{\partial^i}{\partial \delta^i}[J_0(X)K_0(Y)]. \tag{B.28}$$

The quantities X and Y are defined by

$$X = \sqrt{2M}[\sqrt{\delta^2 + q^2} - \delta]^{1/2}, \tag{B.29}$$

$$Y = \sqrt{2M}[\sqrt{\delta^2 + q^2} + \delta]^{1/2}. \tag{B.30}$$

The quantities P_i can further be evaluated by using the formula (see p559 of ref. [46]):

$$F(\nu, \beta; \gamma; z) = (1 - z)^{-\nu} F(\nu, \gamma - \beta; \gamma; \frac{z}{z-1}), \tag{B.31}$$

as listed from eq. (3.61) to eq. (3.64). In a similar way, we can also obtain the Wallace amplitudes for other cases.

Bibliography

[1] C.J. Joachain, K.H. Winters, L. Cartiaux and R.M. Mendez-Moreno, J.Phys. B10 (1977) 1277.

[2] T.S. Ho and F.T. Chan, Phys.Rev.A17(1978)529.

[3] C.J Joachain and K.H Wintetrs, J.Phys.B13(1980)1451.

[4] S. Vucic, R.M Potvliege and C.J Joachain, J.Phys.B20(1987)3157.

[5] R.S. Pundir, R.K. Sharma and K.C. Mathur, Phys.Lett.A19(1982)15.

[6] S. Saxena, G.P. Gupta and K.C. Mathur, J.Phys.B17(1984)3743

[7] N.S. Rao and H.S. Desai, J.Phys.B16(1983)863.

[8] A.C. Yates Phys.Rev.A19(1979)1550.

[9] S.S. Tayal, Phys.Rev.A28(1983)2535.

[10] J.N. Das and P.K. Bhattacharyya, Phys.Rev.A27(1983)2876.

[11] C.N.Chandra Prahba and H.S.Desai,Pramana 21(1983)293.

[12] C.N.Chandra Prahba and H.S.Desai, Ind.J.Pur.App.Phys.23(1985)12.

[13] A.J.Dixon, A.Von.Engel and M.F.A.Harrison, Proc.R.Soc.(Lond)A343(1975)333.

[14] R.J.Glauber, Lectures in Theoretical Physics,P315, Vol.I, ed. W.E. Brittin (Interscience, New York, 1959).

[15] C.J.Joachain, Quantum Collision Theory(North-Holland, Amsterdam, 1975)

[16] J.J. Sakurai, Modern Quantum Mechanics,P392(The Benjamin, 1985).

[17] See ref.[16],P441.

[18] F.W.Byron Jr. and C.J.Joachain, Phys.Rep.34C(1977)P259

[19] F.W. Byron Jr., C.J. Joachain and E.H.Mund, Phys.Rev. D8(1973)2622.

[20] F.W. Byron Jr. and C.J. Joachain, Physica 66(1973)33.

[21] S.J Wallace, Ann.Phys., NY 78(1973)190

[22] H.D.I. Abarbanel and C. Itzykson, Phys.Rev.Lett. 23(1969), 53-56.

[23] R.L. Sugar and R. Blankenbecler, Phys.Rev. 183(1969),1387.

[24] L.I. Schiff, Phys.Rev. 103(1956)443.

[25] See ref.[18]259.

[26] F.W. Byron, C.J. Joachain and E.H. Mund, Phys.Rev.D11(1975)1662; C20(1979)2325

[27] D.M. Chase, Phys.Rev. 104(1956)838.

[28] See ref.[15]Chap.14.

[29] F.W.Byron Jr. and L.J.Latour Jr.,Phys.Rev.A13(1976)649.

[30] F.W. Byron, C.J. Joachain,J.Phys.B8(1975)L284

[31] E. Gerjuoy and B.K. Thomas, J.Math.Phys. 12(1971)1567.

[32] H.S.W.Massey and C.B.O.Mohr, Proc.Roy.Soc.A146(1934)880

[33] B.L.Moiseiwitch and A.Williams, Proc.Roy.Soc.A250(1959)337

[34] H.R.J. Walters, Phys.Rep.116(1984)P22

[35] A.R.Swift Phys.Rev.D9(1974)1740

[36] F.W. Byron Jr., C.J. Joachain and R.M. Potvliege, J.Phys.B15(1982)3915.

[37] V. Franco and Z. Iwinski, Phys.Rev.A25(1982)1900.

[38] K. Unnikrishnan and M.A. Prasad,J.Phys.B15(1982)1549.

[39] F.W. Byron Jr., C.J. Joachain and R.M. Potvliege, J.Phys.B18(1985)1637.

[40] F.W. Byron and C.J. Joachain, J.Phys.B7(1974)L212; B8(1975)L284; B10(1977)207

[41] F.W. Byron and C.J. Joachain, Phys.Rev. A8(1973)1264.

[42] T.T. Gien, Phys.Rep.160(1988)125 and the references therein.

[43] T.T. Gien, J.Phys.B9(1976)5203.

[44] F.W. Byron Jr., C.J. Joachain and R.M. Potvliege, J.Phys.B14(1981)L609.

[45] G.C.King, S.Trajmar and J.W.McConkey, Comments At. Mol.Phys.V.23,No.5(1989).

[46] M.Abramowitz and I.A.Stegun, Hankbook of Math. Fcts. (Nat. Bur. Stds. Washington, D.C.1964)

[47] I.S.Gradshteyn et al.,Table of Integrals, Series, and Products. (Acad. Pre.,1980) PP711, 719.